1967

Solution of space-time kinetic equations for coupled-core nuclear reactors

Neal Edward Carter
Iowa State University

SOLUTION OF SPACE-TIME KINETIC EQUATIONS FOR COUPLED-CORE NUCLEAR REACTORS

by

Neal Edward Carter

A Dissertation Submitted to the
Graduate Faculty in Partial Fulfillment of
The Requirements for the Degree of
DOCTOR OF PHILOSOPHY

Major Subject: Nuclear Engineering

Approved:

Signature was redacted for privacy.

In Charge of Major Work

Signature was redacted for privacy.

Head of Major Department

Signature was redacted for privacy.

Dean of Graduate College

Iowa State University
Of Science and Technology
Ames, Iowa

1967

TABLE OF CONTENTS

I. INTRODUCTION

A review of the literature reveals that much effort has been made to simplify the neutron kinetic equations. (1,2,3,4) These efforts have naturally increased in complexity and generality with time. The early analyses were based upon the continuous slowing down - diffusion model, where the neutron flux distribution was assumed to be separable in space and time. The classic space-independent zero power kinetic equations are then derived by assuming that the space dependency can be represented by some average distribution whose shape does not change with time. (1,2,3,4)

To place these analyses on a more firm theoretical footing, Henry (5) rederived the kinetic equations from the more general transport theory. The purpose of this paper was to obtain a precise statement of the approximations required to derive the reduced equation and to clarify the physical meaning of the parameters appearing in such a reduction. The neutron density is expressed as an amplitude T(t) times a shape function, n(r,t), which is itself time dependent. By the introduction of a static adjoint flux, the spatial dependency of the separable neutron transport equation could be eliminated. The resulting time-dependent equation was indeed of the same form as the classic kinetic equations that had previously been obtained, but the parameters - such as reactivity, neutron lifetime, and the effective delayed neutron fraction - were

precisely defined. This reformulation is only a formality since the unknown space shape, $n(r,t)$, is involved in the evaluation of the reactor parameters. Except in the few cases where the shape is constant and known during the transient, it is necessary to approximate $n(r,t)$. A very common approximation is to use the shape, $n_0(r)$, corresponding to the steady state. In this case use of the static adjoint flux, $\phi_0^*(r)$, causes the first order part of the error in the computation of reactivity to vanish. (5,6) However, other choices of the weighting function have been made; these choices are discussed and compared by Gozani. (7)

The physical interpretation of the adjoint function has been discussed by Hurwitz (8) and Ussachoff (9) in the critical case, Selengut (10) and Kadomtsev (11) in the subcritical case, and Lewins (12) in the time dependent case.

The numerical solution of the space-independent reactor kinetic equations has been treated by various authors. (13,14, 15,16) The various techniques have had varying degrees of success in handling the problems of numerical stability, truncation error, and machine running time.

"More recently it has become both necessary and possible to describe in some detail the space-time kinetic behavior of a nuclear reactor. The necessity has arisen for two reasons. First, the current trend in power reactors is towards very large sizes for which space-time effects can become

limiting design considerations. Second, certain useful experimental techniques for measuring basic reactor parameters and for verifying the adequacy of theoretical models require that space-time phenomena be accounted for, either as an essential part of the analysis or to insure that they are not perturbing the experimental conditions. The possibility of providing a detailed description of space-time effects has arisen from an improved understanding of the basic theory and from an increased capacity to determine numerical solutions to the governing equations through the use of digital computers." (17)

The usual approach that is taken to treat the space-time dynamics problem is to try to break the space-time equations into separate space equations and time equations. The space equations are usually solved on digital computers, and the time equations are solved either digitally, by discretizing the time variable, or by an analog computer with time varying continuously. Several methods which have been used or proposed for accomplishing this breakdown of the space-time equations are now described.

As mentioned previously, most reactor dynamic studies and computer programs use the point kinetic equations, where it is assumed that the space shape is constant, i.e., $n(r,t)=n(r)$. The adiabatic method, as originally suggested by Henry (18), attempts to improve on this assumption while still retaining

the point kinetics formulation. The basic idea is to replace the true shape function, $n(r,t)$, at any instant by the fundamental lambda mode (17), ψ, corresponding to the reactor condition at that instant. A static weighting function given as the adjoint solution for the unperturbed reactor is still necessary as a part of the analysis.

In a series of papers (19,20,6), J. Lewins pointed out that the choice of a static weighting function was arbitrary and could be justified only a posteriori. At the same time, Kaplan and Margolis (21) demonstrated that the adiabatic approximation was not valid for core geometries whose characteristic dimension exceeded about 20 neutron migration lengths. They showed that after a change in the material properties of the core, the flux shape changes part way towards its asymptotic form in a few prompt neutron lifetimes, but the remaining change takes place in times characteristic of the delay precursors. The "prompt" jump component of the asymptotic flux shape decreases as the core size increases. The replacement of n by ψ implies that the flux shape responds instantaneously to changes of the reactor properties; hence, the adiabatic approximation may be a poor method to apply to large reactors.

In a second method for treating the space-time problem, called nodal analysis, the reactor is divided into regions, or nodes, and a set of time dependent equations is found involving

the average fluxes at each node. The space part of the problem consists of the determination of the parameters governing the diffusion of neutrons from node to node.

Finite difference techniques (22) may be considered as a limiting form of nodal analysis in which the nodes are small and closely spaced. This approach has been used for digital computer codes that solve the space-time problems including, in some cases, various feedback effects. The digital code WIGLE (23) solves the two-group space-time equations for one dimensional slab geometry. This program is the only really effective space-time program in existence to date, and it is not readily extended to more energy groups or more dimensions.

When the nodes are few and represent gross regions of the core, different concepts are needed. In this case leakage parameters must be inferred from experiment or from fine mesh, time independent spatial calculations. An example of the latter is the determination of the parameters, k_{ij}, in Avery's theory of coupled reactors. (24) The term "coupled" is taken to mean that in each of the reactors some of the fission neutrons are emitted in fissions induced by neutrons born in other reactors.

The third general method for treating the space-time problem is called modal analysis. In this method the unknown function of space and time is approximated by a linear combination of known space functions (modes) and unknown time

dependent coefficients. The space part of the problem is the selection or construction of the modes; the time part is the determination of the coefficients.

In this discussion several versions of the modal analysis technique will be described corresponding to different methods of choosing the space functions. Once functions are chosen, however, the coefficients of combination are always found in the same manner. The assumed form of the solution is substituted into the governing differential equation, this equation is then multiplied through by other space functions, termed weighting functions, and the result is integrated over space and set equal to zero. This yields a set of differential equations which have the coefficients of combination as unknowns. The substitute-integrate process can be motivated by variational principles (19,25), and this motivation suggests that the weighting functions should be chosen to approximate the time dependent adjoint flux. In principle, many other types of weighting functions may be used. One example would be the weighted residual. (26) However, in this discussion only the adjoint type will be discussed.

Perhaps the most basic and common version of modal analysis is to expand each flux and precursor group in a series of ordinary orthogonal functions. A very common set of functions that has been used (27,28) is the set of eigenfunctions of the Helmholtz equation. This approach is pri-

marily suitable for one-dimensional uniform reactor models. For a more complicated, and typical, reactor configuration many modes are needed and all the expansion coefficients must be solved for simultaneously.

The modal solution for the space-time problem can be expressed in simple expansion form if one can find the set of modes having the so-called finality property, as described by Kaplan. (29) These modes are the set of eigenfunctions diagonalizing the differential operator of the basic differential equations. However, it is generally difficult to solve such an eigenvalue problem.

For more complicated models it is advisable to use modes which are more specific to the problem at hand, e.g., the lambda or omega modes. (30,31) If one writes the reactor equations in the operator form

$$T\dot{\phi} + L\phi = M\phi$$

then the omega modes are defined to be the eigenfunctions of the problem

$$[L-M]\psi_n = \omega_n T \psi_n ,$$

and the lambda modes are the eigenfunctions of the problem

$$L\psi_n = \frac{1}{\lambda_n} M\psi_n .$$

Generally speaking the more effort put into finding the modes the less is required in finding the time dependent coefficients. Thus if the "natural" modes (31) of the system are used, ordinarily only a few modes are needed and the coefficient of each may be found independently of all the others.

The question of completeness of the lambda and omega modes is not fully settled. (32) However, to the designer this question is academic since for practical computations he is able to use only a small number of modes anyway. Therefore the idea is generated that one need not necessarily use eigenfunctions as the basis functions. Indeed, one may use any functions which intuition or experience suggest may yield an adequate approximation. Thus Dougherty and Shen (33) propose the use of Green's Function Modes obtained by solving the diffusion equations with sources fixed in various subregions of the reactor. These modes, although not orthogonal, can be adapted to perturbations in the diffusion parameters about which one has some a priori information.

In order to circumvent the difficulties of an adiabatic approximation and to eliminate the arbitrariness of the static adjoint weighting functions, Lewins (19) suggested extending the work of Selengut (10) and Calame (34) on the use of a variational principle to derive a consistent method of finding approximately separated solutions. Briefly, a Lagrangian is chosen whose Euler equations are given by the time-dependent

equations for the neutron and precursor densities, together with the time-dependent adjoint equations. A separable trial function is substituted into the functional and integrated where possible before variation. The subsequently derived equations then contain time-and space-averaged coefficients that couple the separated equations in a consistent manner. Dougherty and Shen (33) modified the variational principle as originally suggested by Lewins so as to include a natural boundary condition. With this modification the variational principle now requires trial functions that need only be continuous and satisfy homogeneous boundary conditions. The trial functions were also extended to include a modal development of the flux and adjoint.

It is to be noted that the functional used in the variational principle is not selfadjoint; hence, one can only expect to get a saddle point as the stationary point of the functional. This means that the methods that exist for the maximum-minimum case for assessing the errors made in the calculations with the variational principle do not apply here. However, the useful property still exists that first order errors in the flux and adjoint flux do not appear in the numerical value of the functional.

In this thesis the basic modal technique as suggested by Dougherty and Shen (33) has been modified and extended in order to obtain the kinetic response of various model coupled-

core nuclear reactors. The response of the model reactors to step, ramp, and oscillating reactivity inputs is found. The model reactors are one-dimensional slab geometry, and the dynamics of the reactors are described by both one-group and two-group diffusion theory.

II. ANALYTICAL TECHNIQUE

In this section a review will be made of the basic method used in this paper as it was originally suggested by Dougherty and Shen (33).

A solution to the reactor kinetic equations in the operator form $L\phi = v^{-1} \frac{\partial \phi}{\partial t}$ is desired. The solution is to be expressed in the series form

$$\phi(x,t) = \sum_{i=1}^{N} A_i(t)\ \psi_i(x) \ ,$$

where the functions $A_i(t)$ and $\psi_i(x)$ are to be determined. In previous analyses (27,28) the functions $\psi_i(x)$ have been chosen as solutions of the Helmholtz equation

$$\nabla^2 \psi_n(x) + B_n^2\ \psi_n(x) = 0.$$

However, in this analysis the set of functions $\psi_n(x)$ will be derived by obtaining an approximate solution of the kinetic equations by the "Green's Function" method. In this case the functions $\psi_n(x)$ will not be orthogonal, but it will be shown that they converge to the solution $\phi(x,t)$ more readily than the Helmholtz modes.

When the space modes $\psi_n(x)$ have been determined, the corresponding time dependent coefficients, $A_i(t)$, may be obtained by using the method of semidirect calculus of variations. The procedure is to establish a Lagrangian whose Euler equa-

tions are the neutron kinetic equations and the corresponding adjoint kinetic equations. A separable trial function

$$\phi_T(x,t) = \sum_{i=1}^{N} A_i(t)\ \psi_i(x)$$

is substituted into the functional and integrated where possible before variation. The result, after variation, is a set of coupled, first order, ordinary differential equations whose dependent variables are the time coefficients, $A_i(t)$.

The kinetic equations for a given reactor system can, as stated previously, usually be written in the matrix form

$$L\phi = V^{-1}\frac{\partial \phi}{\partial t} \quad , \qquad (1)$$

where L is a space and time dependent matrix operator, and the elements of the diagonal matrix V^{-1} are reciprocals of neutron velocities. The matrix ϕ has as its elements the reactor variables, such as energy group fluxes, temperature, etc.

In deriving a variational principle for Equation 1 it is necessary to define the adjoint multigroup equations

$$L^*\phi^* = -V^{-1}\frac{\partial \phi^*}{\partial t} \quad ,$$

where

$$\int_R d\vec{r}\ \{\phi^* L\phi - \phi L^*\phi^*\} = 0.$$

In order to write the kinetic equations in integral equation form the multigroup operator L is redefined in terms of a

removal operator Lr and a production operator νM such that $L = Lr - \nu M$. Equation 1 is now written as the integral equation

$$\phi(x,t) - \phi_0(x) = \int_0^t \int_{x_o}^{x_N} dx'dt' \{G(x,t;x',t')\nu M(x',t')\phi(x',t')\} \tag{2}$$

where the kernel of Equation 2 is defined by

$$(Lr - v^{-1} \partial/_{\partial t})\ G(x,t;x',t') = \delta(x-x')\delta(t-t')$$

plus the same homogeneous boundary conditions as required for $\phi(x,t)$.

The integrand of Equation 2 is now approximated by a finite sum in the manner

$$G(x,t;x',t')\nu M(x',t')\phi(x',t')$$

$$\approx \sum_{i=1}^{N} C_i(t')G_o(x,x')\nu M_o(x')\phi_o(x')\Delta_i(x) \tag{3}$$

where

zero subscripts denote initial values,

$G_o(x,x')$ is the initial, steady state "Green's Function", defined by

$$Lr_o G_o(x,x') = \delta(x-x'),$$

and

$\Delta_i(x)$ = unity in i^{th} reactor region and zero elsewhere.

By substituting the approximation given in Equation 3 into Equation 2, the following equation is obtained:

$$\phi(x,t)-\phi_o(x)$$

$$= \sum_{i=1}^{N} \left[\int_o^t C_i(t') \left\{ \int_{x_o}^{x_N} dx' G_o(x,x') \nu M_o(x') \phi_o(x') \Delta_i(x') \right\} dt' \right] \tag{4}$$

The space modes are now defined to be

$$\psi_i(x) = \int_{x_o}^{x_N} dx' G_o(x,x') \nu M_o(x') \phi_o(x') \Delta_i(x') \ . \tag{5}$$

It is apparent from the definition of $G_o(x,x')$ that the space modes $\psi_i(x)$ also satisfy the differential equations

$$Lr_o \ \psi_i(x) = \nu M_o(x) \phi_o(x) \Delta_i(x) \ . \tag{6}$$

It is also noted that

$$Lr_o \sum_{i=1}^{N} \psi_i(x) = \nu M_o \phi_o \ ,$$

so the initial steady state flux is equal to the sum of the space modes; that is,

$$\phi_o(x) = \sum_{i=1}^{N} \psi_i(x) \ .$$

The time dependent flux is thus expressed in terms of these space modes as

$$\phi(x,t) = \sum_{i=1}^{N} A_i(t) \ \psi_i(x) \tag{7}$$

where

$$A_i(t) = I + \int_o^t C_i(t')dt' \ .$$

Similarly, it can be shown that the adjoint space modes are determined by

$$Lr_o^* \ \psi_i^*(x) = \nu M_o^* \phi_o^* \Delta_i(x) \qquad (8)$$

where

$$\phi_o^*(x) = \sum_{i=1}^{N} \psi_i^*(x) \ .$$

Associated with Equations 6 and 8 are the same homogeneous boundary conditions as required for $\phi(x,t)$.

Thus, the space modes $\psi_i(x)$ and $\psi_i^*(x)$ may be easily determined by the following procedure:

I. Calculate the initial steady state flux and adjoint flux.

II. Subdivide the reactor into N regions.

III. Calculate the space mode, $\psi_i(x)$, and the adjoint space mode, $\psi_i^*(x)$, by substituting the source $\nu M_o \phi_o$, obtained from step I, into the i^{th} region and zero source elsewhere. Repeat this step for the N regions.

The choice of dividing the reactor into N regions will depend upon the spatial and temporal variations of the core parameters. Note that the calculation of the space modes does not require the usual source iteration. Also, for one-group analyses, it is not necessary to determine adjoint modes.

Semidirect calculus of variations will now be used to determine time coefficients suitable for the space modes $\psi_i(x)$. The functional which will be used is given by

$$F[\phi^*,\phi] = \int_0^\tau \int_{x_0}^{x_N} \{\phi^* V^{-1} \frac{\partial \phi}{\partial t} + (\frac{\partial \phi^*}{\partial x}) D (\frac{\partial \phi}{\partial x}) - \phi^* H \phi\} dt dx \qquad (9)$$

where

$$L = \frac{\partial}{\partial x} (D \frac{\partial}{\partial x}) + H \ .$$

The first variations of $F[\phi^*,\phi]$ will give the equations

$$\delta F[\delta\phi^*,\phi] = \int_0^\tau \int_{x_0}^{x_N} dx dt \left[V^{-1} \frac{\partial \phi}{\partial t} - L\phi \right] \delta\phi^*$$

plus the transition conditions $D \frac{\partial \phi}{\partial x}\Big|_{x_j^-}^{x_j^+} = 0$

and

$$\delta F[\phi^*,\delta\phi] = \int_0^\tau \int_{x_0}^{x_N} dx dt \left[V^{-1} \frac{\partial \phi^*}{\partial t} + L^* \phi^* \right] \delta\phi$$

plus the transition conditions $D \frac{\partial \phi^*}{\partial x}\Big|_{x_j^-}^{x_j^+} = 0$.

Thus requiring the functional $F[\phi^*,\phi]$ to be stationary implies not only that the kinetic equations are satisfied but also that the trial functions satisfy the internal boundary conditions of continuity of current.

Trial functions are assumed of the form

$$\phi_T(x,t) = \sum_{i=1}^{N} A_i(t) \ \psi_i(x)$$

$$\phi_T^*(x,t) = \sum_{i=1}^{N} A_i^*(t)\ \psi_i^*(x)$$

and substituted into Equation 9. After the spatial integration has been performed, the functional reduces to

$$F[\phi^*,\phi] = \int_o^\tau dt \cdot Q(t,a_{ik},a_{ik}^*,\dot{a}_{ik}) \qquad (10)$$

where

$$A_i(t) = \begin{bmatrix} a_{i1}(t) & 0 & 0 & 0 \\ 0 & a_{i2} & 0 & 0 \\ \cdot & \cdot & \cdot & \cdot \\ 0 & 0 & 0 & a_{ig}(t) \end{bmatrix}, \text{ etc.}$$

The result of taking the first variation of Equation 10 is

$$\delta F[\delta\phi^*,\phi] = \int_o^\tau dt \sum_{k=1}^{g} \sum_{i=1}^{N} \frac{\partial\phi}{\partial a_{ik}^*}\,\delta a_{ik}^* \ .$$

Since the variations of δa_{ik}^* are independent, the requirement that $F[\phi^*,\phi]$ be stationary is that

$$\frac{\partial\phi}{\partial a_{ik}^*} = 0; \qquad \begin{matrix} i = 1,2,\ldots,N \\ k = 1,2,\ldots,g \ . \end{matrix} \qquad (11)$$

The solution to the system of coupled differential equations indicated in Equation 11 determines a set of time coefficients, $a_{ik}(t)$, for the space modes $\psi_i(x)$, where

$$\psi_i(x) = \begin{bmatrix} \psi_{i1} \\ \psi_{i2} \\ \cdot \\ \cdot \\ \psi_{ig} \end{bmatrix} .$$

Thus the dynamic behavior of a nuclear reactor may now be analyzed by expressing the flux as

$$\phi(x,t) = \sum_{i=1}^{N} A_i(t)\ \psi_i(x)$$

where the elements $A_i(t)$ and $\psi_i(x)$ are obtained as previously indicated.

III. REFERENCE REACTOR FOR ONE-GROUP ANALYSIS

The one-dimensional reactor shown in Figure 1 will serve as the analytical model for all analyses in which the reactor dynamics are described by one-group diffusion theory, neglecting delayed neutrons. The model is a coupled core reactor consisting of two semi-infinite multiplying regions joined by a non-multiplying coupling region. The reactor parameters, given in Table 1, are analogous to those used by Foderaro (27).

Table 1. Reference reactor critical parameters

Region	Σ_a (cm^{-1})	$\nu\Sigma_f$ (cm^{-1})	D (cm)	V_s (cm/sec)
$0 \leq x \leq 27$	0.00818	0.0161	0.890	220000.
$27 \leq x \leq 47$	0.0210	0	0.890	
$47 \leq x \leq 74$	0.00818	0.0161	0.890	

The kinetics of this reactor are to be described by the one-group diffusion equation

$$D_i \nabla^2 \phi_i(x) - \Sigma_{ai}\phi_i(x) + \nu\Sigma_{fi}\phi_i(x) = \frac{1}{V}\frac{\partial \phi i}{\partial t} ,$$

where the subscripts denote values for the i^{th} region.

After the parameters listed in Table 1 were established, the reactor critical size was determined by the usual technique

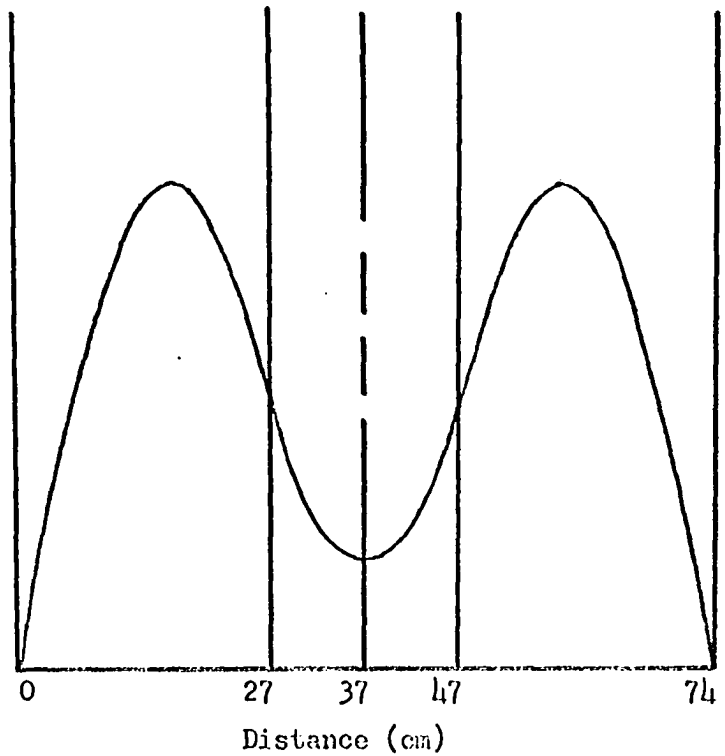

Fig. 1. Reference reactor for One-group analysis with critical flux distribution

of solving the criticality determinant. The equations to be solved are

$$D\nabla^2\phi_1(x) - \Sigma_{a1}\phi_1(x) + \nu\Sigma_{f1}\phi_1(x) = 0 \qquad 0 \leq x \leq \alpha$$

$$D\nabla^2\phi_2(x) - \Sigma_{a2}\phi_2(x) = 0 \qquad \alpha \leq x \leq \beta$$

$$D\nabla^2\phi_3(x) - \Sigma_{a3}\phi_3(x) + \nu\Sigma_{f3}\phi_3(x) = 0 \qquad \beta \leq x \leq C$$

where

C = reactor critical size, to be determined

$\alpha = 0.5C - 10.0$

$\beta = 0.5C + 10.0$

The associated boundary conditions are

$$\phi_1(o) = 0; \quad \phi_1(\alpha) = \phi_2(\alpha); \quad \nabla\phi_1\big|_\alpha = \nabla\phi_2\big|_\alpha$$

$$\phi_3(C) = 0; \quad \phi_2(\beta) = \phi_3(\beta); \quad \nabla\phi_2\big|_\beta = \nabla\phi_3\big|_\beta$$

The resulting set of solutions can be written, in matrix form, as $B \cdot \gamma = 0$, where B is a 6 x 6 matrix. The value of C which establishes the determinant of B as zero is the reactor critical size and was found to be C=74.0 cm.

Since $|B| = 0$, the equations $B \cdot \gamma = 0$ now may be solved for all the unknowns γ, except one. The remaining unknown is a power level factor and was chosen to equal unity. The normalized critical flux distribution was then found to be described by the equations

$$\phi_1(x) = \sin B(1)\cdot x \qquad 0 \leq x \leq 27$$

$$\phi_2(x) = 0.000390\, e^{B(2)\cdot x} + 33.88\, e^{-B(2)\cdot x} \qquad 27 \leq x \leq 47$$

$$\phi_3(x) = -0.765[\sin B(3)\cdot x - 0.846 \cos B(3)\cdot x] \qquad 47 \leq x \leq 74$$

where

$$B^2(1) = \frac{\nu\Sigma_{f1} - \Sigma_{a1}}{D} \; ; \; B^2(2) = \frac{\Sigma_{a2}}{D} \; ; \; B^2(3) = \frac{\nu\Sigma_{f3} - \Sigma_{a3}}{D} \; .$$

This normalized critical flux distribution is also indicated in Figure 1. The problem now to be analyzed is the dynamic response of this reactor to various reactivity inputs.

IV. ONE GROUP ANALYSIS:
STEP RESPONSE

The response of the reactor shown in Figure 1 to step reactivity inputs will be analyzed in this section. Initially, the reactor is divided into three regions as indicated below:

Region 1 $0 \leq x \leq 27$ cm.

Region 2 $27 \leq x \leq 47$ cm.

Region 3 $47 \leq x \leq 74$ cm.

The problem now is to determine the three corresponding space modes using the equation

$$Lr_c \psi_i(x) = \nu M \phi_o(x) \Delta_i(x) \quad , \qquad (6)$$

as developed previously. The kinetic equations for one-group diffusion theory, neglecting delayed neutrons, can be written in the operator form

$$L\phi = V^{-1} \frac{\partial \phi}{\partial t} \quad ,$$

where

$$L = D\nabla^2 - \Sigma_a + \nu\Sigma_f \quad .$$

The operator L is now redefined sc that

$$L = Lr - \nu M$$

where

$$Lr = D\nabla^2 - \Sigma_a$$

$$\nu M = -\nu\Sigma_f \quad .$$

The three space modes will be derived as solutions to the following sets of equations:

Mode 1

$$D\nabla^2\psi_1(x) - \Sigma_{a1o}\psi_1(x) = -\nu\Sigma_{f1}\phi_o(x) \qquad 0\leq x\leq 27$$

$$D\nabla^2\psi_1(x) - \Sigma_{a2o}\psi_1(x) = 0 \qquad 27\leq x\leq 47$$

$$D\nabla^2\psi_1(x) - \Sigma_{a3o}\psi_1(x) = 0 \qquad 47\leq x\leq 74$$

Mode 2

$$D\nabla^2\psi_2(x) - \Sigma_{a1o}\psi_2(x) = 0 \qquad 0\leq x\leq 27$$

$$D\nabla^2\psi_2(x) - \Sigma_{a2o}\psi_2(x) = -\nu\Sigma_{f2}\phi_o(x) \equiv 0 \qquad 27\leq x\leq 47$$

$$D\nabla^2\psi_2(x) - \Sigma_{a3o}\psi_2(x) = 0 \qquad 47\leq x\leq 74$$

Mode 3

$$D\nabla^2\psi_3(x) - \Sigma_{a1o}\psi_3(x) = 0 \qquad 0\leq x\leq 27$$

$$D\nabla^2\psi_3(x) - \Sigma_{a2o}\psi_3(x) = 0 \qquad 27\leq x\leq 47$$

$$D\nabla^2\psi_3(x) - \Sigma_{a3o}\psi_3(x) = -\nu\Sigma_{f3}\phi_o(x) \qquad 47\leq x\leq 74$$

where

Σ_{aio} indicates the critical value of Σ_a in the i^{th} region. In addition, the modes must be continuous functions in the interval $0\leq x\leq 74$, satisfying the boundary conditions

$$\psi_i(0) = 0 \qquad i=1,2,3$$

$$\psi_i(74) = 0 \qquad i=1,2,3$$

and possessing continuous first derivatives in the interval

$0 \leq x \leq 74$. If the diffusion coefficient were not uniform throughout the reactor, the condition of continuous first derivatives would be replaced by the conditions

$$D_j \left.\frac{d\psi_i}{dx}\right|_{x=x_j} = D_{j+1} \left.\frac{d\psi_i}{dx}\right|_{x=x_j} \qquad \begin{matrix} i=1,2,3 \\ j=1,2,\ldots,N-1 \end{matrix}$$

where x_j denotes region interfaces.

Space modes 1 and 3 may be obtained in a completely analytical manner, and their graph is shown in Figure 2. However, mode 2 is required to be the solution of a set of homogeneous equations with homogeneous boundary conditions; thus $\psi_2(x) \equiv 0$. The condition

$$\phi_o(x) = \sum_{i=1}^{3} \psi_i(x)$$

remains valid. The problem is that without the contribution of a mode describing the behavior of the coupling region, it is not possible to obtain a valid expression for $\phi(x,t)$. For instance, if a reactivity change is made in region 2, the expression for $\phi(x,t)$ will become

$$\phi(x,t) = \sum_{i=1}^{3} a_i(t)\psi_i(x) = \phi_o(x)e^{\lambda t} .$$

That is, no flux shape changes will occur. Thus a method must be obtained for generating a mode for the non-multiplying region.

In order to generate a mode $\psi_2(x)$ the operator L was redefined in the various regions as follows.

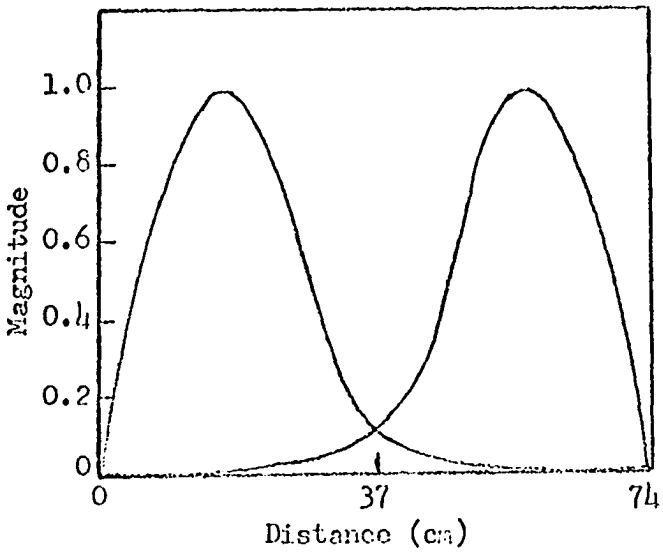

Fig. 2. Two region space modes

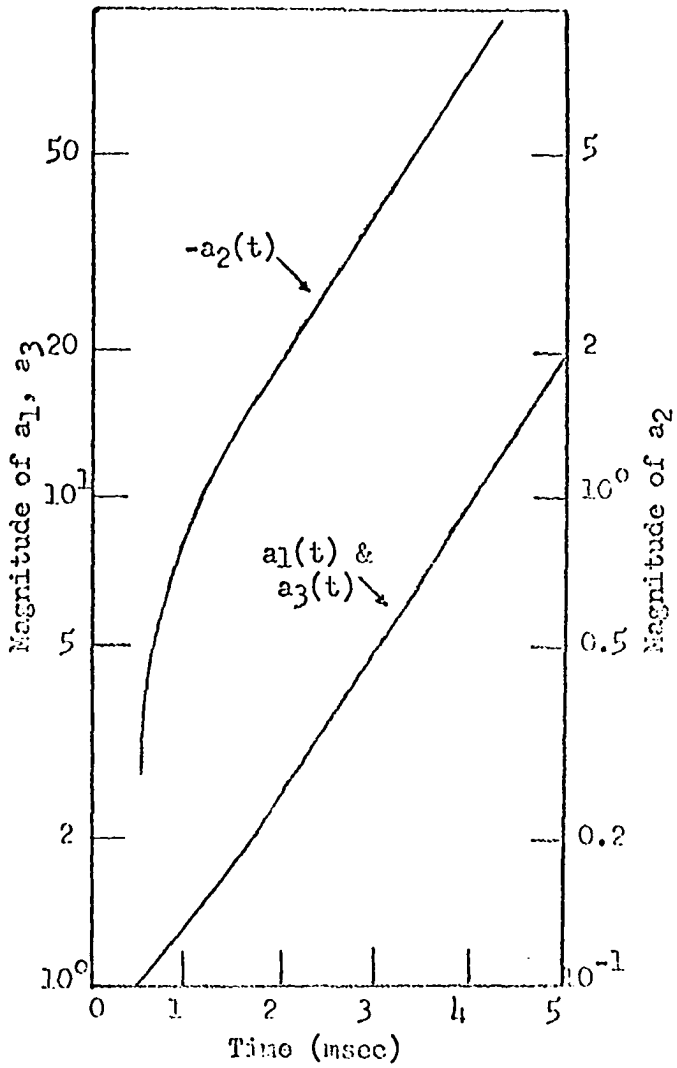

Fig. 3. Time coefficients for three region modes

Region 1

$$L = D\nabla^2 - \Sigma_{a1} + \nu\Sigma_{f1}$$

$$Lr = D\nabla^2 - \Sigma_{a1}$$

$$\nu M = -\nu\Sigma_{f1}$$

Region 3

$$L = D\nabla^2 - \Sigma_{a3} + \nu\Sigma_{f3}$$

$$Lr = D\nabla^2 - \Sigma_{a3}$$

$$\nu M = -\nu\Sigma_{f3}$$

Region 2

$$L = D\nabla^2 - \Sigma_{a2}' - \Sigma_{a2}'' \text{ , where } \Sigma_{a2} = \Sigma_{a2}' + \Sigma_{a2}''$$

$$Lr = D\nabla^2 - \Sigma_{a2}'$$

$$\nu M = \Sigma_{a2}''$$

Note that a pseudo production operator, $\nu M = \Sigma_{a2}''$, has been established by dividing the absorption cross section in region 2 in the manner indicated. The resulting system of equations used to determine the three space modes is given below.

Mode 1

$$D\nabla^2\psi_1 - \Sigma_{a1o}\psi_1 = -\nu\Sigma_{f1}\phi_o \quad 0 \le x \le 27$$

$$D\nabla^2\psi_1 - \Sigma_{a2o}'\psi_1 = 0 \quad 27 \le x \le 47$$

$$D\nabla^2\psi_1 - \Sigma_{a3o}\psi_1 = 0 \quad 47 \le x \le 74$$

Mode 3

$$D\nabla^2\psi_3 - \Sigma_{a1o}\psi_3 = 0$$

$$D\nabla^2\psi_3 - \Sigma_{a2o}'\psi_3 = 0$$

$$D\nabla^2\psi_3 - \Sigma_{a3o}\psi_3 = -\nu\Sigma_{f3}\phi_o$$

Mode 2

$$D\nabla^2\psi_2 - \Sigma_{a1o}\psi_2 = 0 \quad 0 \le x \le 27$$

$$D\nabla^2\psi_2 - \Sigma_{a2o}'\psi_2 = \Sigma_{a2o}''\phi_o \quad 27 \le x \le 47$$

$$D\nabla^2\psi_2 - \Sigma_{a3o}\psi_2 = 0 \qquad 47 \leq x \leq 74$$

It is anticipated that the choice of the ratio $\Sigma_{a2}'/\Sigma_{a2}''$ will not be a critical factor, and it will be shown later that this is indeed the case. Initially, $\Sigma_{a2}'/\Sigma_{a2}''$ was chosen to equal 4×10^{-5}. The resulting three space modes are shown in Figure 4, where again $\phi_o(x) = \sum_{i=1}^{3} \psi_i(x)$. It is also noted that in the case of one-group diffusion theory, $\psi_i^* \equiv \psi_i$.

Next it is required to determine the time coefficients for these space modes. As indicated previously the functional that will be used in applying the calculus of variations is given by

$$F[\phi^*,\phi] = \int_o^\tau \int_{x_o}^{x_N} [\phi^* V^{-1} \frac{\partial \phi}{\partial t} + \frac{\partial \phi^*}{\partial x} D \frac{\partial \phi}{\partial x} - \phi^* H \phi] \, dxdt, \quad (9)$$

where in this case $H = \nu\Sigma_f - \Sigma_a(t)$. Trial functions are assumed of the type

$$\phi(x,t) = \sum_{i=1}^{3} a_i(t)\psi_i(x); \quad \phi^*(x,t) = \sum_{i=1}^{3} a_i^*(t)\psi_i^*(x),$$

and substituted into Equation 3. The result, after substitution, is

$$F(\phi^*,\phi) = \int_o^\tau \int_{x_o}^{x_N} [a_1^*\psi_1^* + a_2^*\psi_2^* + a_3^*\psi_3^*] V^{-1} [\dot{a}_1\psi_1 + \dot{a}_2\psi_2 + \dot{a}_3\psi_3] dxdt$$

$$+ \int_o^\tau \int_{x_o}^{x_N} [a_1^*\partial_x\psi_1^* + a_2^*\partial_x\psi_2^* + a_3^*\partial_x\psi_3^*] D [a_1\partial_x\psi_1 + a_2\partial_x\psi_2 + a_3\partial_x\psi_3] dxdt$$

$$- \int_o^\tau \int_{x_o}^{x_N} [a_1^*\psi_1^* + a_2^*\psi_2^* + a_3^*\psi_3^*] (\nu\Sigma_f - \Sigma_a(t)) [a_1\psi_1 + a_2\psi_2 + a_3\psi_3] dxdt.$$

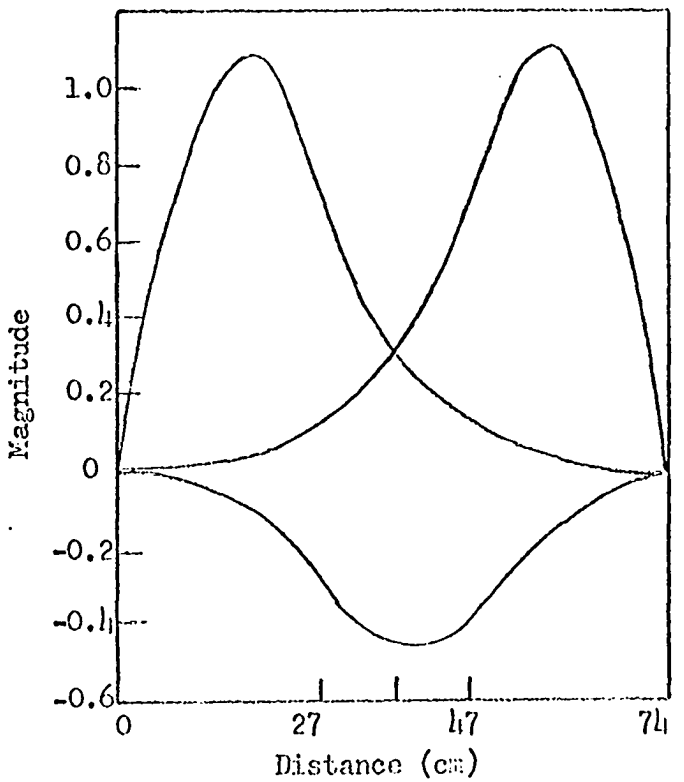

Fig. 4. Three region space modes

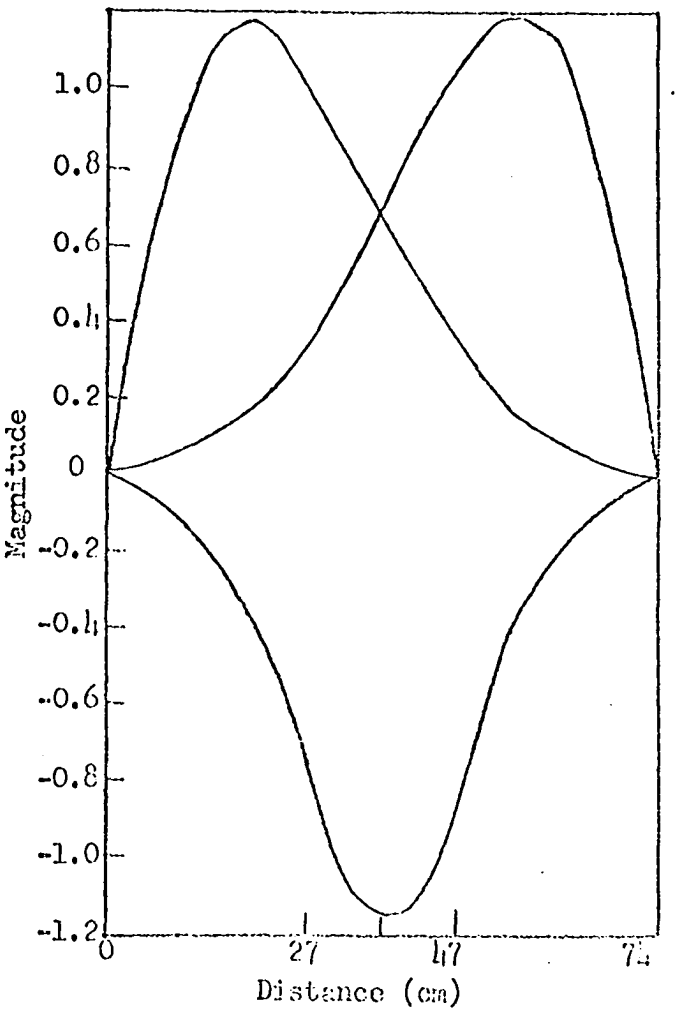

Fig. 5. Three region space modes

The result of performing the spatial integration and taking the first variation with respect to ϕ^* is

$$\delta F(\delta\phi^*,\phi) = \int_o^\tau \int_{x_o}^{x_N} \{[\lambda_{11}\dot{a}_1 + \lambda_{12}\dot{a}_2 + \lambda_{13}\dot{a}_3]\delta a_1^*$$

$$+[a_1(k_{11}-f_{11}) + a_2(k_{12}-f_{12}) + a_3(k_{13}-f_{13})]\delta a_1^*$$

$$+[\lambda_{21}\dot{a}_1 + \lambda_{22}\dot{a}_2 + \lambda_{23}\dot{a}_3 + a_1(k_{21}-f_{21}) + a_2(k_{22}-f_{22})$$

$$+ a_3(k_{23}-f_{23})]\delta a_2^* + \ldots$$

where

$$\lambda_{ij} = [\psi_i^* V^{-1} \psi_j]; \quad f_{ij} = [\psi_i^* (\nu\Sigma_f - \Sigma_a)\psi_j];$$

$$k_{ij} = [\partial_x \psi_i^* \cdot D \cdot \partial_x \psi_j];$$

and

$$\dot{a}_1 \equiv \frac{d}{dt} a_1(t); \quad [\psi_i^* F \psi_j] \equiv \int_{x_o}^{x_N} \psi_i^*(x) F(x,t) \psi_j(x) dx \ .$$

The Euler equations for the Lagrangian thus establish a set of differential equations given, in matrix form, by

$$\Gamma\dot{A} = BA \tag{12}$$

where

$$\Gamma = [\lambda_{ij}]; \ B = [f_{ij}-k_{ij}]; \ A^T = [a_1, a_2, a_3] \ .$$

In order to evaluate the elements of matrices Γ and B, it is necessary to perform integrations of the type

$\int_{x_o}^{x_N} \psi_i^*(x) F(x,t) \psi_j(x) dx$. This integration is performed on a digital computing machine using Gregory's formula of numerical integration (35),

$$\int_{x_o}^{x_N} f(x)dx = h\left[\frac{f_o}{2} + f_1 + \ldots + f_{N-1} + \frac{f_N}{2}\right]$$

$$- \frac{h}{12}\left[\Delta f_{n-1} - \Delta_{fo}\right] - \frac{h}{24}\left[\Delta^2 f_{n-2} + \Delta^2 f_o\right],$$

where h = 1 cm. If the time dependence of $\Sigma_a(x,t)$ is chosen to be a step function, then Equation 12 will represent a first order, linear system of differential equations with constant coefficients. Several methods for solving such equations will now be described and their relative merits investigated.

Eigenvalue method

Due to the nature of the differential equations the following substitutions may be made (35):

$$a_1(t) = \alpha_1 e^{\omega t}$$
$$a_2(t) = \alpha_2 e^{\omega t}$$
$$a_3(t) = \alpha_3 e^{\omega t}$$

This substitution will result in the generalized eigenvalue problem $B\alpha = \omega\Gamma\alpha$. Corresponding to each eigenvalue of the matrix $\Gamma^{-1}B$ is an eigenvector which represents a solution for the α's, within an arbitrary constant. In the case where $\Gamma^{-1}B$ is a 3x3 matrix, the solutions to Equation 12 are given

by

$$a_1(t) = k_1\alpha_{11}e^{\omega_1 t} + k_2\alpha_{12}e^{\omega_2 t} + k_3\alpha_{13}e^{\omega_3 t}$$

$$a_2(t) = k_1\alpha_{21}e^{\omega_1 t} + k_2\alpha_{22}e^{\omega_2 t} + k_3\alpha_{23}e^{\omega_3 t}$$

$$a_3(t) = k_1\alpha_{31}e^{\omega_1 t} + k_2\alpha_{32}e^{\omega_2 t} + k_3\alpha_{33}e^{\omega_3 t}$$

where

$$\alpha_{ji} = \begin{bmatrix} \alpha_{j1} \\ \alpha_{j2} \\ \alpha_{j3} \end{bmatrix}, \; j = 1,2,3, \text{ represent 3 eigenvectors of } \Gamma^{-1}B.$$

The arbitrary constants k_i are determined by applying the initial condition $a_i(0) = 1.0$, i=1,2,3. Various numerical schemes (36,37) are available for determining the eigenvalues and eigenvectors. The major difficulty encountered with this method is the determination of all the eigenvalues of a large matrix with sufficient accuracy.

Numerical method

Many numerical integration schemes are available for solving differential equations. (38,39) A Runge-Kutta technique and its various modifications are commonly employed to solve problems like Equation 12. However, in many situations in which the differential equations are describing the dynamics of a nuclear reactor, numerical schemes have proven unsatisfactory. (40) The problem is that the time increments required for stability of the numerical method are so short

that exceeding long machine running times are required.

In this thesis the subroutine NODE will be used as the numerical scheme that is used to solve the set of differential equations given by Equation 12. The version of NODE written in FORTRAN language as applied to the IBM 360 machine is used. (41) The numerical technique utilized in this program is basically that of Runge-Kutta.

Analog method

A system of differential equations can also be solved on an analog computing machine. One advantage of the analog method becomes apparent when time scaling is applied. A typical equation from Equation 6 is

$$\lambda_{11}\mathring{a}_1(t) + \lambda_{12}\mathring{a}_2 + \lambda_{13}\mathring{a}_3 = b_{11}a_1 + b_{12}a_2 + b_{13}a_3$$

where $\lambda_{ij} << b_{ij}$. When time scaling is applied,

$$\frac{d}{dt} = \alpha \frac{d}{d\tau} ,$$

where τ is machine time and $\alpha < 1$, it can be seen that λ_{ij} and b_{ij} tend to become more comparable in size. This eliminates some of the problems that would be present in numerical techniques, when $\lambda_{ij} << b_{ij}$. The major difficulty associated with an analog computing machine, when applied to problems like Equation 12, is the large equipment requirements.

Exponential method

Consider the set of homogeneous linear differential equations

$$D\bar{a} = B\bar{a} \; ; \; D = \frac{d}{dt} \qquad (13)$$

where $\bar{a}$ is a column vector of n unknowns, and B is a square matrix of coefficients whose magnitudes may, in general, be functions of time. If $\bar{a}_o$ denotes the vector whose elements are the initial values of the variables, then the system given in Equation 13 may be written as an integral equation of the form

$\bar{a} = \bar{a}_o + Q(B)\cdot\bar{a}$ where $Q = \int_o^t (\;)dt'$ is an integral operator. The Peano-Baker method (42) of solving this integral equation is to use the iteration method

$$\bar{a} = [I + Q(B) + Q(B)\cdot Q(B) + Q(B)\cdot Q(B)\cdot Q(B) + \ldots]\bar{a}_o \qquad (14)$$

where I is the n^{th} order unit matrix. If the elements of the matrix B are analytic throughout the range in t, it can be shown that the series in Equation 14 converges absolutely and uniformly. (43) The matrix

$$H(B) = (I + Q(u) + Q(u)Q(u) + \ldots) \qquad (15)$$

has been named the matrizant of B by Baker. (44) The solution to Equation 13 is now written in the form

$$\bar{a} = H(B)\cdot\bar{a}_o$$

If the set of differential equations has constant coefficients, the elements of the matrix B are constants. In this case the series in Equation 15 reduces to

$$M(B) = I + \frac{B \cdot t}{1!} + \frac{B^2}{2!} t^2 + \frac{B^3}{3!} t^3 + \ldots \equiv e^{Bt} \qquad (16)$$

and the solution to Equation 13 is then written as

$$\bar{a} = e^{Bt} \cdot \bar{a}_o \qquad (17)$$

The function e^{Bt} may be interpreted by Sylvester's theorem (45), but this involves use of eigenvalues of B, which are sometimes difficult to obtain. However, the series in Equation 16 does converge analytically and represents the desired solution. It has been found that convergence of a series analytically does not always imply convergence of the series on a numerical computing machine. That is, the time coefficients for the space modes are represented by differential equations of the form

$$\Gamma \dot{\bar{a}} = B\bar{a} \quad \text{or} \quad \dot{\bar{a}} = \Gamma^{-1}B\bar{a} \qquad (18)$$

where the elements of the matrix $\Gamma^{-1}B$ are constants, but the series representation for $e^{\Gamma^{-1}Bt}$ does not always converge rapidly on a digital machine. However, convergence may be obtained by a slight change in the technique. For a specific time t_o the problem reduces to

$\bar{a}(t_o) = e^{[\Gamma^{-1}B] \cdot t_o} \cdot \bar{a}_o \equiv e^u \cdot \bar{a}_o$ Now in series form

$$e^u = \sum_{m=1}^{\infty} \frac{u^m}{m!} \quad .$$

The technique is to evaluate a new matrix, $e^{u/2^n}$, where n is

chosen so that the matrix $u/_{2^n}$ has the sum of the squares of all its elements less than unity. The series

$$e^{u/_{2^n}} = \sum_{m=1}^{\infty} \frac{[u/_{2^n}]^m}{m!}$$

will inevitably converge to some matrix, call it W. The solution to Equation is then obtained as

$$\bar{a} = [W]^{2^n} \cdot \bar{a}_o \ .$$

It will be shown that this method yields solutions for Equation 18 where the other methods mentioned above either fail or become unwieldy.

With techniques available for obtaining both the space modes and their corresponding time coefficients, it is now possible to investigate the kinetic response of the reactor shown in Figure 1. The time dependent flux is expressed as

$$\phi(x,t) = \sum_{i=1}^{3} a_i(t)\psi_i(x) \ , \qquad (19)$$

where the modes $\psi_i(x)$ are shown in Figure 4. In one analysis the absorption cross section in the region $27 \leq x \leq 47$ was reduced to zero in a step wise manner. The time coefficients are solutions of the equations

$$\begin{bmatrix} 22.24 & -5.38 & 4.54 \\ -5.38 & 4.42 & -6.12 \\ 4.54 & -6.12 & 22.24 \end{bmatrix} \begin{bmatrix} \dot{a}_1 \\ \dot{a}_2 \\ \dot{a}_3 \end{bmatrix} = \begin{bmatrix} 9832 & -5592 & 7360 \\ -5592 & -1079 & -5780 \\ 7360 & -5780 & 9832 \end{bmatrix} \begin{bmatrix} a_1 \\ a_2 \\ a_3 \end{bmatrix}$$

These equations were solved successfully by use of all four techniques described previously, and the solutions were iden-

tical in all cases. The solutions are demonstrated in Figure 3. The eigenvalue method leads to an analytical expression for the time coefficients; thus, if this technique is applied, the expression for the time dependent flux, Equation 7, becomes

$$\phi(x,t) = \sum_{i=1}^{N} \psi_i(x) \sum_{\mu=1}^{N} b_\mu \alpha_{\mu i} e^{\omega_\mu t} \qquad (20)$$

where

$$\sum_{\mu=1}^{N} b_\mu \alpha_{\mu i} e^{\omega_\mu t}$$

represents the expression for $A_i(t)$. Table 2 lists the constants of Equation 20 as they were determined for the case $\Sigma_a=0$ in region $27 \leq x \leq 47$.

Table 2. Eigenvalue expansion coefficients: $\Sigma_{a2}=0$

μ	$\alpha_{\mu 1}$	$\alpha_{\mu 2}$	$\alpha_{\mu 3}$	b_μ	ω_μ
1	6.29×10^{-1}	-4.84×10^{-1}	6.08×10^{-1}	1.03×10^{0}	6.82×10^{2}
2	-7.19×10^{-1}	-1.05×10^{-3}	6.94×10^{-1}	2.13×10^{-2}	1.52×10^{2}
3	2.30×10^{-1}	9.47×10^{-1}	2.24×10^{-1}	1.58×10^{0}	-2.48×10^{3}

Application of Equation 20 and the constants listed in Table 2 leads to the time dependent flux distributions shown in Figure 6. It is interesting to note that an asymptotic flux shape is attained at some time t_o, and after time t_o the flux rises exponentially, with this asymptotic shape, on a period

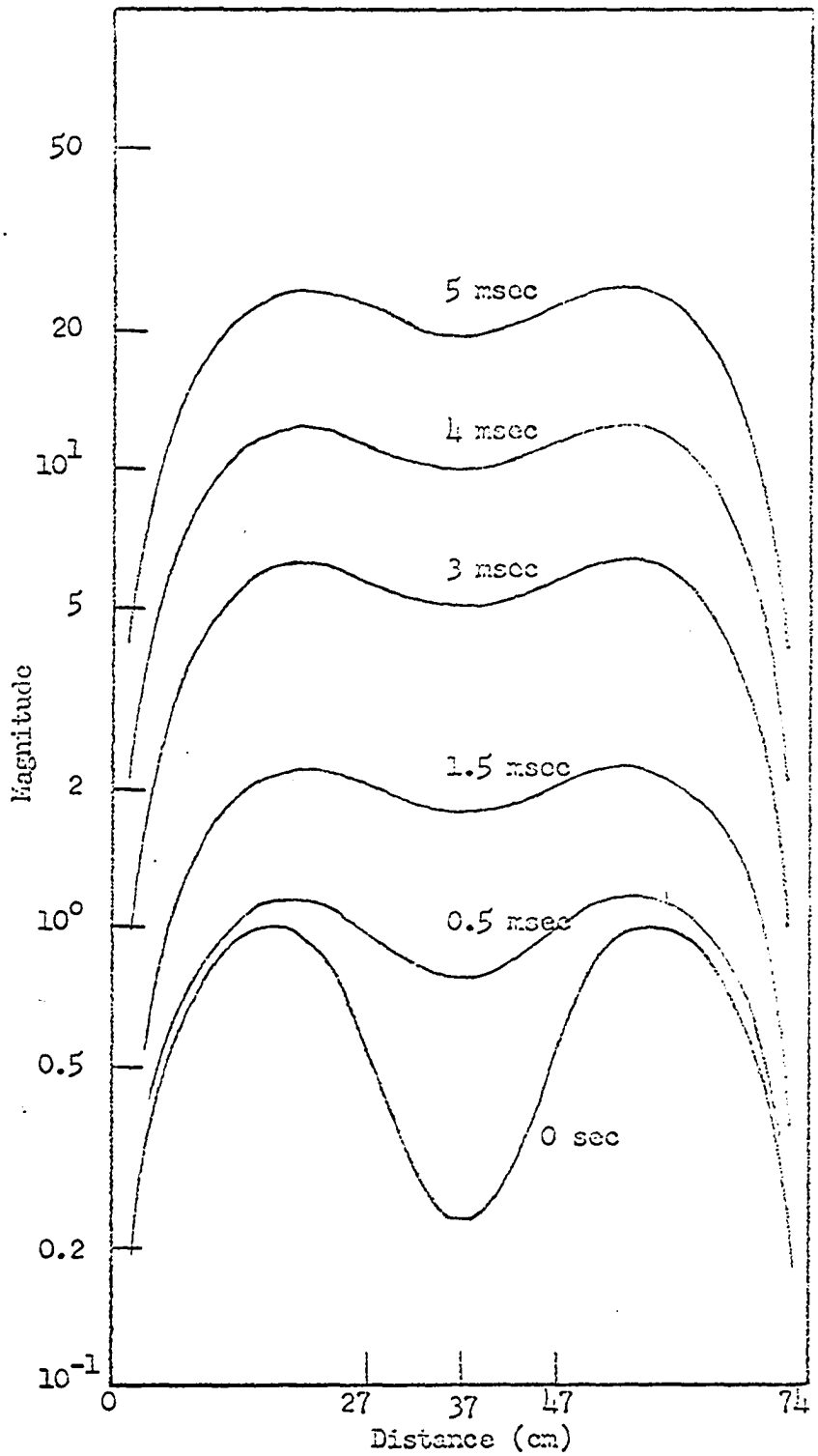

Fig.6 . Time dependent flux for $\Sigma_a = 0$ in region 2

determined by the predominant positive eigenvalue found in solutions for $A_i(t)$.

In a second analysis the absorption cross section in the region $27 \leq x \leq 47$ was reduced stepwise to $\Sigma_a = 0.013$ cm^{-1}. In this case the constants needed for Equation 20 are as listed in Table 3.

Table 3. Eigenvalue expansion coefficients: $\Sigma_{a2}=0.013$ cm^{-1}

μ	$\alpha_{\mu 1}$	$\alpha_{\mu 2}$	$\alpha_{\mu 3}$	b_μ	ω_μ
1	6.45×10^{-1}	4.32×10^{-1}	6.30×10^{-1}	1.46×10^{0}	1.49×10^{2}
2	-7.21×10^{-1}	-9.02×10^{-4}	6.93×10^{-1}	1.71×10^{-2}	-3.18×10^{1}
3	1.87×10^{-1}	9.65×10^{-1}	1.83×10^{-1}	3.83×10^{-1}	-4.50×10^{3}

The time dependent flux distributions are shown in Figure 7, and again it is noted that an asymptotic flux shape is achieved.

As noted previously the space modes shown in Figure 4 were obtained by choosing $\Sigma_{a2}'/\Sigma_{a2}'' = 4\times10^{-5}$, and it was predicted that this choice would not affect the final form for $\phi(x,t)$. When $\Sigma_{a2}'/\Sigma_{a2}''$ was chosen to equal 4×10^{-1}, the space modes for the three region case were obtained as shown in Figure 5. These modes are somewhat different than the modes shown in Figure 4; but when they were substituted into Equation 12 and the corresponding time coefficients were ob-

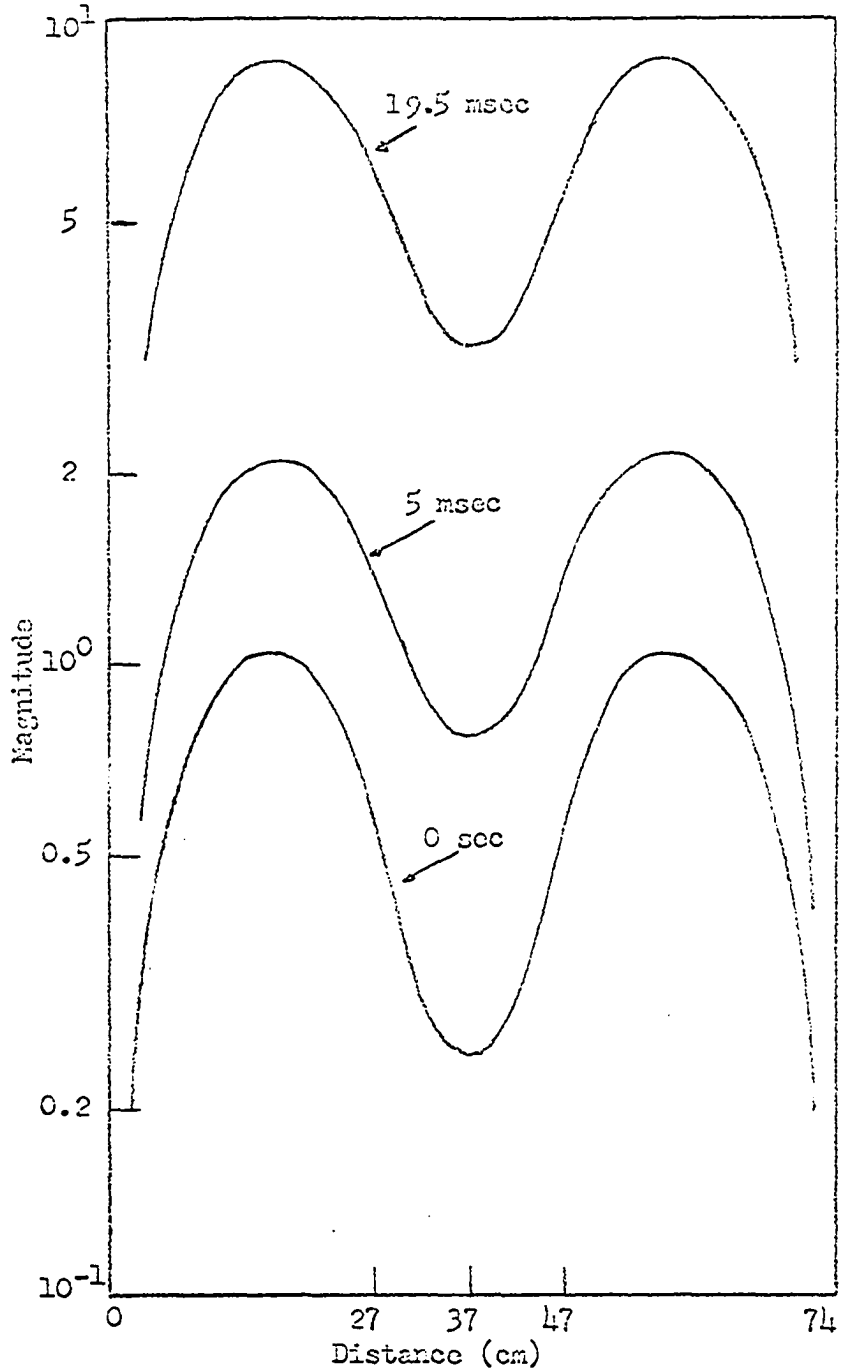

Fig. 7. Time dependent flux for $\sum_a = 0.013$ cm^{-1} in region 2

tained, the final form for $\phi(x,t)$ agreed with the distribution shown in Figures 6 and 7.

Note that when the statement is made in this paper that two results "agreed", it is meant to imply that the first two significant figures of each result were identical. In some cases even better agreement was obtained, but it is felt that two significant figures constitutes very sufficient agreement for results obtained in this paper.

The criterion for determining whether sufficient modes have been chosen in a flux synthesis technique is to compare the results of an N+1 mode expansion with those of an N mode expansion. In order to apply this criterion to the previous analyses, the region $27 \leq x \leq 47$ was divided into two equal regions, and four space modes were determined as shown in Figure 9. When Σ_{a2} was again reduced to zero in the region $27 \leq x \leq 47$, the flux distributions derived from the expression

$$\phi(x,t) = \sum_{i=1}^{4} a_i(t)\psi_i(x) \qquad (21)$$

agreed with those obtained from the previous three mode expansion, as displayed in Figure 6. The time coefficients used in Equation 21 were obtained by the eigenvalue method, and the constants used in Equation 20 for this four mode case are listed in Table 4.

However, when the absorption cross section in the region $0 \leq x \leq 27$ was reduced stepwise to $\Sigma_a = 0.004$ cm^{-1}, the results of a three mode expansion did not agree with those of a four

Table 4. Eigenvalue expansion coefficients: $\Sigma_{a2}=0$

μ	$\alpha_{\mu 1}$	$\alpha_{\mu 2}$	$\alpha_{\mu 3}$	$\alpha_{\mu 4}$	b_μ	ω_μ
1	5.60×10^{-1}	-4.36×10^{-1}	-4.28×10^{-1}	5.59×10^{-1}	1.14×10^{0}	6.82×10^{2}
2	-6.45×10^{-1}	2.93×10^{-1}	-2.88×10^{-1}	6.44×10^{-1}	2.26×10^{-4}	1.62×10^{2}
3	1.67×10^{-1}	6.94×10^{-1}	6.80×10^{-1}	1.67×10^{-1}	2.17×10^{0}	-2.48×10^{3}
4	6.23×10^{-2}	7.10×10^{-1}	-6.98×10^{-1}	-6.23×10^{-2}	-1.44×10^{-2}	-7.18×10^{3}

Table 5. Eigenvalue expansion coefficients: $\Sigma_{a1} = 0.004\ cm^{-1}$

μ	$\alpha_{\mu 1}$	$\alpha_{\mu 2}$	$\alpha_{\mu 3}$	$\alpha_{\mu 4}$	b_μ	ω_μ
1	7.12×10^{-1}	6.94×10^{-1}	1.05×10^{-1}	2.25×10^{-2}	1.52×10^{0}	8.19×10^{2}
2	-5.30×10^{-2}	5.49×10^{-2}	6.36×10^{-1}	7.68×10^{-1}	1.26×10^{0}	-5.69×10^{1}
3	1.23×10^{-1}	7.39×10^{-1}	6.51×10^{-1}	1.22×10^{-1}	-6.06×10^{-2}	-5.83×10^{3}
4	5.45×10^{-2}	7.05×10^{-1}	-7.05×10^{-1}	-5.72×10^{-2}	-1.11×10^{-1}	-1.03×10^{4}

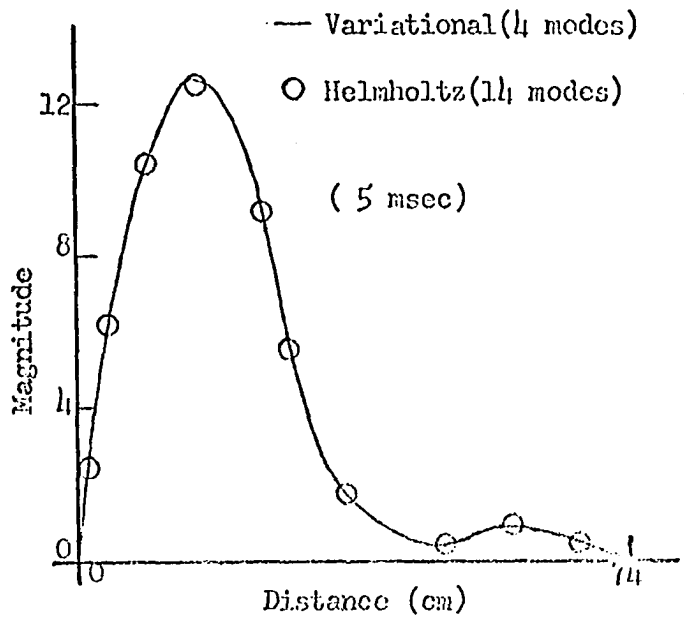

Fig. 8. Comparison of Helmholtz and variational results

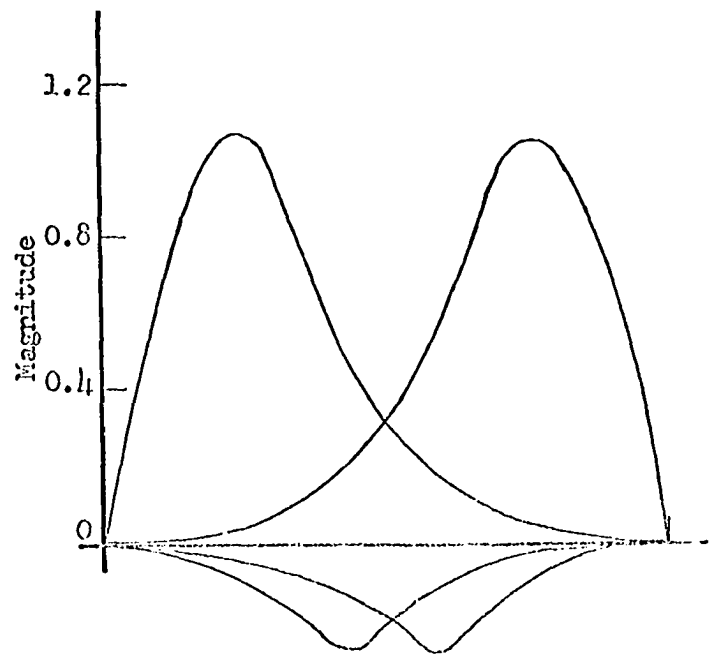

Fig. 9. Four region space modes

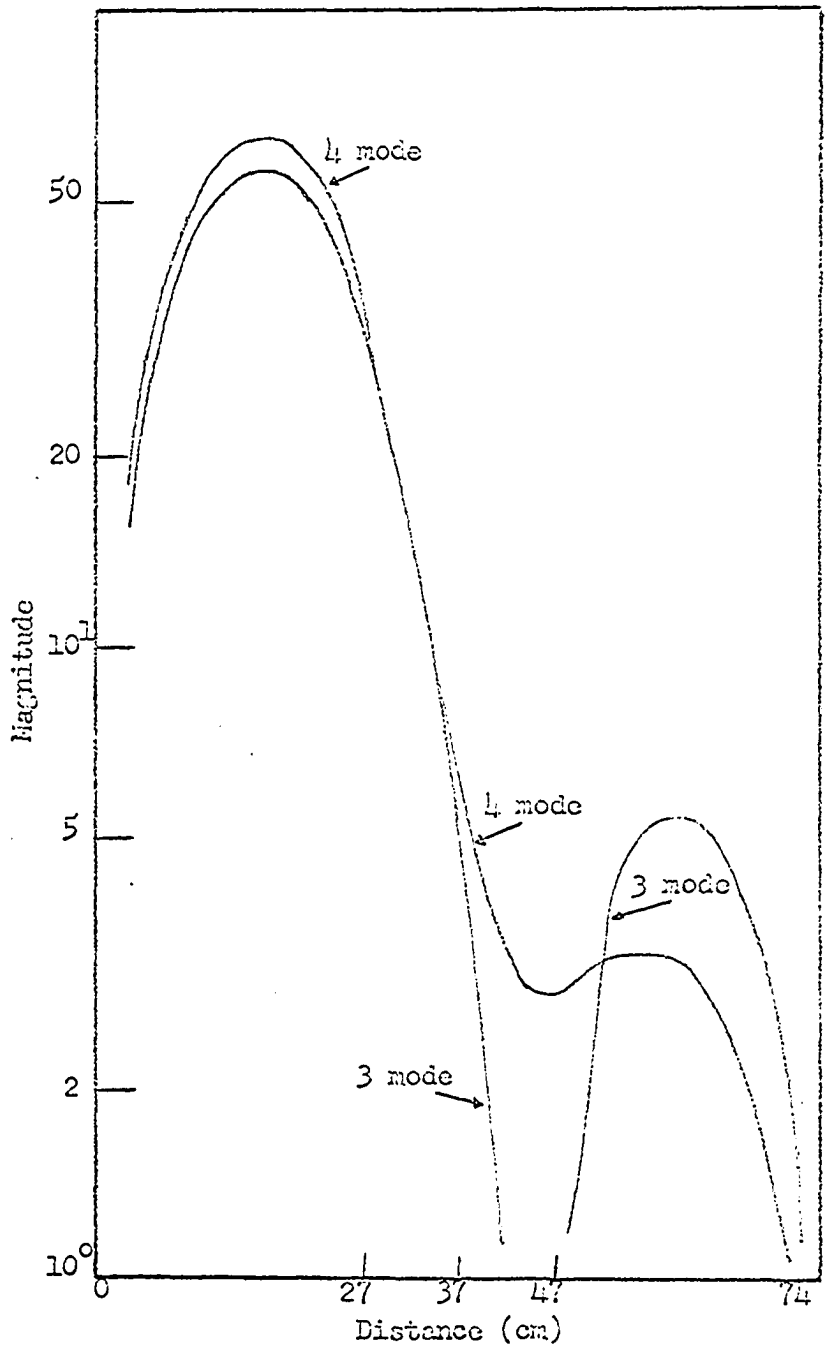

Fig. 10. Comparison of three mode and four mode results

mode expansion. A graphic comparison of this results is shown in Figure 10. This situation seems to infer that three modes are not sufficient to attain the correct form for nonsymmetric flux variations. The constants used in evaluating the time coefficients for the nonsymmetric four mode expansion are listed in Table 5, as obtained from the eigenvalue method.

Helmholtz modal analysis

Another method for solving reactor kinetic equations that has been applied previously (27) is a technique commonly called Helmholtz modal analysis. This technique consists of expressing the flux in the form

$$\phi(x,t) = \sum_{\nu=1}^{N} T\nu(t)\ W\nu(x), \qquad (22)$$

where the space functions $W\nu(x)$ are now eigenfunctions of the Helmholtz equation $\nabla^2 W\nu(x) + B\nu^2 W\nu(x) = 0$ with the associated boundary conditions $W\nu(o) = 0$ and $W\nu(c) = 0$, where $r = 0$ and $r = c$ are the reactor extrapolated boundaries.

The reactor shown in Figure 1 will now be analyzed using this method and assuming the kinetics of the reactor are described by the equation

$$D\nabla^2\phi(x,t) - \Sigma_a\phi(x,t) + \nu\Sigma_f\phi(x,t) = \frac{1}{V}\ \frac{\partial\phi(x,t)}{\partial t}\ . \qquad (23)$$

Substituting Equation 22 into Equation 23 gives the result

$$\sum_{\nu} DT\nu(t)\ \nabla^2 W\nu(x) - \sum_{\nu}\ \Sigma_a T\nu(t) W\nu(x) \qquad (24)$$

$$+ \sum_{\nu} \nu\Sigma_f T\nu(t) W\nu(x) = \frac{1}{V} \sum_{\nu} A\nu \dot{T}_{\nu}(t) W\nu(x) \ .$$

If the eigenfunctions have been normalized, the orthonormal condition

$$\int_o^c W\nu(x) W\mu(x) dx = \delta\mu\nu \qquad (25)$$

will hold. Now integrating Equation 24 over the reactor volume, applying Equation 25, and substituting

$$\nabla^2 W\nu(x) = -B\nu^2 W\nu(x),$$

the result obtained is

$$\sum_{\nu} - \int_o^c DT\nu(t) B\nu^2 W\mu(x) W\nu(x) dx$$

$$- \sum_{\nu} \int_o^c \Sigma_a A\nu T\nu(t) W\mu(x) W\nu(x) dx$$

$$+ \sum_{\nu} \int_o^c \nu\Sigma_f T\nu(t) W\mu(x) W\nu(x) dx$$

$$= \frac{1}{V} \sum_{\nu} \dot{T}\nu(t) \int_o^c W\mu(x) W\nu(x) dx \ .$$

This equation may be rewritten in the form

$$\sum_{\nu} R_{\mu\nu} T\nu(t) + \sum_{\nu} Q_{\mu\nu} T\nu(t) = \frac{1}{V} \sum_{\nu} T\nu(t) \delta\mu\nu \qquad (26)$$

where

$$R_{\mu\nu} = -DB\nu^2 \delta\mu\nu - \int_o^c \Sigma_a(x) W\mu(x) W\nu(x) dx$$

$$Q_{\mu\nu} = \int_o^c \nu\Sigma_f(x) W\mu(x) W\nu(x) dx \ .$$

Equation 26 is a system of ordinary differential equations having $T\nu(t)$ as its dependent variables. If the flux were expressed by an infinite series of the form,

$$\phi(x,t) = \sum_{\nu=1}^{\infty} T\nu(t)W\nu(x),$$

then the series would converge to the function $\phi(x,t)$ since the eigenfunctions $W\nu(x)$ constitute a complete set. (46) However, in modal analysis a finite approximation is applied where in Equation 26 becomes a finite set by letting

$$\mu = 1,2,\ldots,N$$

$$\nu = 1,2,\ldots,N.$$

Hence, the function $\phi(x,t)$ is approximated by a set of N harmonics.

The solution to a linear system of homogeneous differential equations is of the form $e^{\omega t}$, so the substitution

$$T\nu(t) = \alpha\nu e^{\omega t}$$

is made in Equation 26. The result is the equation

$$\sum_{\nu=1}^{N} [R_{\mu\nu} - \frac{\omega}{V}\delta_{\mu\nu}]\alpha\nu = -\sum_{\nu=1}^{N} Q_{\mu\nu}\,\alpha\nu \,. \qquad (27)$$

By defining $B_{ij}=(R_{ij}+Q_{ij})\cdot V$ and allowing the index μ to take on its values $1,2,\ldots,N$, the system of equations given in Equation 27 may be written in matrix form as

$$\begin{bmatrix} B_{11} & B_{12} & \cdots & B_{1N} \\ B_{21} & B_{22} & \cdots & B_{2N} \\ \vdots & & & \\ B_{N1} & \cdots & & B_{NN} \end{bmatrix} \begin{bmatrix} \alpha_1 \\ \alpha_2 \\ \vdots \\ \alpha_N \end{bmatrix} = \omega \begin{bmatrix} \alpha_1 \\ \alpha_2 \\ \vdots \\ \alpha_N \end{bmatrix}$$

or $B\bar{\alpha} = \omega\bar{\alpha}$.

Hence, the solution for the time coefficients is

$$T_\nu(t) = \sum_{k=1}^{N} A_k \alpha_{k\nu} e^{\omega_k t} \tag{28}$$

where

ω_k = N eigenvalues of matrix B,

$\alpha_{k\nu}$ = elements of the corresponding N eigenvectors of B, and

A_k = arbitrary constants involved in the eigenvectors.

The arbitrary constants A_k are determined by applying the initial condition that

$$\phi(x,o) = \sum_{\nu=1}^{N} T\nu(o) W\nu(x) \ .$$

Application of Equation 25 to Equation 28 leads to the condition

$$T\nu(o)\,\delta_{\mu\nu} = \sum_{k=1}^{N} A_k \alpha_{k\nu} = \int_o^c \phi(x,o) W\mu(x)\,dx, \quad \mu=1,2,\ldots,N.$$

Hence, the flux is now expressed as

$$\phi(x,t) = \sum_{\nu=1}^{N} W\nu(x) \sum_{k=1}^{N} A_k \alpha_{k\nu}\, e^{\omega_k t} \ . \tag{29}$$

In the case of the reactor shown in Figure 1 the eigenfunctions $W_\nu(x)$ are given by

$$W_\nu(x) = \sqrt{2}/\sqrt{74} \quad \sin \frac{\nu\pi}{74} x$$

The response of the reactor shown in Figure 1 to various reactivity perturbations was determined using Equation 29. When the absorption cross section in the entire center region was again reduced to zero stepwise, it was found that 7 modes were required for convergence of the series. Actually N was equal to 14, but no odd harmonics were needed to describe the symmetric flux distribution. The results obtained agreed with those obtained by the three mode variational expression, Equation 19.

In a second analysis the absorption cross section in the region $0 \leq x \leq 27$ was reduced to 0.004 cm^{-1}, and the resulting flux distribution was determined from Equation 29. In this case 14 modes were required for convergence of the series, and the resulting flux distributions agreed with those obtained by the four mode variational expression, Equation 21. A comparison of the variational method and Helmholtz method for this particular analysis is shown in Figure 8.

It is felt that these comparisons serve not only to verify the validity of the variational method but also establish the superior convergence rate of the variational method.

Six mode analysis

In order to perform a more detailed analysis the reactor in Figure 1 is subdivided into the six regions shown in Figure 12. Formation of these regions and application of the equation (with νM properly defined in coupling region)

$$L_{ro}\psi_i(x) = \nu M\phi_o\Delta_i(x), \quad i=1,2,\ldots,6$$

leads to solutions for the corresponding six space modes; these modes are illustrated in Figure 14. Again these six modes will sum to $\phi_o(x)$. It is anticipated that region 2, centered in the left core, might represent a control rod which could be removed in a step or ramp manner or could be oscillated. The time-dependent flux for this analysis is now expressed as

$$\phi(x,t) = \sum_{i=1}^{6} a_i(t)\psi_i(x), \qquad (30)$$

where the $\psi_i(x)$ are shown in Figure 14. Application of the calculus of variations to determine the coefficients $a_i(t)$ will result, as before, in a set of differential equations of the form $\Gamma\dot{A} = BA$, where Γ and B are now square matrices of order 6, and A is a column matrix of the 6 unknown coefficients $a_i(t)$.

Initially, the absorption cross section in the region $27 \leq x \leq 47$ was reduced to zero, and the resulting flux distribution was determined by Equation 30. In this case the time coefficients were determined by the eigenvalue method. As

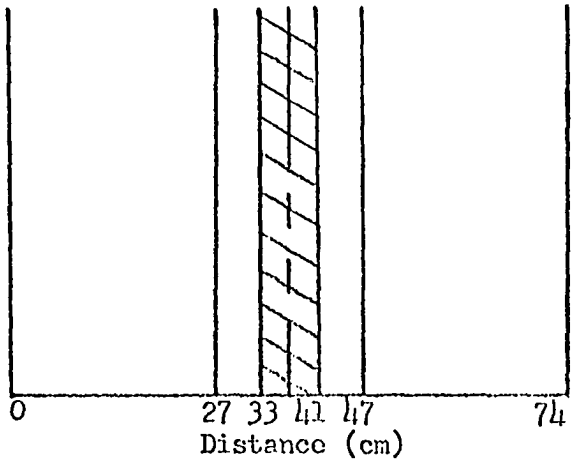

Fig. 11. Division of reactor for five mode analysis

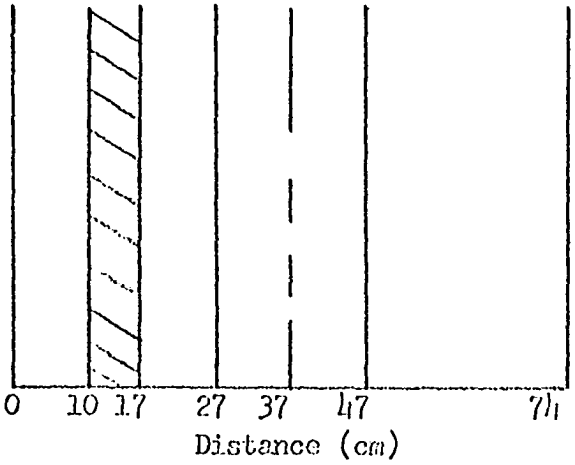

Fig. 12. Division of reactor for six mode analysis

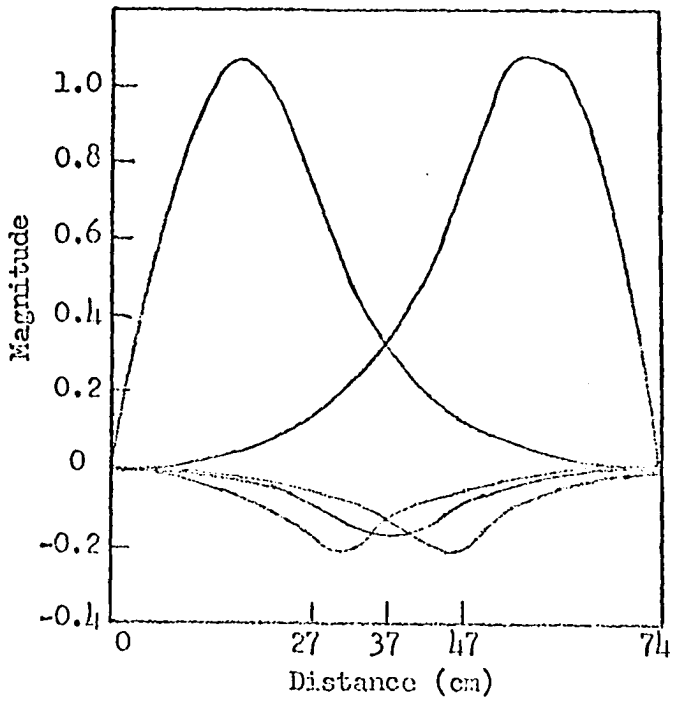

Fig. 13. Five region space modes

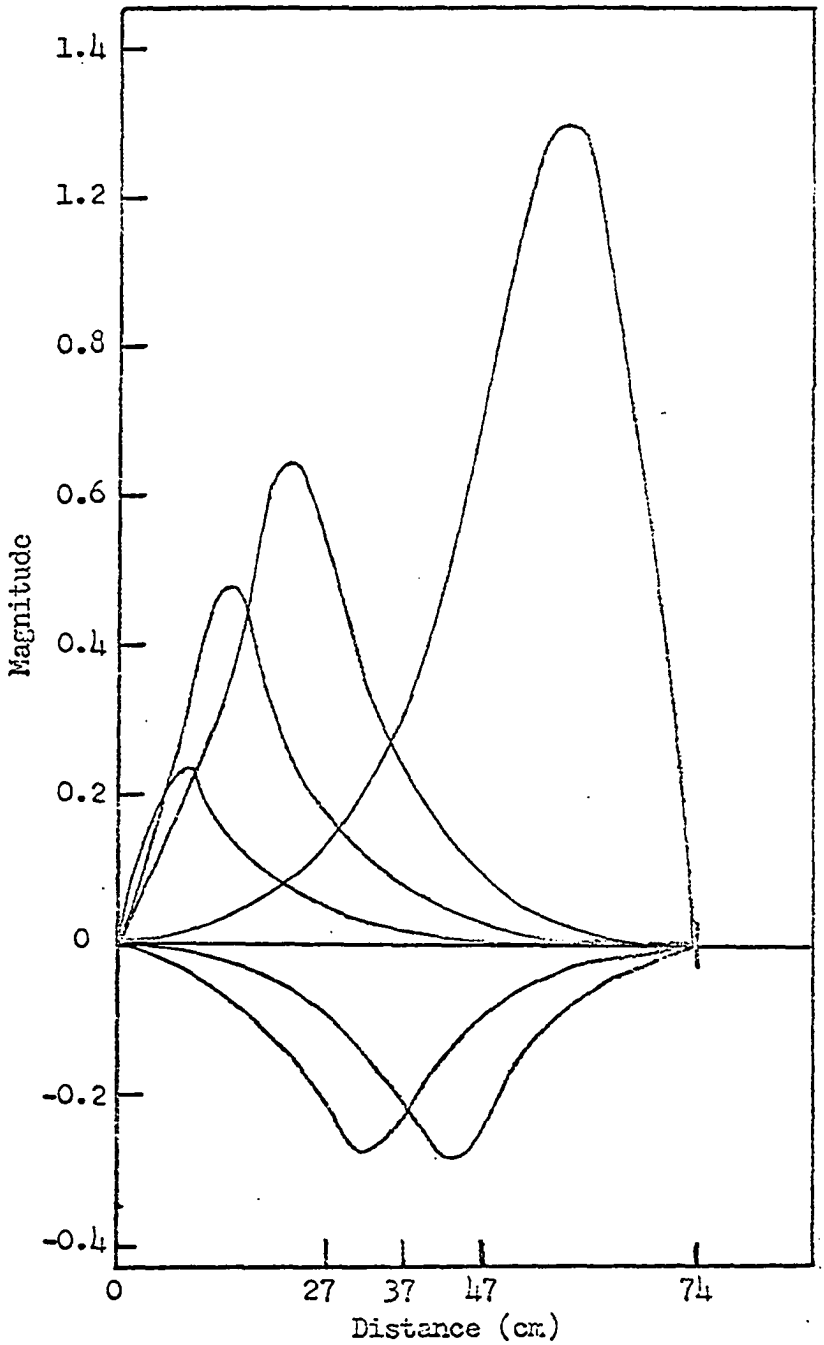

Fig. 14. Six region space modes

expected the flux distributions obtained agreed with those of the three mode analysis shown in Figure 6. The constants used in determining the $a_i(t)$ are given in Table 6.

Secondly, Σ_a in the region $0 \leq x \leq 27$ was reduced stepwise to $\Sigma_a = 0.004$ cm^{-1}, and the resulting flux distribution was determined using Equation 30. In this case the flux distributions obtained agreed with those of the corresponding four mode analysis, as shown in Figure 10. The constants used in determining the $a_i(t)$ are given in Table 7. Also a display of these time coefficients as a function of time is given in Figure 15.

The six mode expression, Equation 30, was then used to obtain the response of the reactor shown in Figure 12 to reactivity perturbations in various other regions. The eigenvalue method was used in all cases to determine the time coefficients $a_i(t)$. The eigenvalues obtained for the various investigations are listed in Table 8. Figures 16,17,18, 19, and 20 display the flux distributions obtained for the reactivity perturbations as indicated on the graphs. The time coefficients corresponding to the analysis where $\Sigma_a = 0.004$ cm^{-1} in the region $10 \leq x \leq 17$ were also determined by the exponential method. This method converged rapidly, and the resulting time coefficients were comparable with those obtained by the eigenvalue technique. A comparison of the two results is given in Figure 21. It might be noted that in the

Table 6. Eigenvalue expansion coefficients: $\Sigma_a = 0$: $27 \leq x \leq 47$

μ	$\alpha_{\mu 1}$	$\alpha_{\mu 2}$	$\alpha_{\mu 3}$	$\alpha_{\mu 4}$	$\alpha_{\mu 5}$	$\alpha_{\mu 6}$	b_μ	ω_μ
1	0.386	0.396	0.539	-0.282	-0.360	0.441	1.42	6.86×10^{2}
2	0.468	0.464	0.506	-0.201	0.214	-0.473	-0.0327	1.62×10^{2}
3	0.371	0.273	0.0137	0.611	0.624	0.158	2.07	-2.31×10^{3}
4	-0.446	-0.171	0.248	-0.297	0.784	0.0863	0.492	-5.34×10^{3}
5	-0.451	0.0808	0.222	0.732	-0.452	-0.031	0.322	-1.07×10^{4}
6	0.656	-0.544	0.304	0.398	-0.150	-0.00815	0.0976	-2.22×10^{4}

Table 7. Eigenvalue expansion coefficients: $\Sigma_a = 0.004$ cm^{-1}, $0 \leq x \leq 27$

μ	$\alpha_{\mu 1}$	$\alpha_{\mu 2}$	$\alpha_{\mu 3}$	$\alpha_{\mu 4}$	$\alpha_{\mu 5}$	$\alpha_{\mu 6}$	b_μ	ω_μ
1	0.524	0.515	0.482	0.471	0.0772	0.0155	2.16	8.20×10^{2}
2	-0.0733	-0.0683	-0.0316	0.0736	0.641	0.757	1.28	-5.66×10^{1}
3	0.810	0.327	-0.422	0.210	0.109	0.0448	-0.0914	-4.21×10^{3}
4	-0.468	-0.0339	0.284	0.164	0.813	0.101	-0.0426	-7.11×10^{3}
5	-0.478	0.194	0.121	0.687	-0.496	-0.0339	-0.0936	-1.27×10^{4}
6	0.613	-0.522	0.312	0.466	-0.194	-0.0105	-0.0441	-2.20×10^{4}

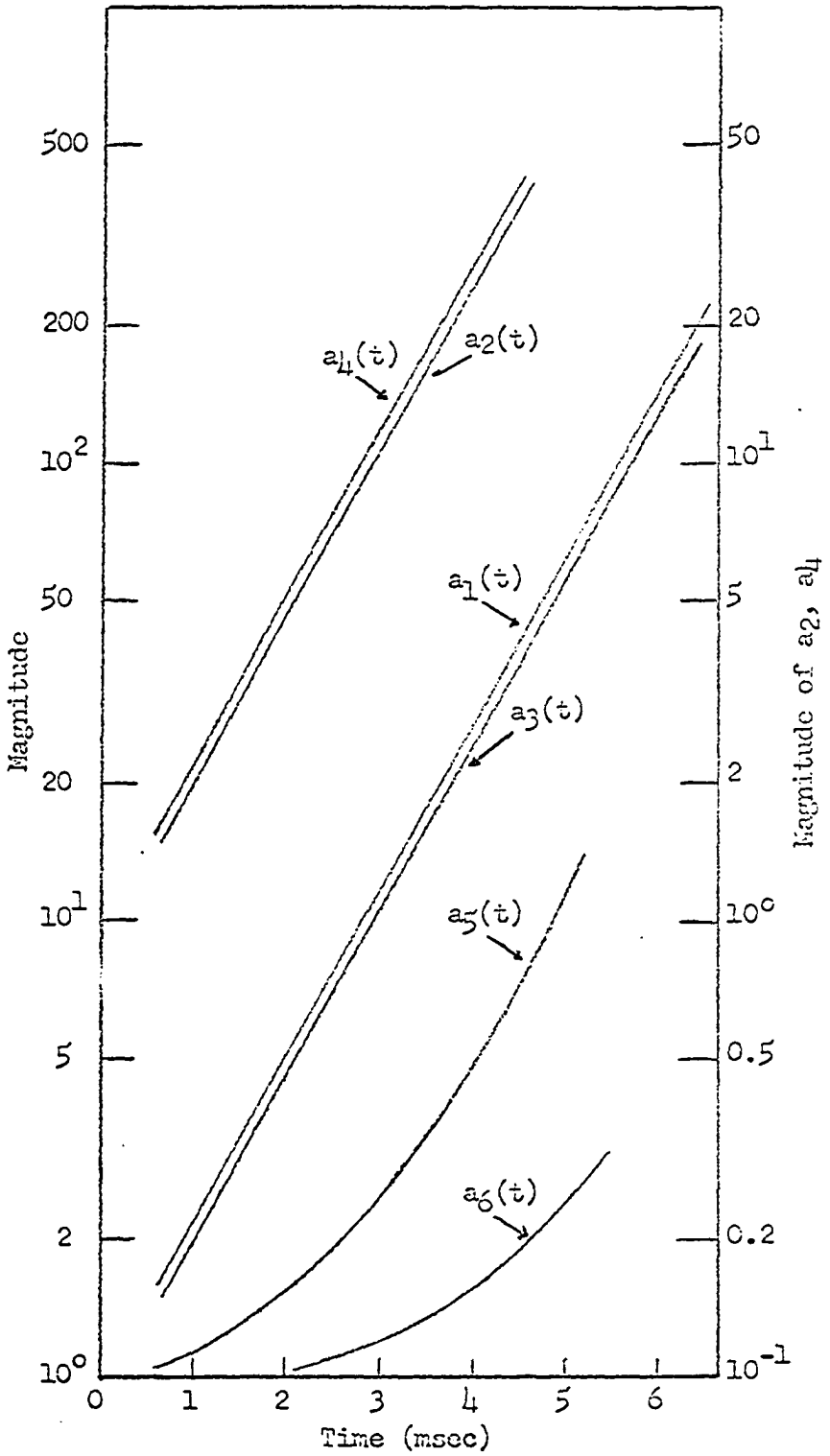

Fig. 15. Time coefficients for six mode analysis

Table 8. Eigenvalues for six mode analyses

Σ_a (cm^{-1})	region	ω_1 (10^2)	ω_2 (10^1)	ω_3 (10^3)	ω_4 (10^3)	ω_5 (10^4)	ω_6 (10^4)
0.004	$0 \leq x \leq 10$	1.10	-6.68	-4.54	-7.24	-1.29	-2.25
0.004	$10 \leq x \leq 17$	3.05	-6.00	-4.66	-7.32	-1.30	-2.24
0	$0 \leq x \leq 10$	2.74	-6.00	-4.31	-7.15	-1.27	-2.23
0	$27 \leq x \leq 37$	3.78	-6.82	-3.13	-7.00	-1.15	-2.23
0	$10 \leq x \leq 17$	6.63	-5.66	-4.56	-7.30	-1.29	-2.21

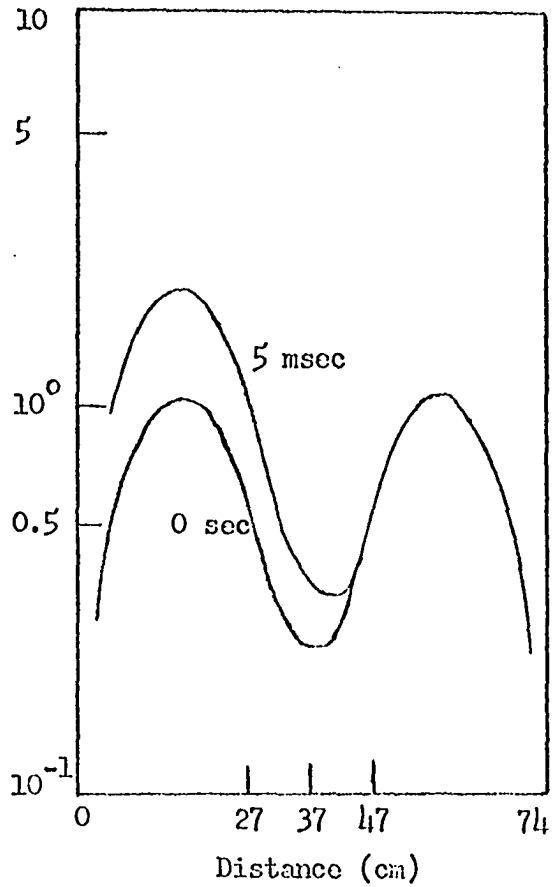

Fig. 16. Time dependent flux for $\Sigma_a = 0.004$ cm^{-1} in region 1

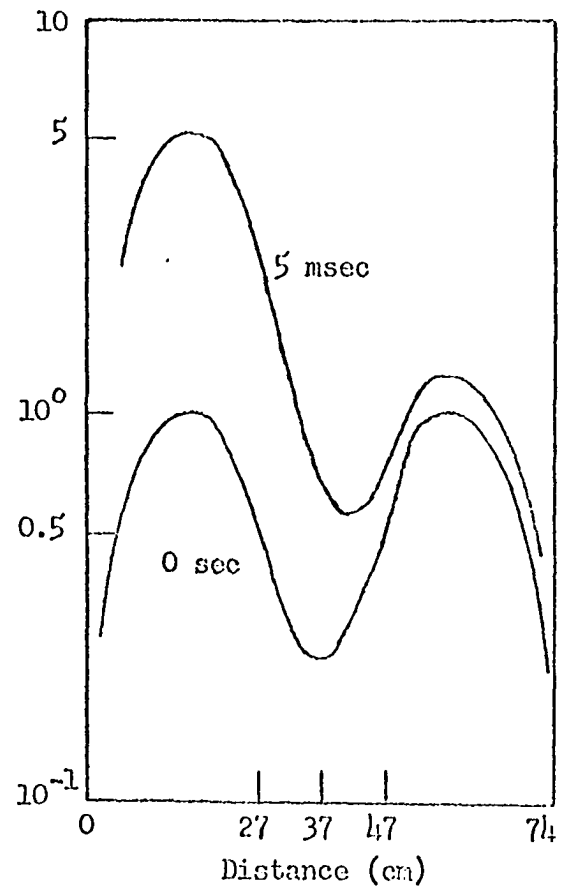

Fig. 17. Time dependent flux for $\Sigma_a = 0.004$ cm^{-1} in region 2

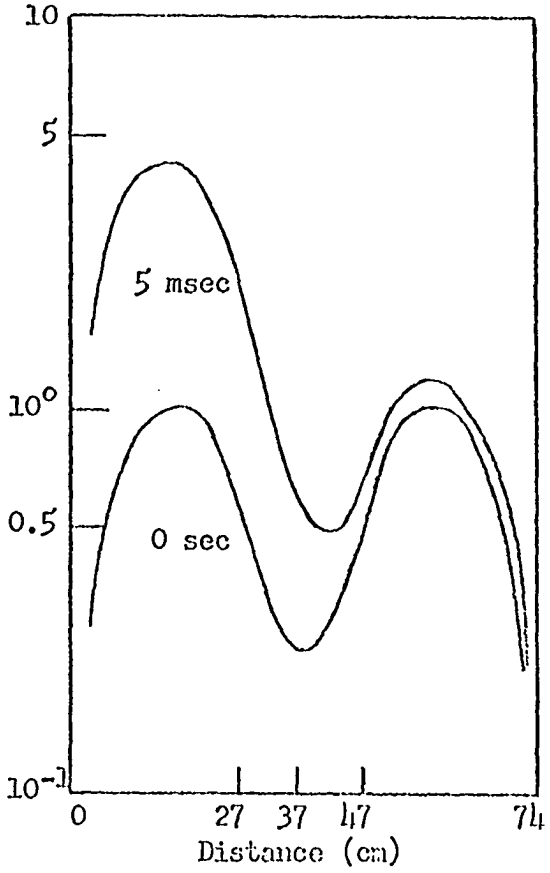

Fig. 18. Time dependent flux for $\Sigma_a = 0$ in region 1

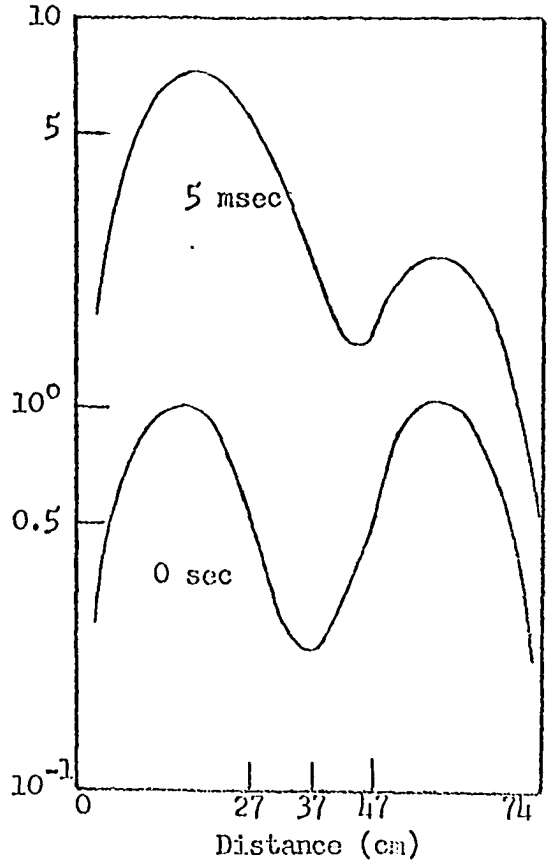

Fig. 19. Time dependent flux for $\Sigma_a = 0$ in region 4

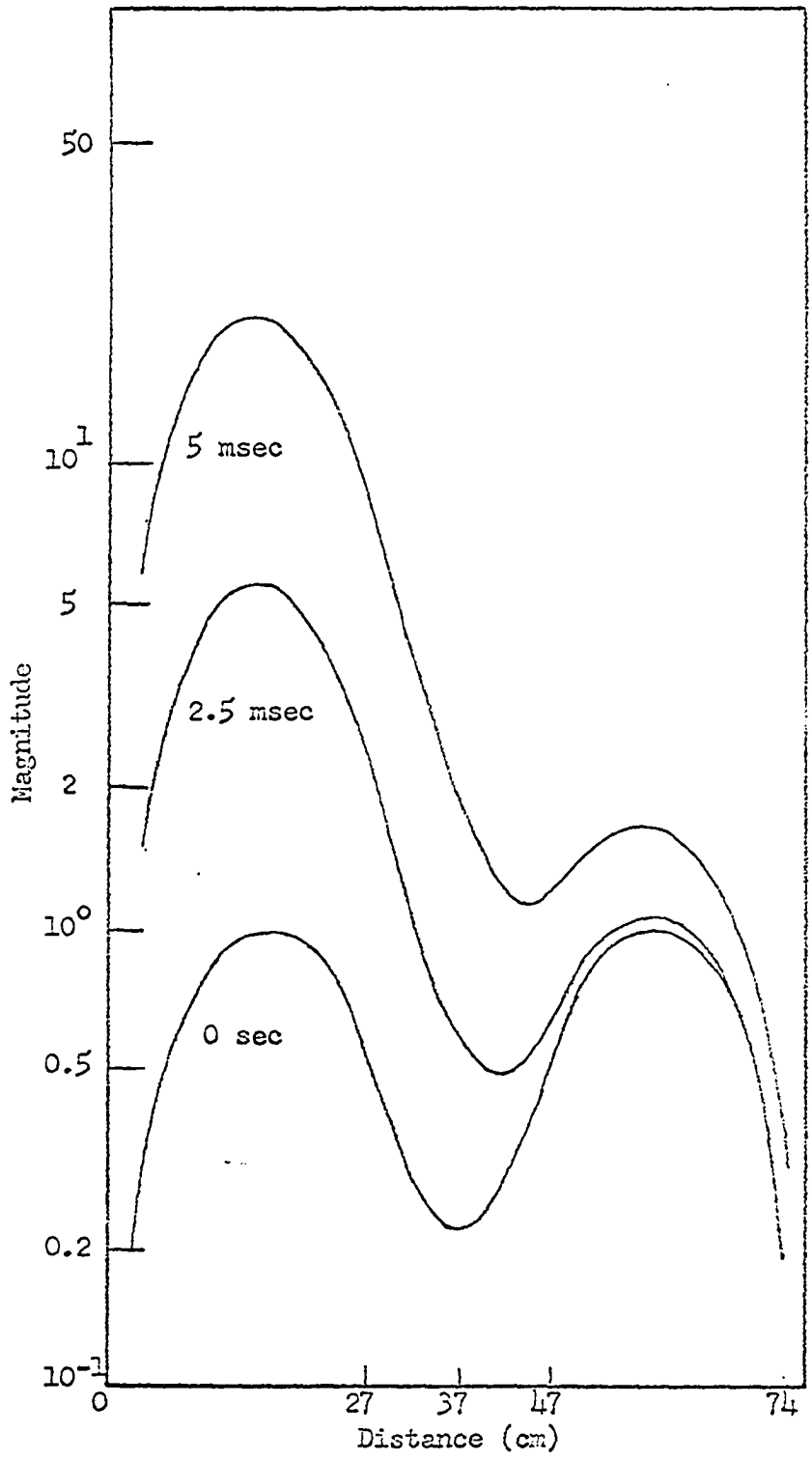

Fig. 20. Time dependent flux for $\Sigma_a = 0$ in region 2

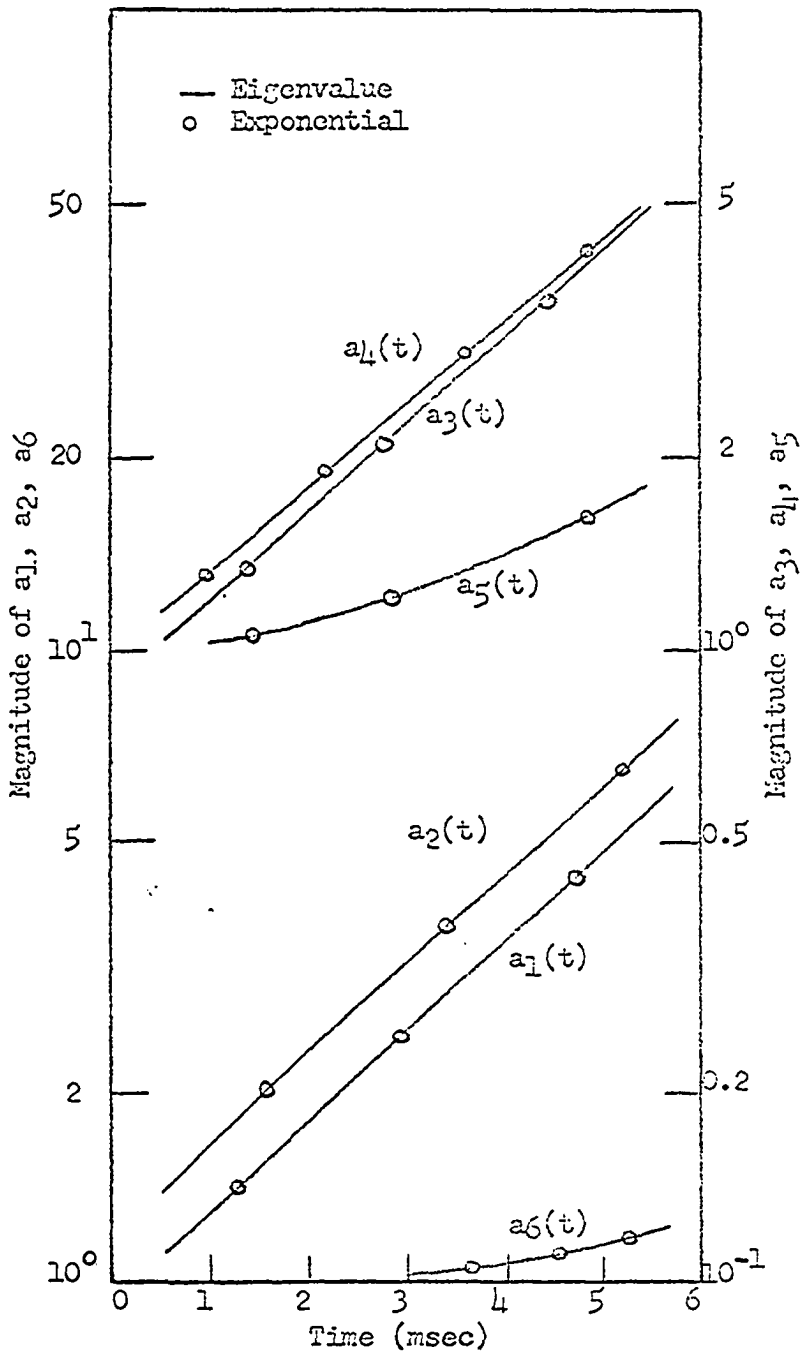

Fig. 21. Comparison of time coefficients as determined by eigenvalue and exponential methods

exponential method the maximum-value of N chosen was 8.

No further investigations were made concerning the step response of the reactor shown in Figure 1. It is felt that the results displayed in this section indicate the following conclusions:

1. Obtaining the space modes is merely a simple algebraic problem. Extension of the analysis to coupled cores is also easily accomplished.

2. Solving the differential equations obtained for the time coefficients is the only major problem in the analysis. These differential equations are describing the kinetics of a nuclear reactor, so it is not surprising that their solution might present some problems. However, as far as the one-group analysis is concerned, the equations were solved successfully by four separate techniques. The numerical method, the eigenvalue method, and the exponential method are all methods applicable to a digital computing machine, and all three methods seemed to operate with about equal ease. It is felt that the analog method would also work quite well, due especially to the time scaling effect, but sufficient equipment was not available to apply this technique to any analyses other than the simplest 3 region model.

3. The Helmholtz analysis serves to indicate both the validity and the improved convergence of the variational method.

V. ONE GROUP ANALYSIS: FREQUENCY RESPONSE

The response of the reactor shown in Figure 1 to an oscillating absorber located in some region is to be determined by applying the same basic technique that was utilized in obtaining step responses. Recall that the variational method generated differential equations for the time coefficients of the form

$$\Gamma\dot{A} = BA \tag{12}$$

where

$$\Gamma = [[\psi_i^* V^{-1} \psi_j]_{ij}];$$

$$B = [[\psi_i^* F \psi_j - (\partial_x \psi_i^*) D (\partial_x \psi_j)]_{ij}] .$$

In the one group case, $F = \nu\Sigma_f - \Sigma_a(t)$. In this analysis it will be assumed that Σ_a in some region of the reactor can be expressed in the form

$$\Sigma_a = \Sigma_{ao} + \delta\Sigma_a e^{i\omega t} \tag{31}$$

where

Σ_{ao} = critical value of Σ_a in the region of oscillation

$\delta\Sigma_a$ = small amplitude variation in Σ_a that is being oscillated in the region.

When Equation 31 is substituted into Equation 12, it can be seen that the matrix B will now be of the form

$$B = [[\psi_i^* F_o \psi_j + \psi_i^* \Delta F \psi_j - (\partial_x \psi_i^*) D (\partial_x \psi_j)]_{ij}]$$

$$\equiv B_o + \delta B$$

where

$\delta B = -\delta \sum_a e^{i\omega t} [[\psi_i^* \psi_j]']_{ij}$; the integration $[\psi_i^* \psi_j]'$ is over the region of oscillation only

and

$B_o = [[\psi_i^* F_o \psi_j] - (\partial_x \psi_i^*) D (\partial_x \psi_j)]_{ij}]$; the parameters D and F_o are the critical reactor parameters.

Thus, Equation 1 may now be written as

$$\Gamma \dot{A} = (B_o + \delta B) A \ . \qquad (32)$$

It is also noted that the matrix A may be expressed in the form

$$A = A_o + \delta A e^{i\omega t} \qquad (33)$$

where

$$A_o = \begin{bmatrix} 1 \\ 1 \\ \cdot \\ \cdot \\ \cdot \\ 1 \end{bmatrix} \quad \text{and} \quad \delta A = \begin{bmatrix} \delta a_1 \\ \delta a_2 \\ \cdot \\ \cdot \\ \cdot \\ \delta a_N \end{bmatrix}$$

Substitution of Equation 33 into Equation 32 leads to the result

$$\Gamma \cdot \frac{d}{dt} \delta A e^{i\omega t} = (B_o + \delta B)(A_o + \delta A e^{i\omega t}) \ ,$$

or

$$e^{i\omega t}\cdot i\omega\cdot\Gamma\cdot\delta A = B_o A_o + \delta B\cdot A_o + B_o\cdot\delta A e^{i\omega t} + \delta B\cdot\delta A e^{i\omega t}$$

$$= \delta B\cdot A_o + B_o\cdot\delta A e^{i\omega t} \qquad (34)$$

where second order term $\delta B\cdot\delta A$ has been neglected and where it has been noted that $B_o\cdot A_o=0$, the criticality condition.

Now Equation 34 may be written in the matrix form

$$[i\omega\Gamma - B_o]\delta A = -\delta\Sigma_a[[\psi_i^*\psi_j]'_{ij}]\cdot \begin{bmatrix} 1 \\ 1 \\ \cdot \\ \cdot \\ 1 \end{bmatrix} \qquad (35)$$

Several observations are now made concerning the previous analysis.

1. The condition $B_o\cdot A_o = 0$ provides a good check on the calculations that have been performed. That is, when the elements of the matrix B have been evaluated using critical reactor parameters, one may determine their correctness, to some extent, by observing the values of $B_o\cdot A_o$.

2. When the statement is made that $A = A_o+\delta A e^{i\omega t}$, what is really being stated is that the flux may be expressed in the form

$$\phi(x,t) = [1 + \delta a_1 e^{i\omega t}]\psi_1(x) + [1 + \delta a_2 e^{i\omega t}]\psi_2(x)+\ldots+$$
$$[1 + \delta a_N e^{i\omega t}]\psi_N(x)$$
$$= \phi_o(x) + \delta\phi(x)e^{i\omega t}.$$

That is, the flux is oscillating about $\phi_o(x)$ with the same

frequency as the oscillator but with different phase and magnitude.

3. The elements of δA are then really the coefficients for the space modes, evaluated in the frequency domain. Hence, these elements are complex numbers and may be written in the form

$$\delta a_k = \gamma_k + i\beta_k \cdot$$

Thus, Equation 35 may be written in the form

$$[i\omega\Gamma - B_o] \begin{bmatrix} \gamma_1 + i\beta_1 \\ \vdots \\ \gamma_N + i\beta_N \end{bmatrix} = -\delta\sum_a [[\psi_i^* \psi_j]'_{ij}] \begin{bmatrix} 1 \\ \vdots \\ 1 \end{bmatrix} \qquad (36)$$

Equation 36 represents a set of algebraic equations for the unknowns γ_k and β_k, k=1,2,...,N. The equations are solved by separating the 2N equations into N equations representing the real parts and N equations for the imaginary part; this results in a set of equations of the form

$$\begin{aligned} D\gamma - B_o\beta &= 0 \\ + B_o\gamma + D\beta &= -\gamma \end{aligned} \qquad \text{or} \qquad \begin{bmatrix} D & -B_o \\ B_o & D \end{bmatrix} \begin{bmatrix} \gamma \\ \beta \end{bmatrix} = \begin{bmatrix} 0 \\ -\gamma \end{bmatrix} \qquad (37)$$

where

$$\beta = [\beta_i];\ \gamma = [\gamma_i];\ D = \omega \cdot \Gamma = \omega[\Gamma_{ij}].$$

and where

$$\gamma_i = -\delta\sum_a ([\psi_i^* \psi_1]' + [\psi_i^* \psi_2]' + \ldots + [\psi_i^* \psi_N]')$$

The solution for the coefficients δA can then be determined by simple matrix manipulation as

$$\begin{bmatrix} \gamma \\ \beta \end{bmatrix} = \begin{bmatrix} D & -B_o \\ B_o & D \end{bmatrix}^{-1} \cdot \begin{bmatrix} 0 \\ -\gamma \end{bmatrix} .$$

The frequency dependent flux is expressed in the form

$$\phi(x,\omega) = (\gamma_1+i\beta_1)\psi_1(x) + (\gamma_2+i\beta_2)\psi_2(x) + \ldots$$

$$= \gamma_1\psi_1(x)+\gamma_2\psi_2(x)+\ldots+\gamma_N\psi_N(x)+i(\beta_1\psi_1(x)+\beta_2\psi_2(x)+\ldots)$$

$$\equiv W(x,\omega)+iY(x,\omega) \qquad (38)$$

where the modes $\psi_i(x)$ are same as those used in step analysis.

The frequency response of the reactor is obtained by noting that magnitude and phase of this response are given by

$$\text{Magnitude} \equiv |\phi(x,\omega)| = [W^2+Y^2]^{\frac{1}{2}}$$

$$\text{Phase} = \tan^{-1} Y/W .$$

The frequency response of the reactor shown in Figure 1 is to be determined using the technique just described and assuming that the kinetics of the reactor are described by one-group diffusion theory, excluding delayed neutrons. Initially it was assumed that an absorber of magnitude $\delta\Sigma_a = 0.001\ cm^{-1}$ was being oscillated in the region $27 \leq x \leq 47$. The magnitude and phase diagrams shown in Figures 22 and 23

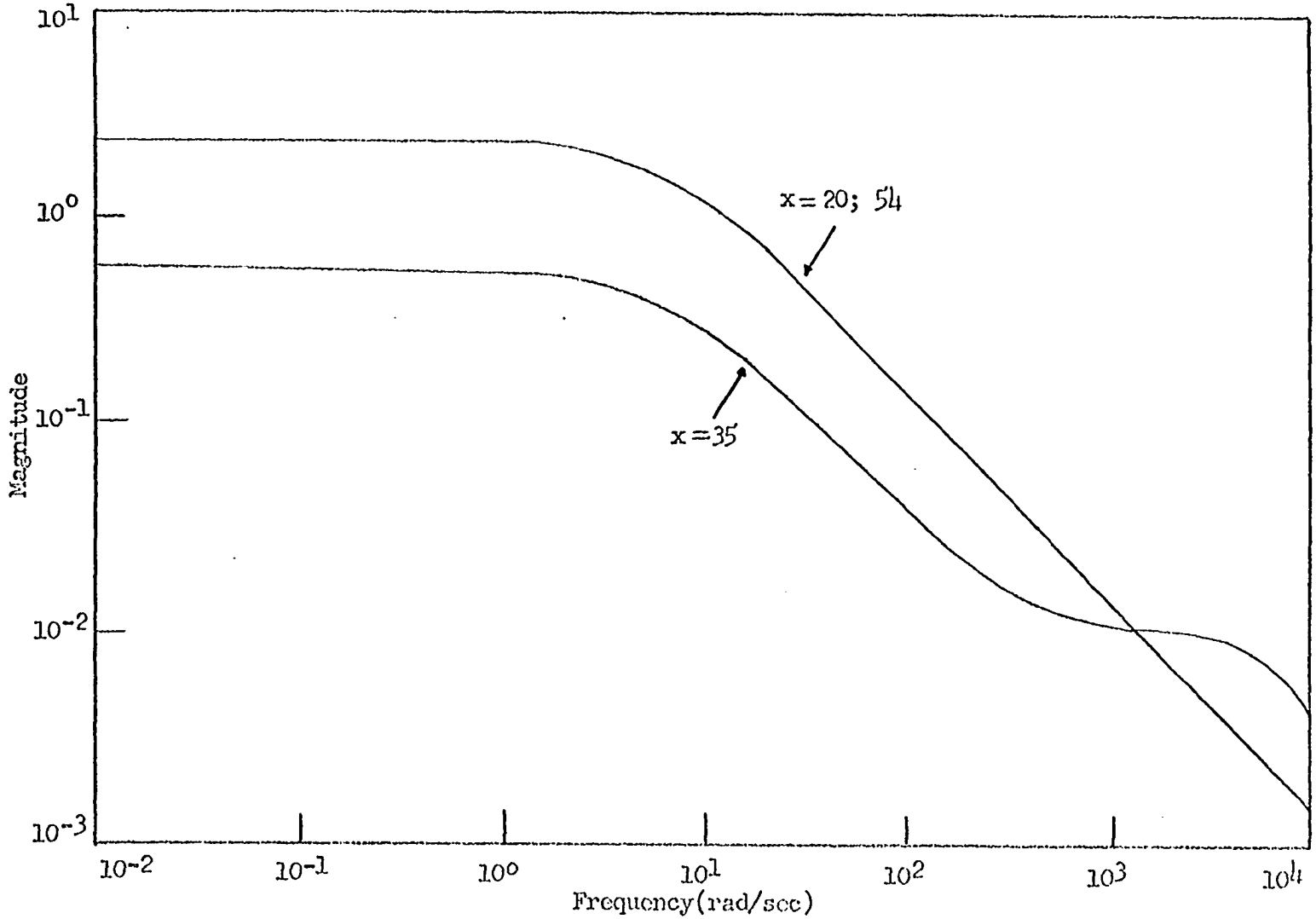

Fig. 22. Magnitude of frequency response for three mode analysis

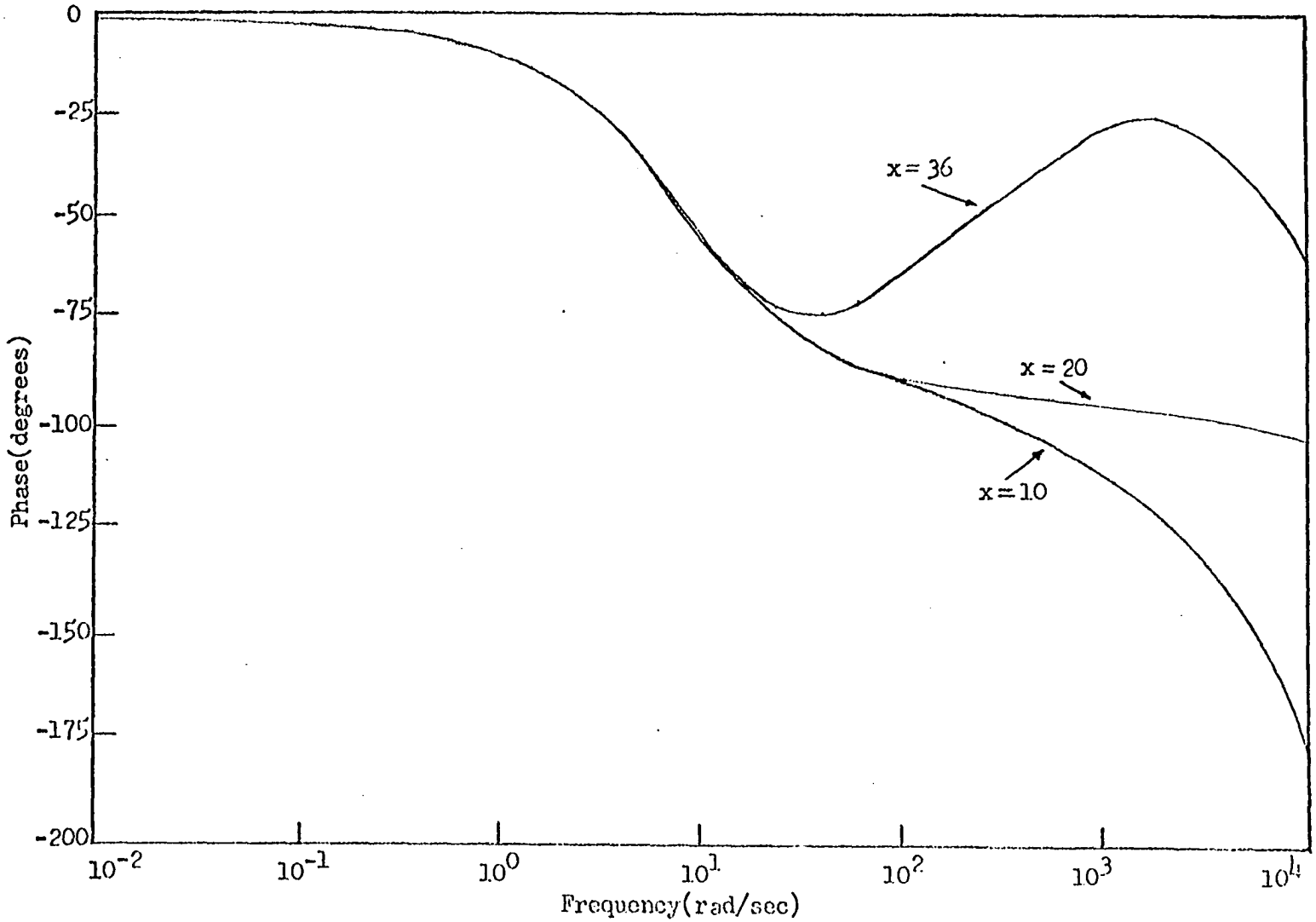

Fig. 23. Phase angle of frequency response for three mode analysis

represent the frequency response of the reactor for this situation. Note that x in the frequency response diagrams refers to distance in cm. measured from the left face of the reactor. The diagrams do indicate some spatial dependence of the frequency response, but this effect is small due to the large area being oscillated.

The reactor shown in Figure 1 was next divided into five regions, as shown in Figure 11. The 8 cm. region in the center of the reactor was assumed to have an oscillator of amplitude $\delta\Sigma_a = 0.0021\ cm^{-1}$. The five space modes used in this situation are displayed in Figure 13. Magnitude and phase diagrams representing the frequency response of the reactor shown in Figure 11 are displayed in Figures 24 and 25. It is noted that more spatial dependence of the frequency response appears in this situation.

When the reactor was divided into six regions as shown in Figure 12, six space modes were derived as shown in Figure 14. These space modes were used to obtain the frequency response of this reactor when the region $10 \leq x \leq 17$ was oscillated with an amplitude of oscillation $\delta\Sigma_a = 0.0008\ cm^{-1}$. The magnitude and phase diagrams of this frequency response are displayed in Figures 26 and 27. It is interesting to note the very pronounced spatial dependence in this situation. For example, the magnitude of the frequency response evaluated in right hand core is falling off approximately twice as

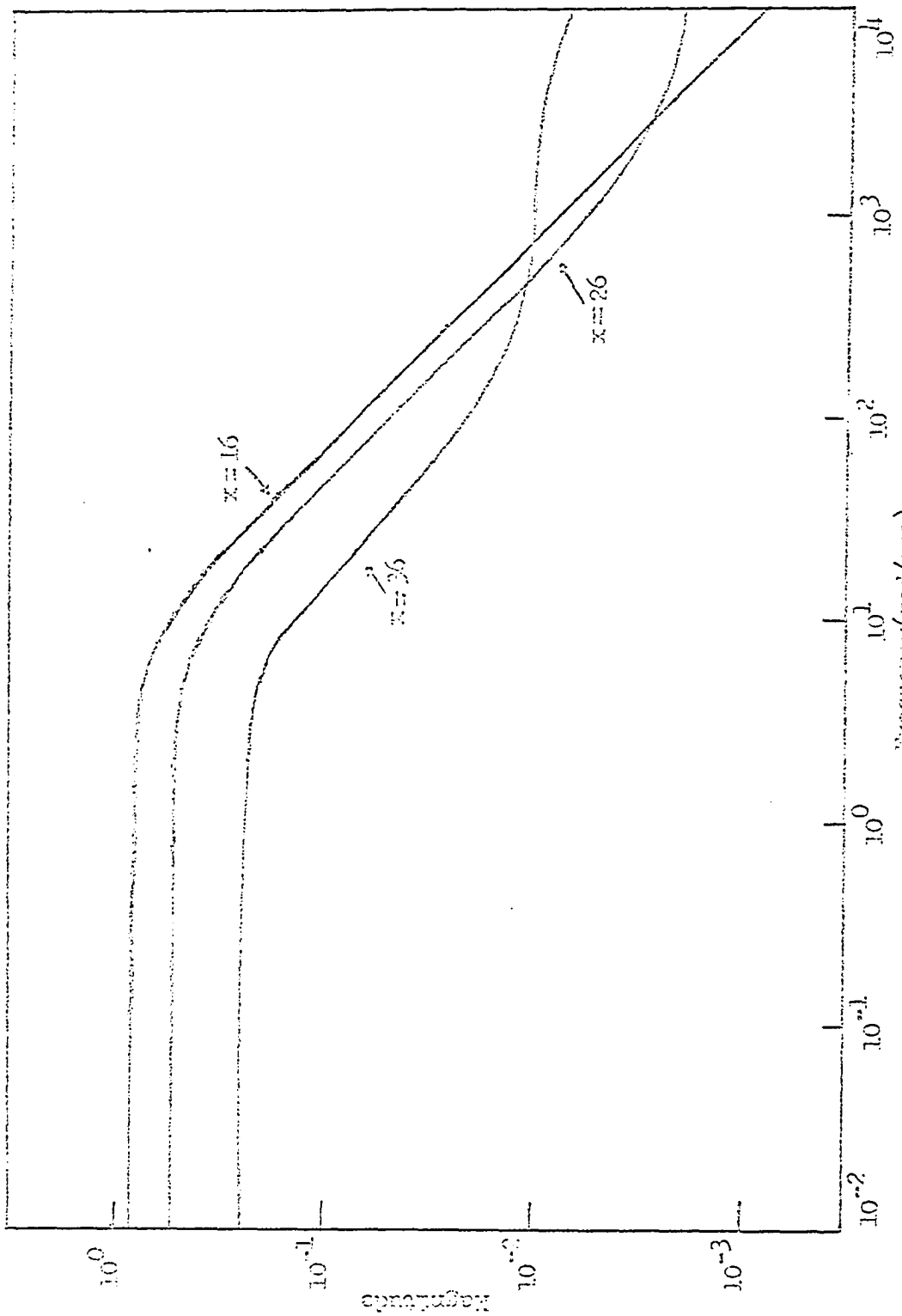

Fig. 24. Magnitude of frequency response for five mode analysis

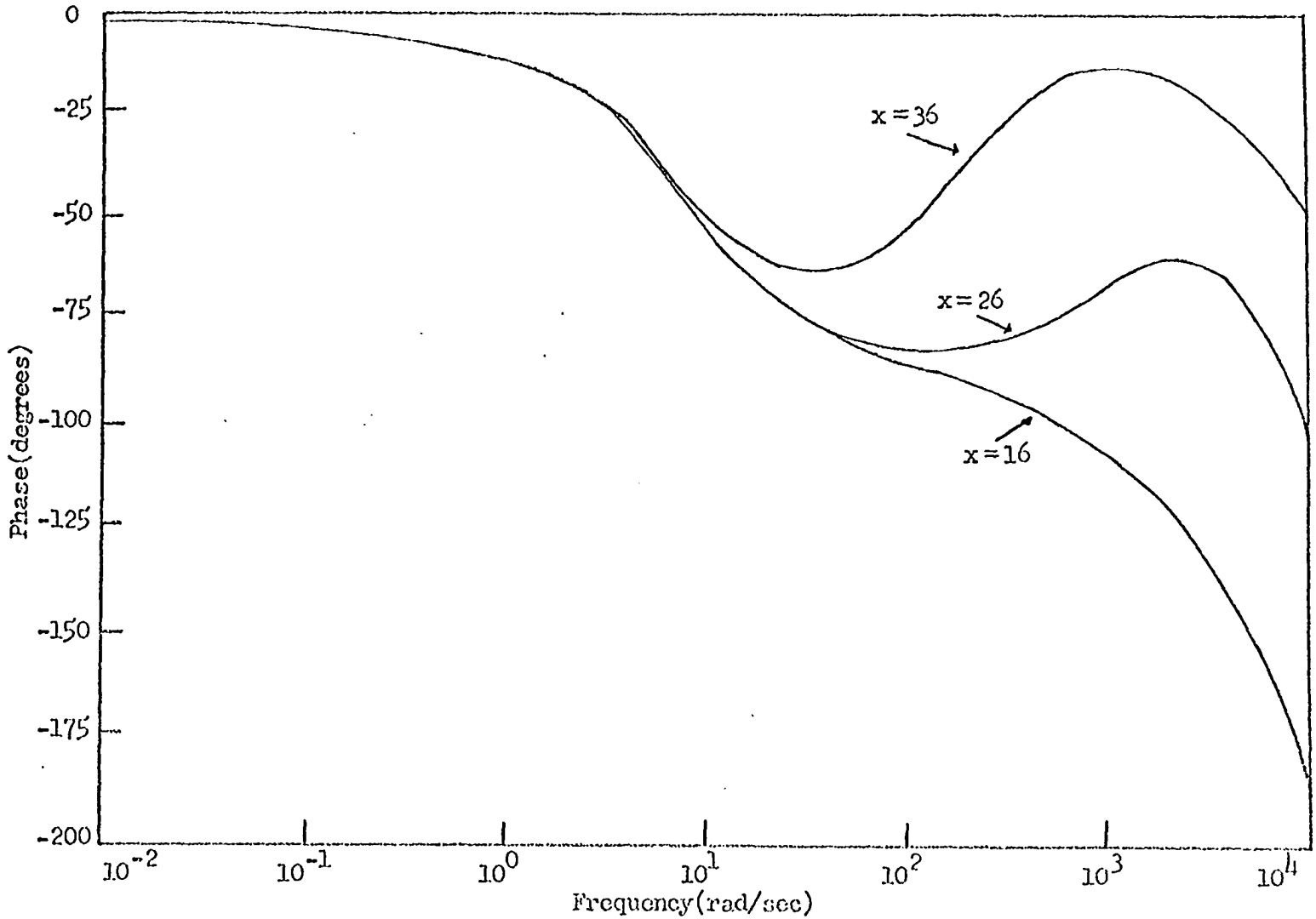

Fig. 25. Phase angle of frequency response for five mode analysis

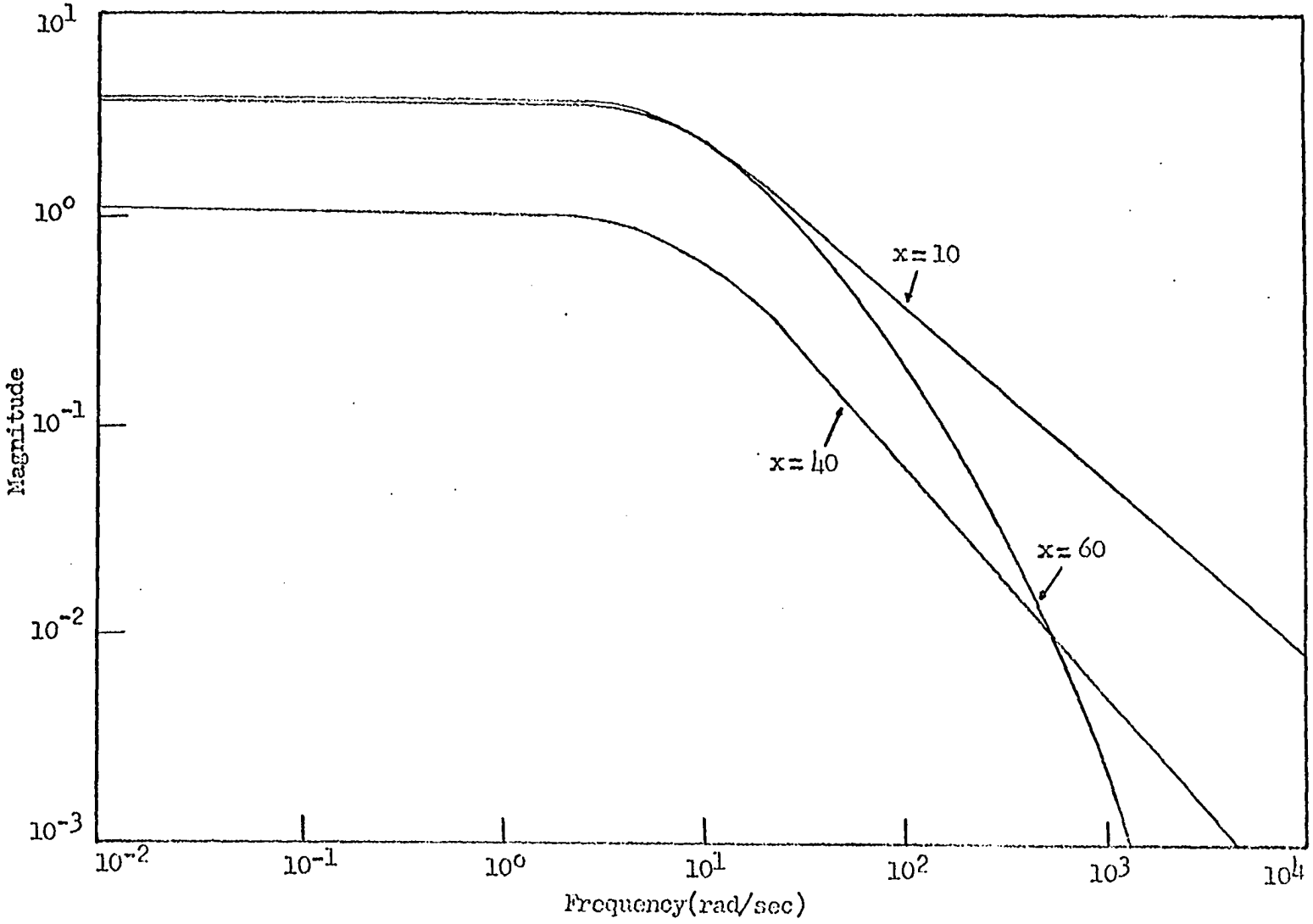

Fig. 26. Magnitude of frequency response for six mode analysis

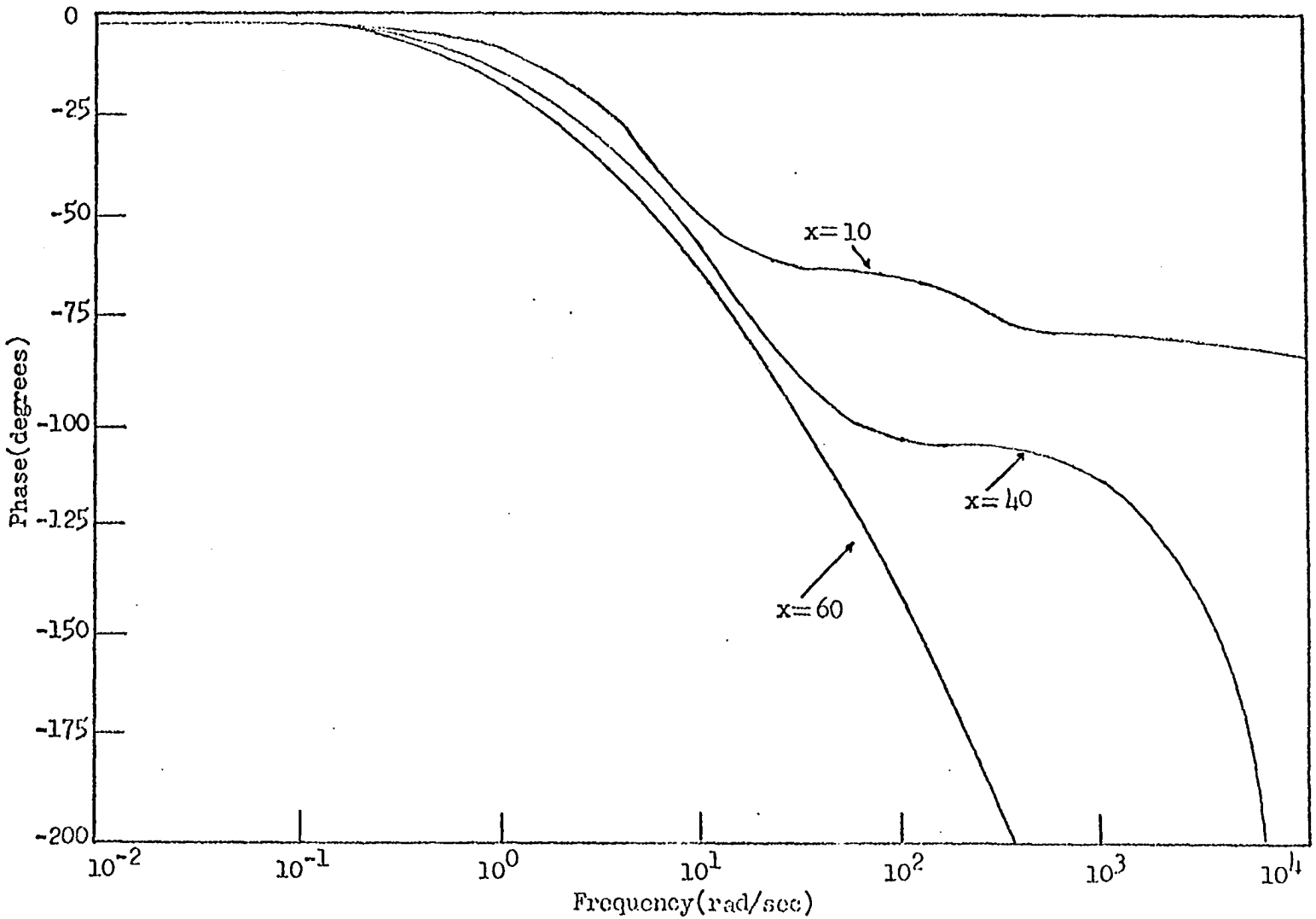

Fig. 27. Phase angle of frequency response for six mode analysis

rapidly as the magnitude in left hand core.

A six-mode analysis was also applied to obtain the frequency response of the reactor when the region $27 \leq x \leq 47$ was oscillated with an amplitude of oscillation $\delta\Sigma_a = 0.001\ cm^{-1}$. As expected, this six-mode analysis of the frequency response agreed with that obtained previously by the three mode analysis as displayed in Figures 22 and 23

It should be noted that since the equations describing the frequency response of the reactor have been linearized, the value of $\delta\Sigma_a$ chosen only affects the magnitude of the frequency response, and this is merely a relative effect. That is, changing the value of $\delta\Sigma_a$ will only shift the magnitude diagram of the frequency response along the ordinate.

VI. REFERENCE REACTOR FOR TWO-GROUP ANALYSIS

Two-group diffusion theory, including one group of delayed neutrons, will be used to describe the kinetic behavior of the reference reactor shown in Figure 28. This analytical model is again a coupled core reactor consisting of two semi-infinite multiplying regions joined by a non-multiplying coupling region. The critical reactor parameters are given in Table 9.

Table 9. Reference reactor critical parameters

Region	Σ_a (cm^{-1})	$\nu\Sigma_f$ (cm^{-1})	D (cm)	Σ_R (cm^{-1})
$0 \leq x \leq 50$	0.00818	0.0161	1.0	0.00340
$50 \leq x \leq 70$	0.01622	0	1.0	0.00340
$70 \leq x \leq 120$	0.00818	0.0161	1.0	0.00340

The kinetic response of this reactor is to be described by the two-group diffusion equations

$$D\nabla^2\phi_{Fi} - \Sigma_{Ri}\phi_{Fi} + \nu\Sigma_{fi}(1-\beta)\phi_{Si} + \lambda C_i = \frac{1}{V_F}\frac{\partial}{\partial t}\phi_{Fi}$$

$$D\nabla^2\phi_{Si} - \Sigma_{ai}\phi_{Si} + \Sigma_{Ri}\phi_{Fi} = \frac{1}{V_S}\frac{\partial}{\partial t}\phi_{Si}$$

$$\beta\nu\Sigma_{fi}\phi_{Si} - \lambda C_i = \frac{\partial}{\partial t} C_i$$

where

$V_S = 2.2\times10^5$ cm/sec; $V_F = 4.36\times10^8$ cm/sec.

and

subscripts denote values for i^{th} region

λ = decay constant for delayed neutrons = 0.08 sec^{-1}

β = delayed neutron fraction = 0.007

C = precursor concentration

ϕ_F = fast neutron flux

ϕ_S = slow neutron flux.

In the steady state situation the kinetic equations reduce to the form

$$D\nabla^2\phi_F - \Sigma_R\phi_F + \nu\Sigma_f\phi_S = 0$$

$$D\nabla^2\phi_S - \Sigma_a\phi_S + \Sigma_R\phi_F = 0 \qquad (39)$$

$$C = \frac{\beta\nu\Sigma_f}{\lambda}\phi_S$$

The steady state equations are solved in the manner suggested in Glasstone and Edlund (47), wherein solutions are assumed of the form

$$\nabla^2\phi_F + B^2\phi_F = 0$$

$$\nabla^2\phi_S + B^2\phi_S = 0.$$

In this manner the two-group critical flux distributions are found to be

$$\left.\begin{aligned}\phi_F &= H \sin \mu x + B \cos \mu x + Ce^{\nu x} + Ee^{-\nu x} \\ \phi_S &= S_1 A \sin \mu x + S_1 B \cos \mu x + S_2 Ce^{\nu x} + S_2 Ee^{-\nu x}\end{aligned}\right] 0 \leq x \leq 50$$

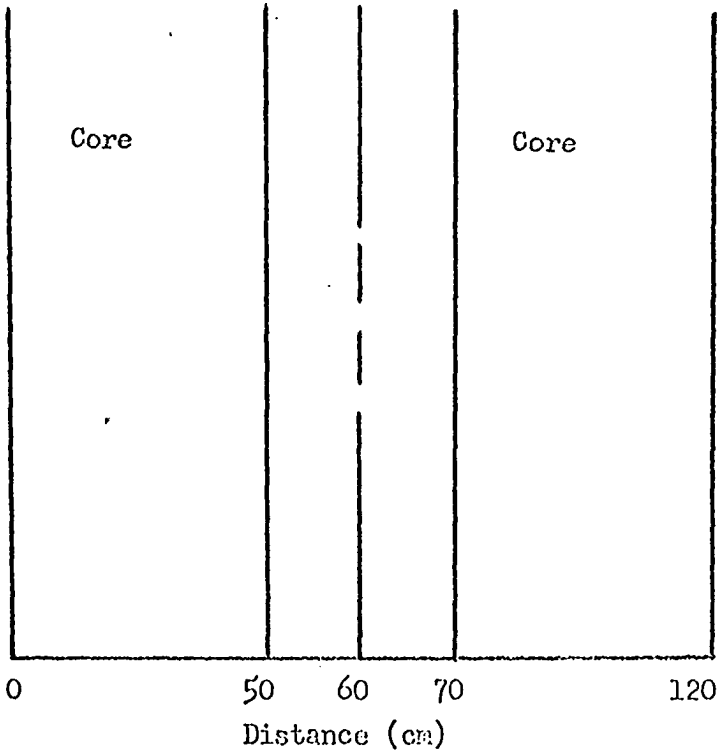

Fig. 28. Reference reactor for two-group analyses

$$\left.\begin{aligned}\phi_F &= Fe^{B_1x} + Ge^{-B_1x} \\ \phi_S &= S_3Fe^{B_1x} + S_3Ge^{-B_1x} + He^{B_2x} + Ie^{-B_2x}\end{aligned}\right] \quad 50 \leq x \leq 70$$

$$\left.\begin{aligned}\phi_F &= J \sin \mu x + K \cos \mu x + Le^{\nu x} + Me^{-\nu x} \\ \phi_S &= S_1J \sin \mu x + S_1K \cos \mu x + S_2Le^{\nu x} + S_2Me^{-\nu x}\end{aligned}\right] 70 \leq x \leq 120$$

where

$$S_1 = \frac{D\mu^2+\Sigma_R}{\nu\Sigma_f} \; ; \; S_2 = \frac{\Sigma_R-D\mu^2}{\nu\Sigma_f} \; ; \; S_3 = \frac{\Sigma_R}{\Sigma a_2-\Sigma_R}$$

$$B_1^2 = \Sigma_R/D; \; B_2^2 = \Sigma_{a2}/D \; ;$$

$$\mu^2 = \frac{-(\gamma_1+\gamma_2) + [(\gamma_1+\gamma_2)^2+4(\gamma_1\gamma_3-\gamma_1\gamma_2)]^{\frac{1}{2}}}{2}$$

$$-\nu^2 = \frac{-(\gamma_1+\gamma_2)-[(\gamma_1+\gamma_2)^2+4(\gamma_1\gamma_3-\gamma_1\gamma_2)]^{\frac{1}{2}}}{2} \; ;$$

and

$$\gamma_1 = \Sigma_R/D; \quad \gamma_2 = \Sigma_{a1}/D; \quad \gamma_3 = \nu\Sigma_f/D \; .$$

When these equations are coupled by the boundary condition at the reactor interfaces, a set of homogeneous equations is determined of the form $B\alpha = 0$, where B is a 12x12 matrix and α is a column matrix of the 12 unknowns A,B,C,...,M. The reactor critical size is found by solving the criticality condition, $|B| = 0$.

After the reactor critical size was determined, the critical flux distributions were determined as shown in Figure

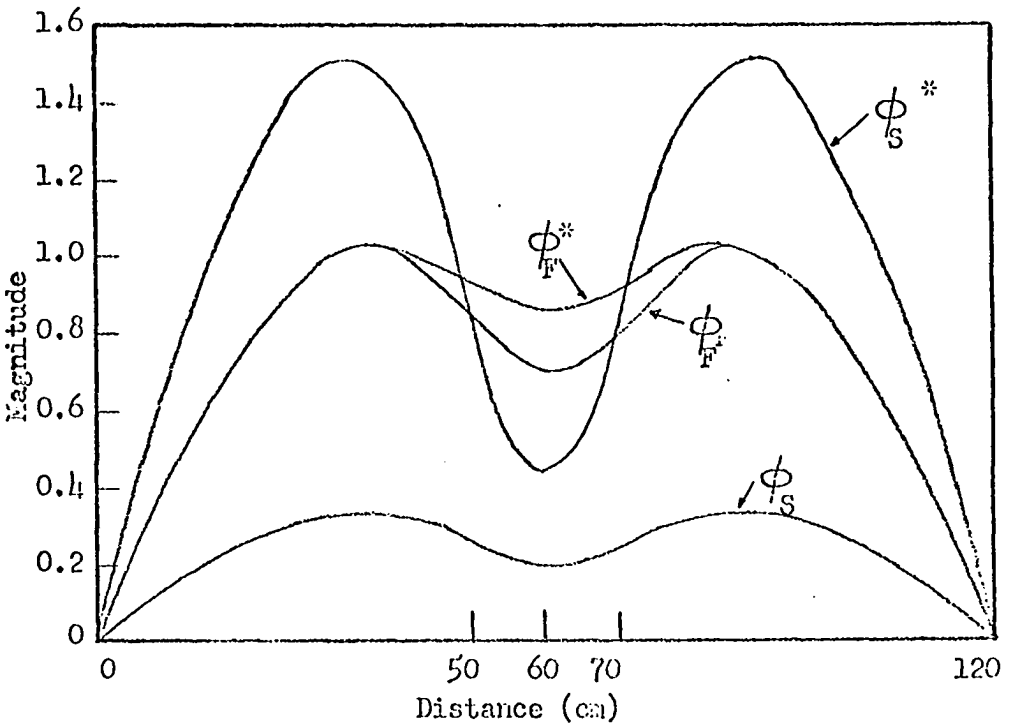

Fig. 29. Normalized two-group critical fluxes

29. The fluxes have been normalized by choosing the power level variable to be A = 1.0.

The steady state neutron equations, Equation 39, can be written in operator form as $L\phi = 0$ where

$$L = \begin{bmatrix} D\nabla^2 - \Sigma_R & \nu\Sigma_f(1-\beta) & \lambda \\ \Sigma_R & D\nabla^2 - \Sigma_a & 0 \\ 0 & \beta\nu\Sigma_f & -\lambda \end{bmatrix} ; \qquad \phi = \begin{bmatrix} \phi_F \\ \phi_S \\ C \end{bmatrix}$$

The adjoint variables are solutions of the operator equations $L^*\phi^* = 0$, where the adjoint operator L^* is defined by the relation

$$\int_{x_o}^{x_N} [\phi^* L\phi - \phi L^*\phi^*]dx = 0.$$

In this case L^* is given by

$$L^* = \begin{bmatrix} D\nabla^2 - \Sigma_R & \Sigma_R & 0 \\ \nu\Sigma_f(1-\beta) & D\nabla^2-\Sigma_a & \nu\Sigma_f\beta \\ \lambda & 0 & -\lambda \end{bmatrix} .$$

Thus the steady state adjoint equations are

$$\begin{aligned} D\nabla^2\phi_F^* - \Sigma_R\phi_F^* + \Sigma_R\phi_S^* &= 0 \\ D\nabla^2\phi_S^* - \Sigma_a\phi_S^* + \nu\Sigma_f\phi_F^* &= 0 \qquad (40) \\ C^* &= \phi_F^* \end{aligned}$$

The adjoint steady state equations are solved in the same manner as Equations 39, and the solutions are

$$\left.\begin{aligned}\phi_F^* &= A \sin \mu x + B \cos \mu x + Ce^{\nu x} + Ee^{-\nu x} \\ \phi_S^* &= S_1 A \sin \mu x + S_1 B \cos \mu x + S_2 Ce^{\nu x} + S_2 Ee^{-\nu x}\end{aligned}\right] 0 \leq x \leq 50$$

$$\left.\begin{aligned}\phi_F^* &= S_3 Fe^{B_3 x} + S_3 Ge^{-B_3 x} + He^{B_2 x} + Ie^{-B_2 x} \\ \phi_S^* &= Fe^{B_3 x} + Ge^{-B_3 x}\end{aligned}\right] 50 \leq x \leq 70$$

$$\left.\begin{aligned}\phi_F^* &= J \sin \mu x + K \cos \mu x + Le^{\nu x} + Me^{-\nu x} \\ \phi_S^* &= S_1 J \sin \mu x + S_1 K \cos \mu x + LS_2 e^{\nu x} + MS_2 e^{-\nu x}\end{aligned}\right] 70 \leq x \leq 120$$

where

$$S_1 = \frac{D\mu 2 + \Sigma_R}{\Sigma_R} \; ; \; S_2 = \frac{\Sigma_R - D\mu 2}{\Sigma_R} \; ; \; S_3 = \frac{\Sigma_R}{\Sigma_R - \Sigma_{a2}} \; ;$$

$$B_3^2 = \Sigma_{a2}/D; \; B_2^2 = \Sigma_R/D \; ;$$

and

μ^2, ν^2 are as defined previously .

These equations are again coupled by the interface boundary conditions of continuity of flux and current, and the resulting set of equations is written in the form $B^T \eta = 0$, where B^T is the transpose of the matrix determined in the ordinary steady state equations. Hence, the condition $|B^T| = 0$ is satisfied and the adjoint critical flux distribu-

tions can be determined as shown in Figure 29.

The values for the variables found in solving the steady state equations

$$B\alpha = 0$$

$$B^T\eta = 0$$

are given in Table 10.

Now the problem to be analyzed is the response of the reactor shown in Figure 28, with critical flux distributions as shown in Figure 29, to various reactivity inputs.

Table 10. Critical flux solution constants

Flux	A	B	C	E	F	G
Critical	1.0	-0.0006152	0.00005944	0.0005558	0.01046	11.43
Adjoint	1.0	-0.0006119	0.0004102	0.0002017	0.0001053	452.2

Flux	H	I	J	K	L	M
Critical	0.0000046	19.66	-0.5931	-0.8064	0	69.82
Adjoint	0.01486	16.24	-0.5931	-0.8064	0	481.9

Flux	S_1	S_2	S_3	B_1	B_2	B_3
Critical	0.3345	-0.6314	0.2656	0.05831	0.1273	-
Adjoint	1.584	-2.990	-0.2656	-	0.05831	0.1273

Flux	μ	ν
Critical	0.04455	0.1165
Adjoint	0.04455	0.1165

VII. TWO GROUP ANALYSIS: STEP RESPONSE

In this section two-group diffusion theory will be used to analyze the kinetic response of the reactor shown in Figure 28 to step inputs of reactivity. That is, the absorption cross section in some region of the reactor will be reduced in a stepwise manner, and the resulting time dependent flux distributions are then to be determined.

The analysis is analogous to the previously described one-group analysis in that the kinetic equations may again be written in the form $L\phi = V^{-1} \frac{\partial \phi}{\partial t}$, but now in the two-group situation the operators and L and V^{-1} and the variable ϕ are matrices given by

$$L = \begin{bmatrix} D\nabla^2 - \Sigma_R & \nu\Sigma_f(1-\beta) & \lambda \\ \Sigma_R & D\nabla^2 - \Sigma_a & 0 \\ 0 & \beta\nu\Sigma_f & -\lambda \end{bmatrix};$$

$$V^{-1} = \begin{bmatrix} V_F^{-1} & 0 & 0 \\ 0 & V_S^{-1} & 0 \\ 0 & 0 & 1.0 \end{bmatrix}; \quad \phi = \begin{bmatrix} \phi_F \\ \phi_S \\ C \end{bmatrix}.$$

The operator L is again to be divided into a production and a loss operator in the form $L = Lr - \nu M$, and the kinetic equations written in integral equation form as

$$\phi(x,t)-\phi_o(x) = \int_o^t\int_{x_o}^{x_N} dt'dx'[G(x,t;x',t')M(x',t')\phi(x',t')],$$

where

$$(Lr - V^{-1}\frac{\partial}{\partial t})\ G(x,t;x',t') = \delta(x-x')\delta(t-t').$$

The only difference between this analysis and the one-group analysis then is that all variables are now matrices. The space modes are obtained as solutions to the equations

$$Lr_o\psi_i = \nu M_o\phi_o\Delta_i(x),$$

and the adjoint space modes are obtained as solutions to the equations

$$Lr_o^*\psi_i^* = \nu M_o^*\phi_o^*\Delta_i(x)\ .$$

It is noted that now $\psi_i \neq \psi_i^*$.

Initially, the reactor is divided into three regions as indicated below:

Region 1 $0 \leq x \leq 50$ cm

Region 2 $50 \leq x \leq 70$

Region 3 $70 \leq x \leq 120$,

and the corresponding space modes are to be determined.

It is noted that the equations describing the steady state fluxes are coupled, and this situation makes their solution more difficult. It was found that this complication could be avoided when solving for the space modes if the matrix operators Lr and νM are defined in the manner,

$$Lr = \begin{bmatrix} D\nabla^2 - \Sigma_R & 0 & 0 \\ 0 & D\nabla^2 - \Sigma_a & 0 \\ 0 & 0 & -\lambda \end{bmatrix};$$

$$\nu M = \begin{bmatrix} 0 & -\nu\Sigma_f(1-\beta) & -\lambda \\ -\Sigma_R & 0 & 0 \\ 0 & -\beta\nu\Sigma_f & 0 \end{bmatrix}.$$

The space modes are solutions to the equations

$$\begin{bmatrix} D\nabla^2 - \Sigma_{Ro} & 0 & 0 \\ 0 & D\nabla^2 - \Sigma_{ao} & 0 \\ 0 & 0 & -\lambda \end{bmatrix} \begin{bmatrix} \psi_{Fi} \\ \psi_{Si} \\ \psi_{Ci} \end{bmatrix}$$

$$= \begin{bmatrix} 0 & -\nu\Sigma_{fo}(1-\beta) & -\lambda \\ -\Sigma_{Ro} & 0 & 0 \\ 0 & -\beta\nu\Sigma_{fo} & 0 \end{bmatrix} \begin{bmatrix} \phi_{Fo} \\ \phi_{So} \\ C_o \end{bmatrix} \Delta_i(x) ,$$

for i=1,2,3 in the three region situation. It can be seen that the equations are, in fact, uncoupled;

$$D\nabla^2\psi_{Fi} - \Sigma_{Ro}\psi_{Fi} = -\nu\Sigma_{fo}(1-\beta)\phi_{So}\Delta_i(x) - \lambda C_o\Delta_i(x)$$

$$D\nabla^2\psi_{Si} - \Sigma_{ao}\psi_{Si} = -\Sigma_{Ro}\phi_{Fo}\Delta_i(x) \qquad (41)$$

$$-\lambda\psi_{Ci} = -\beta\nu\Sigma_{fo}\phi_{So}\Delta_i(x) \ .$$

The equations given in Equations 41 will determine three spaces modes to describe the fast flux, three modes for the slow flux, and three modes for the precursor. However, since $\nu\Sigma_f=0$ in the region $50\leq x\leq 70$, it was found that $\psi_{F2}\equiv 0$. In order to generate a mode ψ_{F2} the matrix operators Lr and νM are defined in the region $50\leq x\leq 70$ as follows:

$$Lr=\begin{bmatrix} D\nabla^2 - \Sigma_R' & 0 & 0 \\ 0 & D\nabla^2 - \Sigma_a & 0 \\ 0 & 0 & -\lambda \end{bmatrix} \quad \nu M=\begin{bmatrix} \Sigma_R'' & -\nu\Sigma_f(1-\beta) & -\lambda \\ -\Sigma_R & 0 & 0 \\ 0 & -\beta\nu\Sigma_f & 0 \end{bmatrix},$$

Where $\Sigma_R = \Sigma_R' + \Sigma_R''$.

The system of equations used to determine the space modes is given below.

Fast Modes

Mode 1

$$D\nabla^2\psi_{F1} - \Sigma_{Ro}\psi_{F1} = -\nu\Sigma_{fo}\phi_{So} \qquad 0\leq x\leq 50$$

$$D\nabla^2\psi_{F1} - \Sigma_{Ro}'\psi_{F1} = 0 \qquad 50\leq x\leq 70$$

$$D\nabla^2\psi_{F1} - \Sigma_{Ro}\psi_{F1} = 0 \qquad 70\leq x\leq 120$$

Mode 2

$$D\nabla^2\psi_{F2} - \Sigma_{Ro}\psi_{F2} = 0 \qquad 0 \le x \le 50$$

$$D\nabla^2\psi_{F2} - \Sigma_{Ro}'\psi_{F2} = \Sigma_{Ro}''\phi_{Fo} \qquad 50 \le x \le 70$$

$$D\nabla^2\psi_{F2} - \Sigma_{Ro}\psi_{F2} = 0 \qquad 70 \le x \le 120$$

Mode 3

$$D\nabla^2\psi_{F3} - \Sigma_{Ro}\psi_{F3} = 0 \qquad 0 \le x \le 50$$

$$D\nabla^2\psi_{F3} - \Sigma_{Ro}'\psi_{F3} = 0 \qquad 50 \le x \le 70$$

$$D\nabla^2\psi_{F3} - \Sigma_{Ro}\psi_{F3} = -\nu\Sigma_{fo}\phi_{So} \qquad 70 \le x \le 120$$

Precursor Modes

Mode 1

$$\psi_{C1} = \frac{\beta\nu\Sigma_f}{\lambda}\phi_{So} \qquad 0 \le x \le 50$$

$$\psi_{C1} = 0 \qquad 50 \le x \le 120$$

Mode 2

$$\psi_{C2} = 0 \qquad 0 \le x \le 120$$

Mode 3

$$\psi_{C3} = 0 \qquad 0 \le x \le 70$$

$$\psi_{C3} = \frac{\beta\nu\Sigma_f}{\lambda}\phi_{So} \qquad 70 \le x \le 120$$

Slow Modes

Mode 1

$$D\nabla^2\psi_{S1} - \Sigma_{a1o}\psi_{S1} = -\Sigma_{Ro}\phi_{Fo} \qquad 0 \le x \le 50$$

$$D\nabla^2\psi_{S1} - \Sigma_{a2o}\psi_{S1} = 0 \qquad 50 \le x \le 70$$

$$D\nabla^2\psi_{S1} - \Sigma_{a3o}\psi_{S1} = 0 \qquad 70 \le x \le 120$$

Mode 2

$$D\nabla^2\psi_{S2} - \Sigma_{a1o}\psi_{S2} = 0 \qquad 0 \le x \le 50$$

$$D\nabla^2\psi_{S2} - \Sigma_{a2o}\psi_{S2} = -\Sigma_{Ro}\phi_{Fo} \qquad 50 \le x \le 70$$

$$D\nabla^2\psi_{S2} - \Sigma_{a3o}\psi_{S2} = 0 \qquad 70 \le x \le 120$$

Mode 3

$$D\nabla^2\psi_{S3} - \Sigma_{a1o}\psi_{S3} = 0 \qquad 0 \le x \le 50$$

$$D\nabla^2\psi_{S3} - \Sigma_{a2o}\psi_{S3} = 0 \qquad 50 \le x \le 70$$

$$D\nabla^2\psi_{S3} - \Sigma_{a3o}\psi_{S3} = -\Sigma_{Ro}\phi_{Fo} \qquad 70 \le x \le 120$$

The space modes are shown in Figures 30 and 31. Again it is noted that

$$\phi_{Fo} = \sum_{i=1}^{3} \psi_{Fi}; \quad \phi_{So} = \sum_{i=1}^{3} \psi_{Si}; \quad C_o = \sum_{i=1}^{3} \psi_{Ci}.$$

The adjoint kinetic equations can be written in the form

$$L^*\phi^* = v^{-1} \frac{\partial \phi^*}{\partial t}$$

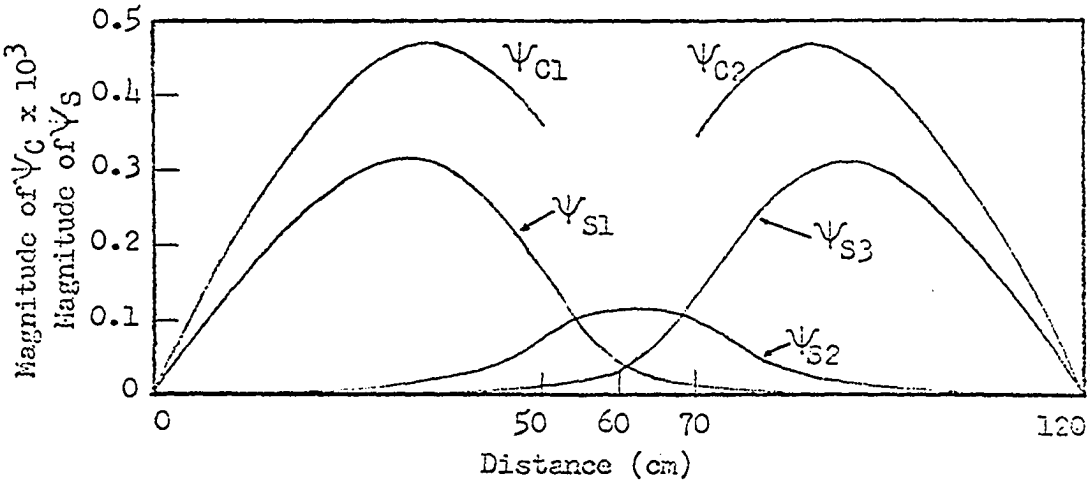

Fig. 30. Three region space modes for two-group analysis

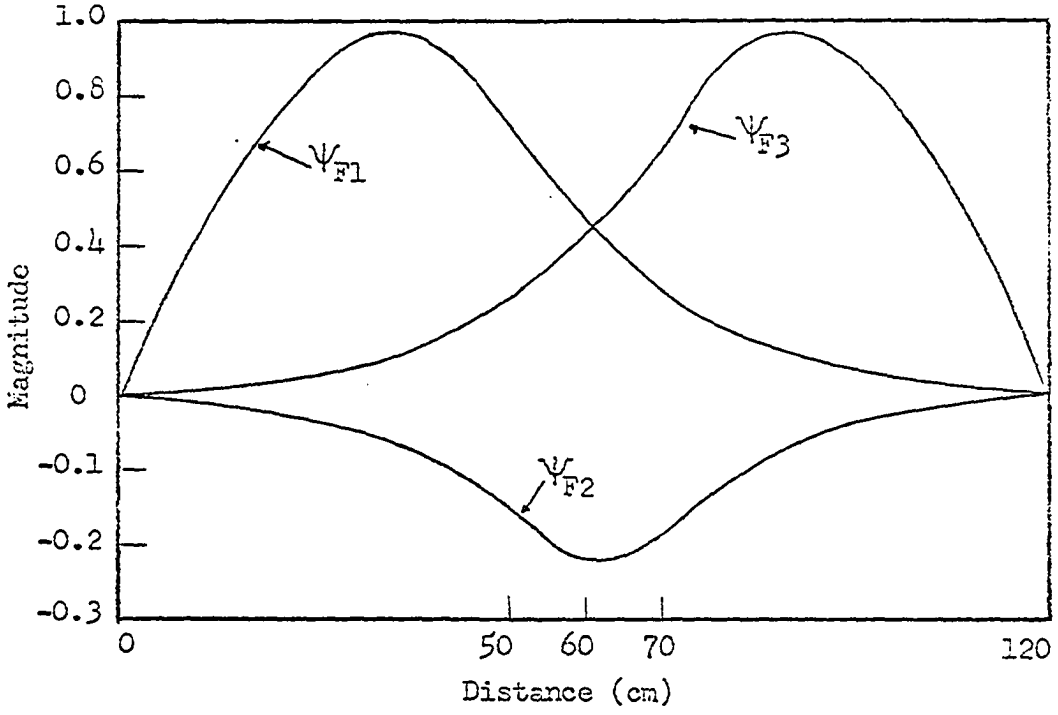

Fig. 31. Three region space modes for two-group analysis

where

$$L^* = \begin{bmatrix} D\nabla^2 - \Sigma_R & \Sigma_R & 0 \\ \nu\Sigma_f(1-\beta) & D\nabla^2 - \Sigma_a & \beta\nu\Sigma_f \\ \lambda & 0 & -\lambda \end{bmatrix}.$$

In order to generate adjoint space modes, operators Lr* and νM^* are defined as follows:

$$Lr^* = \begin{bmatrix} D\nabla^2 - \Sigma_R & 0 & 0 \\ 0 & D\nabla^2 - \Sigma_a & 0 \\ 0 & 0 & -\lambda \end{bmatrix}; \nu M^* = \begin{bmatrix} 0 & -\Sigma_R & 0 \\ -\nu\Sigma_f(1-\beta) & 0 & -\beta\nu\Sigma_f \\ -\lambda & 0 & 0 \end{bmatrix}$$

The adjoint space modes are determined by solving the system of equations

$$L_{ro}^*\psi_i^* = \nu M_o^*\phi_o^*\Delta_i(x)$$

or, in non-matrix form,

$$D\nabla^2\psi_F^* - \Sigma_R\psi_F^* = -\Sigma_R\phi_{So}^*\Delta_i(x)$$

$$D\nabla^2\psi_S^* - \Sigma_a\psi_S^* = -\nu\Sigma_f(1-\beta)\phi_{Fo}^*\Delta_i(x) - \beta\nu\Sigma_f C_o^*\Delta_i(x)$$

$$-\lambda\psi_C^* = -\lambda\phi_{Fo}^*\Delta_i(x) .$$

In this case it can be seen that when the slow adjoint modes are determined, it will be found that $\psi_{S2} \equiv 0$. Hence, in the region $50 \leq x \leq 70$ the operators $L\overset{*}{r}$ and νM^* are defined as

$$L_r^* = \begin{bmatrix} D\nabla^2 - \Sigma_R & 0 & 0 \\ 0 & D\nabla^2 - \Sigma_a' & 0 \\ 0 & 0 & -\lambda \end{bmatrix}; \quad \nu M^* = \begin{bmatrix} 0 & -\Sigma_R & 0 \\ 0 & \Sigma_a'' & 0 \\ -\lambda & 0 & 0 \end{bmatrix},$$

where $\Sigma_a = \Sigma_a' + \Sigma_a''$.

The adjoint space modes are given in Figures 32 and 33, where

$$\phi_{Fo}^* = \sum_{i=1}^{3} \psi_{Fi}^* \; ; \; \phi_{So}^* = \sum_{i=1}^{3} \psi_{Si}^* ; \; C_o^* = \sum_{i=1}^{3} \psi_{Ci}^* \; .$$

Now it is required to determine the corresponding time coefficients for these space modes. The functional that will be used in the calculus of variations technique is

$$F[\phi_F^*, \phi_S^*, C^*, \phi_F, \phi_S, C] = \int_o^\tau \int_{x_o}^{x_N} \{ [\phi_F^*, \phi_S^*, C^*] \begin{bmatrix} V_F^{-1} & 0 & 0 \\ 0 & V_S^{-1} & 0 \\ 0 & 0 & 1.0 \end{bmatrix} \begin{bmatrix} \dot{\phi}_F \\ \dot{\phi}_S \\ \dot{C} \end{bmatrix}$$

$$+ \left[\frac{\partial \phi_F^*}{\partial x} , \frac{\partial \phi_S^*}{\partial x} , \frac{\partial C^*}{\partial x} \right] \begin{bmatrix} D & 0 & 0 \\ 0 & D & 0 \\ 0 & 0 & 0 \end{bmatrix} \begin{bmatrix} \partial \phi_F / \partial x \\ \partial \phi_S / \partial x \\ \partial C / \partial x \end{bmatrix} \qquad (42)$$

$$- [\phi_F^*, \phi_S^*, C^*] \begin{bmatrix} -\Sigma_R & \nu\Sigma_f(1-\beta) & \lambda \\ \Sigma_R & -\Sigma_a & 0 \\ 0 & \beta\nu\Sigma_f & -\lambda \end{bmatrix} \begin{bmatrix} \phi_F \\ \phi_S \\ C \end{bmatrix} \} \; dx dt.$$

The Euler equations for this functional are the two-group kinetic equations; i.e.,

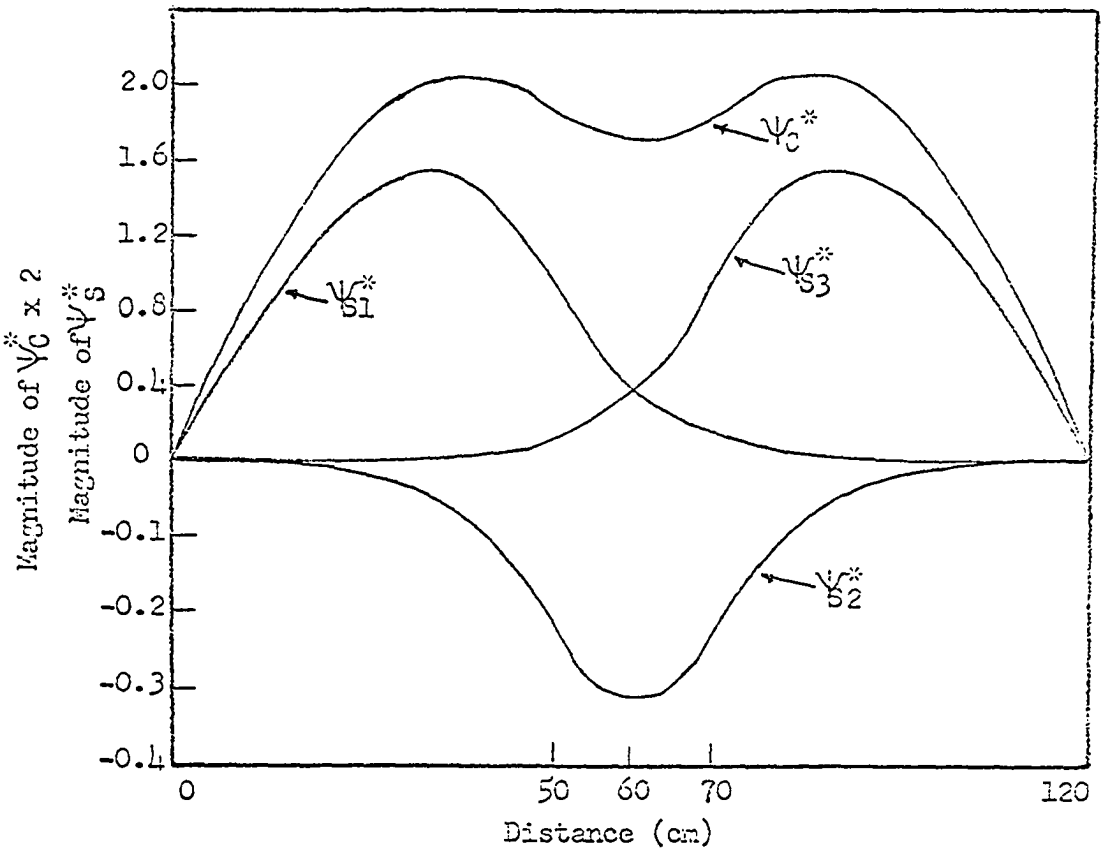

Fig. 32. Three region adjoint space modes for two-group analysis

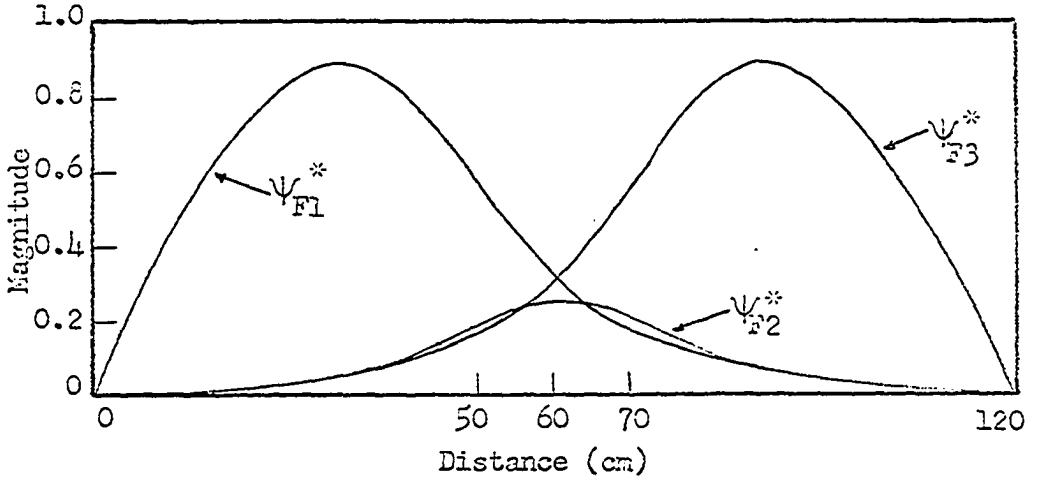

Fig. 33. Three region space modes for two-group analysis (adjoint modes)

$$\delta F[\delta\phi_F^*, \phi_S^*, \ldots, C] = \int_0^{\tau}\int_{x_o}^{x_N} [V_F^{-1}\dot{\phi}_F - D\frac{\partial^2\phi_F}{\partial x^2} + \Sigma_R\phi_F - \nu\Sigma_f(1-\beta)\phi_S - \lambda C]\,\delta\phi_F^* dx dt,$$

etc.

Trial functions are assumed of the type

$$\phi_F = \sum_{i=1}^{N} a_i(t)\psi_{Fi}(x);\quad \phi_F^* = \sum_{i=1}^{N} a_i^*(t)\psi_{Fi}^*(x);$$

$$\phi_S = \sum_{i=1}^{N} b_i(t)\psi_{Si}(x);\quad \phi_S^* = \sum_{i=1}^{N} b_i^*(t)\psi_{Si}^*(x);$$

$$C = \sum_{i=1}^{N} d_i(t)\psi_{ci}(x);\quad C^* = \sum_{i=1}^{N} d_i^*(t)\psi_{ci}^*(x),$$

and substituted into Equation 42. Variations are taken, after performing the spatial integration, with respect to a_i^*, b_i^*, and d_i^*. The resulting Euler equations can be written in matrix form as, for the case of N=2,

$$\Gamma\dot{\theta} = B\theta$$

where

$$\theta = \begin{bmatrix} a_1 \\ a_2 \\ b_1 \\ b_2 \\ d_1 \\ d_2 \end{bmatrix}$$

and the matrices Γ and B are shown on the following pages.

$$\Gamma = \begin{bmatrix}
[\psi_{1F}^{*} V_F^{-1} \psi_{1F}] & [\psi_{1F}^{*} V_F^{-1} \psi_{2F}] & 0 & 0 & 0 & 0 \\
[\psi_{2F}^{*} V_F^{-1} \psi_{1F}] & [\psi_{2F}^{*} V_F^{-1} \psi_{2F}] & 0 & 0 & 0 & 0 \\
0 & 0 & [\psi_{1S}^{*} V_S^{-1} \psi_{1S}] & [\psi_{1S}^{*} V_S^{-1} \psi_{2S}] & 0 & 0 \\
0 & 0 & [\psi_{2S}^{*} V_S^{-1} \psi_{1S}] & [\psi_{2S}^{*} V_S^{-1} \psi_{2S}] & 0 & 0 \\
0 & 0 & 0 & 0 & [\psi_{1C}^{*} V_D^{-1} \psi_{1C}] & [\psi_{1C}^{*} V_D^{-1} \psi_{2C}] \\
0 & 0 & 0 & 0 & [\psi_{2C}^{*} V_D^{-1} \psi_{1C}] & [\psi_{2C}^{*} V_D^{-1} \psi_{2C}]
\end{bmatrix}$$

Matrix 1. Coefficient matrix Γ

$$
B=\begin{bmatrix}
-[\psi_{1Fx}^{*D}\psi_{1Fx}] & -[\psi_{1Fx}^{*D}\psi_{2Fx}] & [\psi_{1F}^{*\nu}\Sigma_f(1-\beta)\psi_{1S}] & [\psi_{1F}^{*\nu}\Sigma_f(1-\beta)\psi_{2S}] & [\psi_{1F}^{*}\bar{\lambda}\psi_{1C}] & [\psi_{1F}^{*}\bar{\lambda}\psi_{2C}] \\
-[\psi_{1F}^{*}\Sigma_R\psi_{1F}] & -[\psi_{1F}^{*}\Sigma_R\psi_{2F}] & & & & \\
-[\psi_{2Fx}^{*D}\psi_{1Fx}] & -[\psi_{2Fx}^{*D}\psi_{2Fx}] & [\psi_{2F}^{*\nu}\Sigma_f(1-\beta)\psi_{1S}] & [\psi_{2F}^{*\nu}\Sigma_f(1-\beta)\psi_{2S}] & [\psi_{2F}^{*}\bar{\lambda}\psi_{1C}]+[\psi_{2F}^{*}\bar{\lambda}\psi_{2C}] & \\
-[\psi_{2F}^{*}\Sigma_R\psi_{1F}] & -[\psi_{2F}^{*}\Sigma_R\psi_{2F}] & & & & \\
[\psi_{1S}^{*}\Sigma_R\psi_{1F}] & [\psi_{1S}^{*}\Sigma_R\psi_{2F}] & -[\psi_{1Sx}^{*D}\psi_{1Sx}] & -[\psi_{1Sx}^{*D}\psi_{2Sx}] & & \\
 & & -[\psi_{1S}^{*}\Sigma_a\psi_{1S}] & -[\psi_{1S}^{*}\Sigma_a\psi_{2S}] & 0 & 0 \\
[\psi_{2S}^{*}\Sigma_R\psi_{1F}] & [\psi_{2S}^{*}\Sigma_R\psi_{2F}] & -[\psi_{2Sx}^{*D}\psi_{1Sx}] & -[\psi_{2Sx}^{*D}\psi_{2Sx}] & & \\
 & & -[\psi_{2S}^{*}\Sigma_a\psi_{1S}] & -[\psi_{2S}^{*}\Sigma_a\psi_{2S}] & 0 & 0 \\
0 & 0 & [\psi_{1C}^{*\beta\nu}\Sigma_f\psi_{1S}] & [\psi_{1C}^{*\nu}\Sigma_f\psi_{2S}] & -[\psi_{1C}^{*}\bar{\lambda}\psi_{1C}]-[\psi_{1C}^{*}\bar{\lambda}\psi_{2C}] & \\
0 & 0 & [\psi_{2C}^{*\beta\nu}\Sigma_f\psi_{1S}] & [\psi_{2C}^{*\beta\nu}\Sigma_f\psi_{2S}] & -[\psi_{2C}^{*}\bar{\lambda}\psi_{1C}]-[\psi_{2C}^{*}\bar{\lambda}\psi_{2C}] &
\end{bmatrix}
$$

Matrix 2. Coefficient matrix B

The elements of the matrices are determined, as before, by Gregory's method of numerical integration. The problem then is reduced to solving a system of differential equations of the form

$$\Gamma\dot{\theta} = B\theta, \qquad (43)$$

which is a problem very comparable to that encountered in the one-group analysis, Equation 12. It was found, however, that Equation 43 was not as easily solved as Equation 12.

3 mode analysis

In the first analysis the reactor was divided into three regions, as mentioned previously, and space modes were obtained as shown in Figures 30,31,32, and 33. The time dependent fluxes are expressed as

$$\phi_F(x,t) = \sum_{i=1}^{3} a_i(t)\psi_{Fi}(x); \quad \phi_S(x,t) = \sum_{i=1}^{3} b_i(t)\psi_{si}(x),$$

where the time coefficients are determined as solutions to equations like Equation 43. When the absorption cross section in the region $50 \leq x \leq 70$ was reduced stepwise to $\Sigma_a = 0.0005$ cm^{-1}, the matrices Γ and B in Equation 43 were found to be as shown in Matrices 3 and 4.

$$B=\begin{bmatrix}
-1.47\times10^{-1} & 1.11\times10^{-2} & -1.77\times10^{-2} & 1.28\times10^{-1} & 1.23\times10^{-2} & 1.25\times10^{-2} & 9.87\times10^{-4} & 8.67\times10^{-5} \\
-1.80\times10^{-2} & 7.61\times10^{-3} & -1.80\times10^{-2} & 1.23\times10^{-2} & 3.52\times10^{-3} & 1.23\times10^{-2} & 1.01\times10^{-4} & 9.71\times10^{-5} \\
-1.77\times10^{-2} & 1.11\times10^{-2} & -1.48\times10^{-1} & 1.25\times10^{-2} & 1.23\times10^{-2} & 1.28\times10^{-1} & 9.05\times10^{-5} & 9.84\times10^{-4} \\
1.66\times10^{-1} & -1.79\times10^{-2} & 3.48\times10^{-2} & -1.46\times10^{-1} & -7.28\times10^{-3} & 2.31\times10^{-4} & 0 & 0 \\
-1.82\times10^{-2} & 5.87\times10^{-3} & -1.82\times10^{-2} & 2.86\times10^{-3} & 4.70\times10^{-3} & 2.86\times10^{-3} & 0 & 0 \\
3.48\times10^{-2} & -1.79\times10^{-2} & 1.67\times10^{-1} & 2.31\times10^{-4} & -7.29\times10^{-3} & -1.47\times10^{-1} & 0 & 0 \\
0 & 0 & 0 & 1.06\times10^{-3} & 9.92\times10^{-5} & 1.65\times10^{-5} & -1.18\times10^{-3} & 0 \\
0 & 0 & 0 & 1.59\times10^{-5} & 9.60\times10^{-5} & 1.06\times10^{-3} & 0 & -1.17\times10^{-3}
\end{bmatrix}$$

Matrix 3. Coefficient matrix B for three mode analysis

$$
\Gamma = \begin{bmatrix}
6.69\times10^{-8} & -8.04\times10^{-9} & 1.87\times10^{-8} & 0 & 0 & 0 & 0 & 0 \\
1.16\times10^{-8} & -3.37\times10^{-9} & 1.17\times10^{-8} & 0 & 0 & 0 & 0 & 0 \\
1.87\times10^{-8} & -8.05\times10^{-9} & 6.71\times10^{-8} & 0 & 0 & 0 & 0 & 0 \\
0 & 0 & 0 & 6.59\times10^{-5} & 9.77\times10^{-6} & 4.26\times10^{-6} & 0 & 0 \\
0 & 0 & 0 & -4.43\times10^{-6} & -3.87\times10^{-6} & -4.44\times10^{-6} & 0 & 0 \\
0 & 0 & 0 & 4.26\times10^{-6} & 9.78\times10^{-6} & 6.60\times10^{-5} & 0 & 0 \\
0 & 0 & 0 & 0 & 0 & 0 & 1.46\times10^{-2} & 0 \\
0 & 0 & 0 & 0 & 0 & 0 & 0 & 1.46\times10^{-2}
\end{bmatrix}
$$

Matrix 4. Coefficient matrix Γ for three mode analysis

The problem now is to solve Equation 43 with Γ and B as shown. The first technique attempted was the eigenvalue method. The eigenvalues and eigenvectors of the matrix $\Gamma^{-1}B$ were determined using the "power method". (45) The eigenvalues are listed in Table 11.

Table 11. Eigenvalues for two-group analysis: $\Sigma_{a2}=0.005$ cm^{-1}

$\omega_1= -4.743\text{x}10^{6}$	$\omega_4= -2.184\text{x}10^{3}$	$\omega_7= -6.013\text{x}10^{-2}$
$\omega_2= -2.686\text{x}10^{6}$	$\omega_5= +5.159\text{x}10^{2}$	$\omega_8= -8.025\text{x}10^{-1}$
$\omega_3= -1.79\text{x}10^{6}$	$\omega_6= -4.799\text{x}10^{2}$	

The second technique attempted was the exponential method, and it was found to converge rapidly to a solution that agreed with the results of the eigenvalue method. In this case it was found that the elements of the matrix $\Gamma^{-1}B$ in $e^{\Gamma^{-1}Bt}$ had to be divided by 2^N, where N=13, in order to insure convergence. The first attempt at using the numerical algorithm NODE was unsuccessful. The time increment required for stability of the scheme was found to be on the order of 10^{-8} sec. This condition is very unsatisfactory since it would require very long running times on the digital machine before results could be found for times on the order of 10^{-3} sec., which are the times being investigated. The time increment required for stability of the numerical scheme in the one-group analysis was about $5\text{x}10^{-4}$ sec. The sharp

difference in this time for the two-group case is thought to be due to the fast neutron lifetime that has been introduced. However, it was found that this problem could be alleviated by a slight change in the analysis. Recall that the matrix Γ has elements like $[\psi_i {}^{+}V_F^{-1}\psi_j]$ which multiply the elements $\dot{a}_i(t)$, the fast derivatives. Since $V_F >> V_S$, it was thought that perhaps these elements could be neglected. Hence, these terms in Γ, $[\psi_i {}^{+}V_F^{-1}\psi_j]$, were set to zero and the numerical routine NODE was again used to solve the system of equations

$$\Gamma'\dot{\theta} = B\theta,$$

where Γ' is the matrix Γ with fast terms set equal to zero. The numerical routine now required a time increment of 5×10^{-4} sec. and converged rapidly to solutions for the time coefficients that agreed with the previous results. This result seems to be a very interesting and useful fact. The presence of the terms $[\psi_i {}^{+}V_F^{-1}\psi_j]$ is not required for the proper solution to Equations 43 but is sufficient to cause very serious numerical problems.

The solution for the time coefficients determined for the situation where $\Sigma_{a2}=0.0005$ cm^{-1} is shown in Figure 34. Also the time dependent flux distributions are shown in Figures 35 and 36.

In a second analysis the absorption cross section in the region $50 \leq x \leq 70$ was reduced stepwise to $\Sigma_{a2}=0.008$ cm^{-1}.

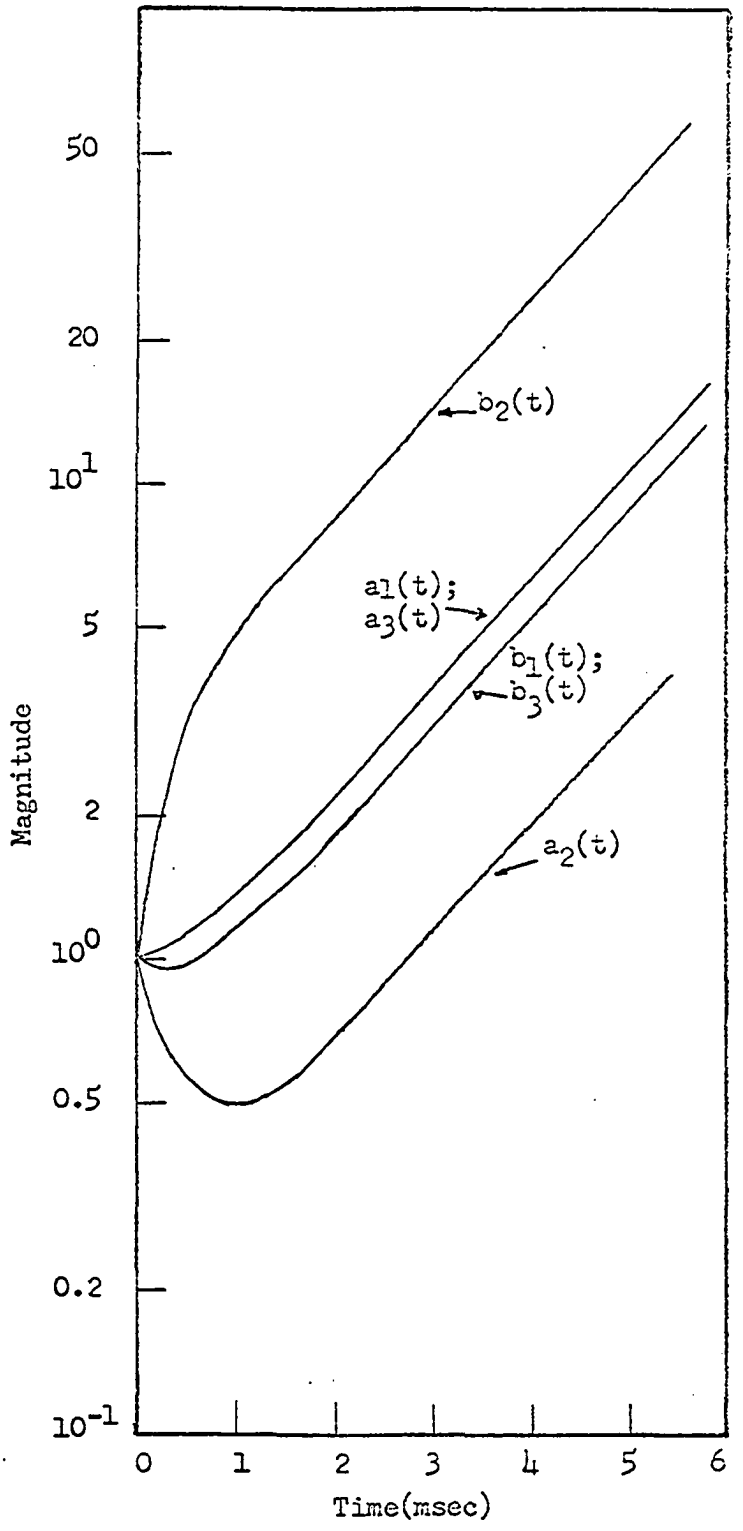

Fig. 34. Time coefficients for three region two-group analysis

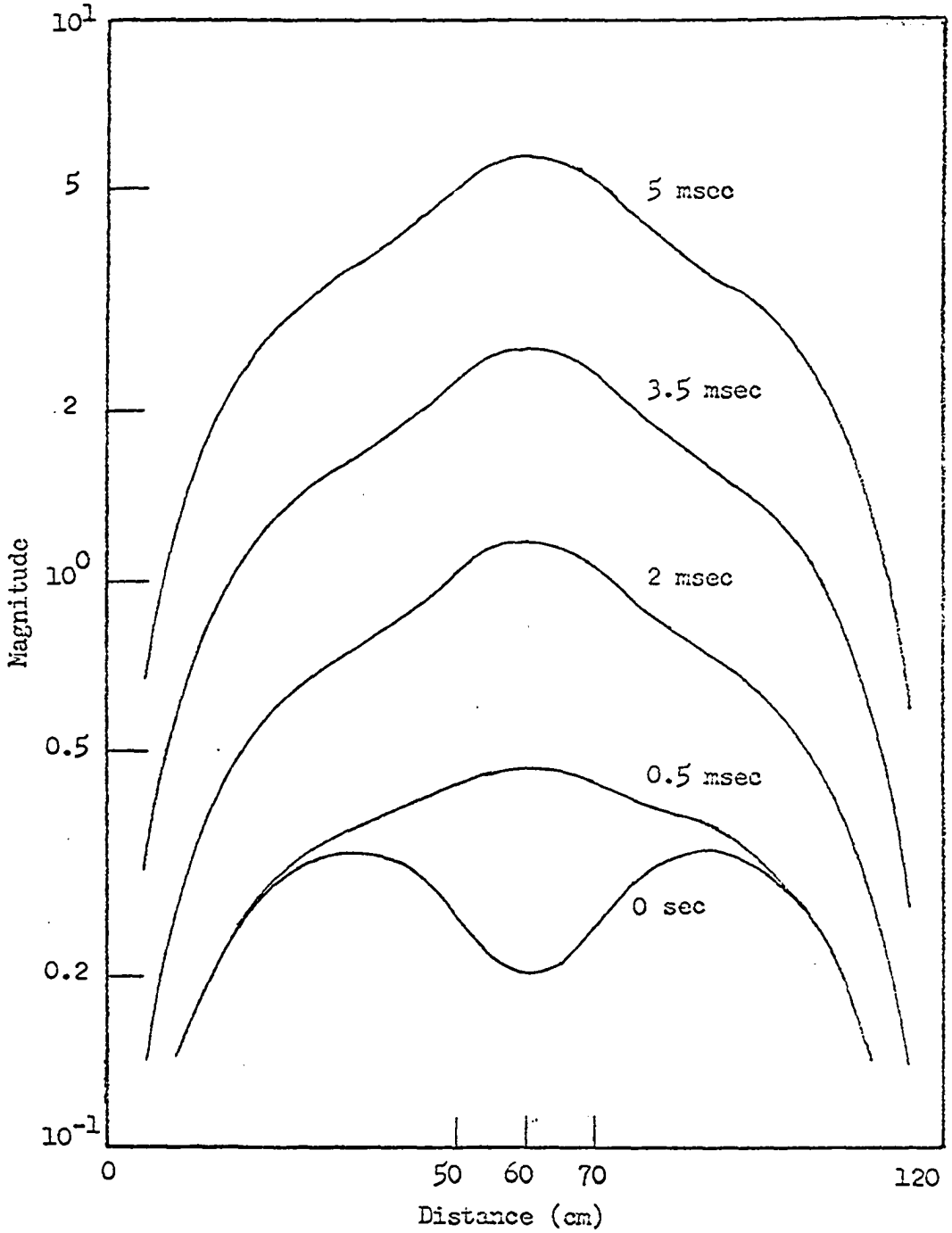

Fig. 35. Time dependent slow flux for three region two-group analysis where $\Sigma_a = 0.0005$ cm^{-1}

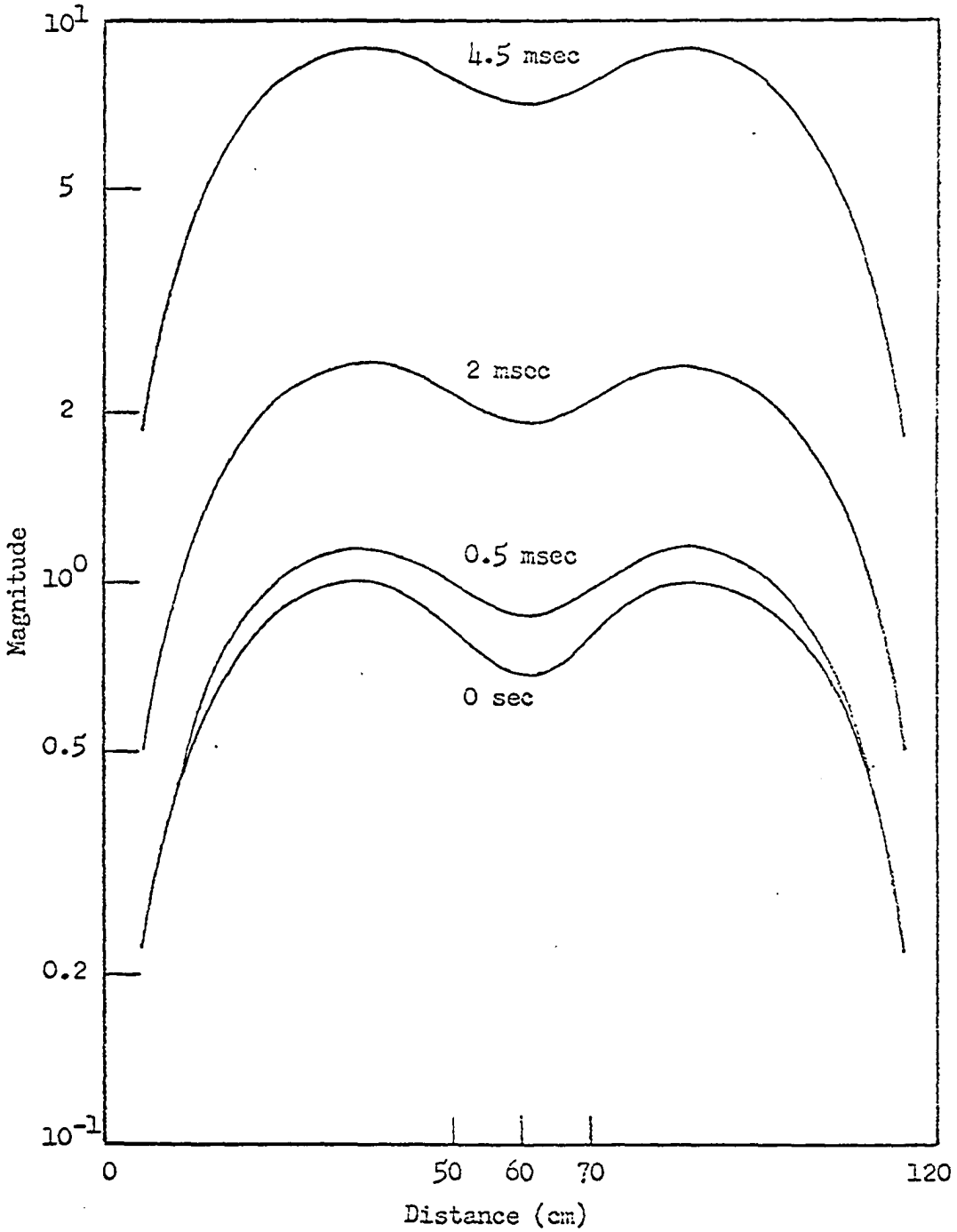

Fig. 36. Time dependent fast flux for three region two-group analysis where $\Sigma_a = 0.0005$ cm^{-1}

When the eigenvalue method was applied to determine the time coefficients for this situation some problems developed. As seen from Table 11 there are usually some very large negative eigenvalues found before a predominant positive eigenvalue is found, corresponding to the asymptotic reactor period. For small reactivity changes this positive eigenvalue becomes so small that it becomes very difficult to converge to it by numerical methods. Most numerical schemes for finding eigenvalues converge to the eigenvalues of largest magnitudes first; thus the errors of the numerical scheme may become very large before the smaller eigenvalues are found. This was the case in all two-group analyses except the case for $\Sigma_{a2}=0.0005\ cm^{-1}$; thus the eigenvalue method had to be discarded.

However, both the exponential method and the numerical routine, NODE, with the extension as mentioned previously, continued to converge rapidly to solutions for the time coefficients, and the solutions agreed. The flux distributions for the case $\Sigma_{a2}=0.008\ cm^{-1}$ are shown in Figures 37 and 38 as obtained from these methods.

Since the two-group analysis included the effect of delayed neutrons, an attempt was made to perform an analysis wherein their effect could be detected. In the investigations reported previously the reactivity changes were so large that the delayed neutrons had no effect, but for smaller reactiv-

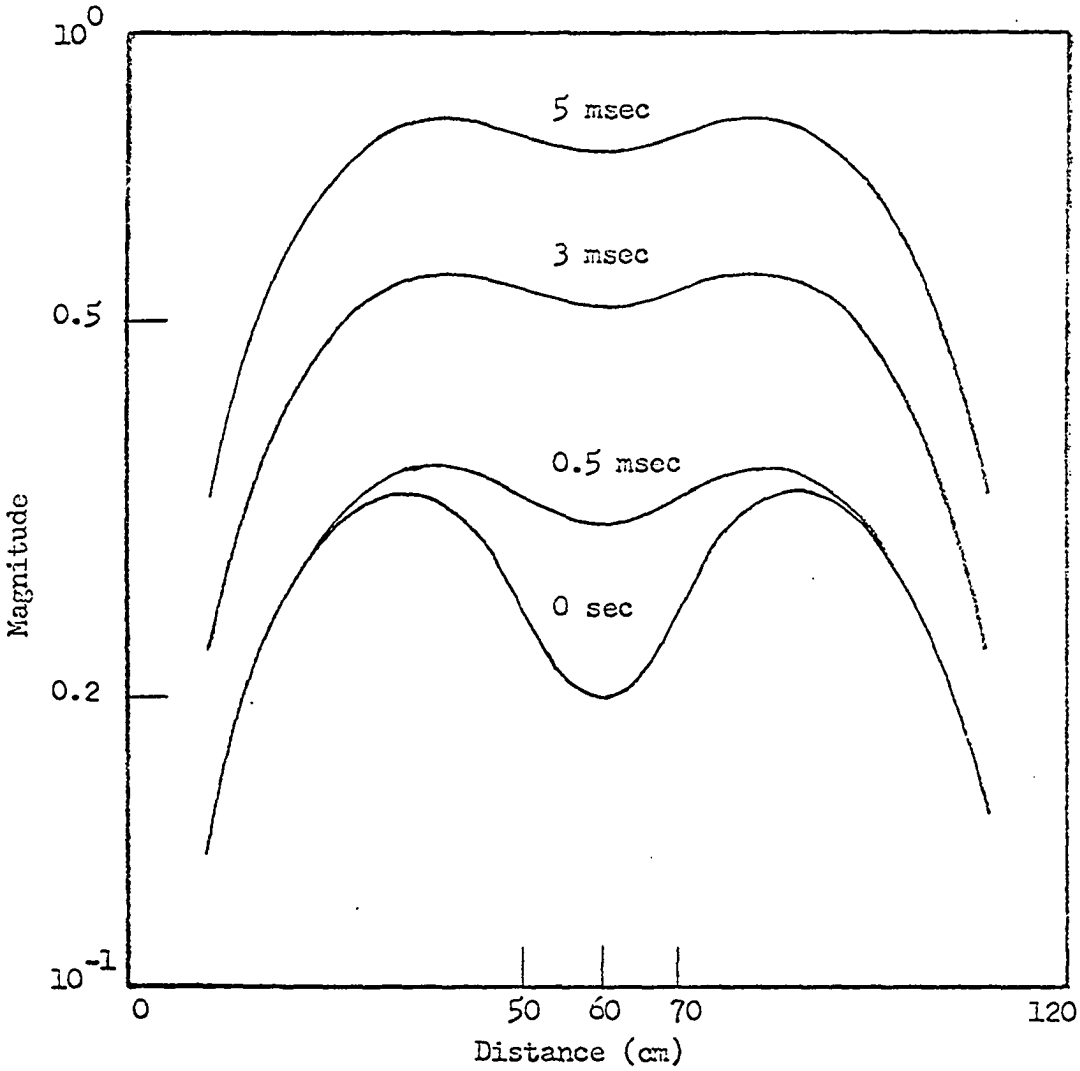

Fig. 37. Time dependent slow flux for three region two-group analysis where $\Sigma_a = 0.008$ cm^{-1}

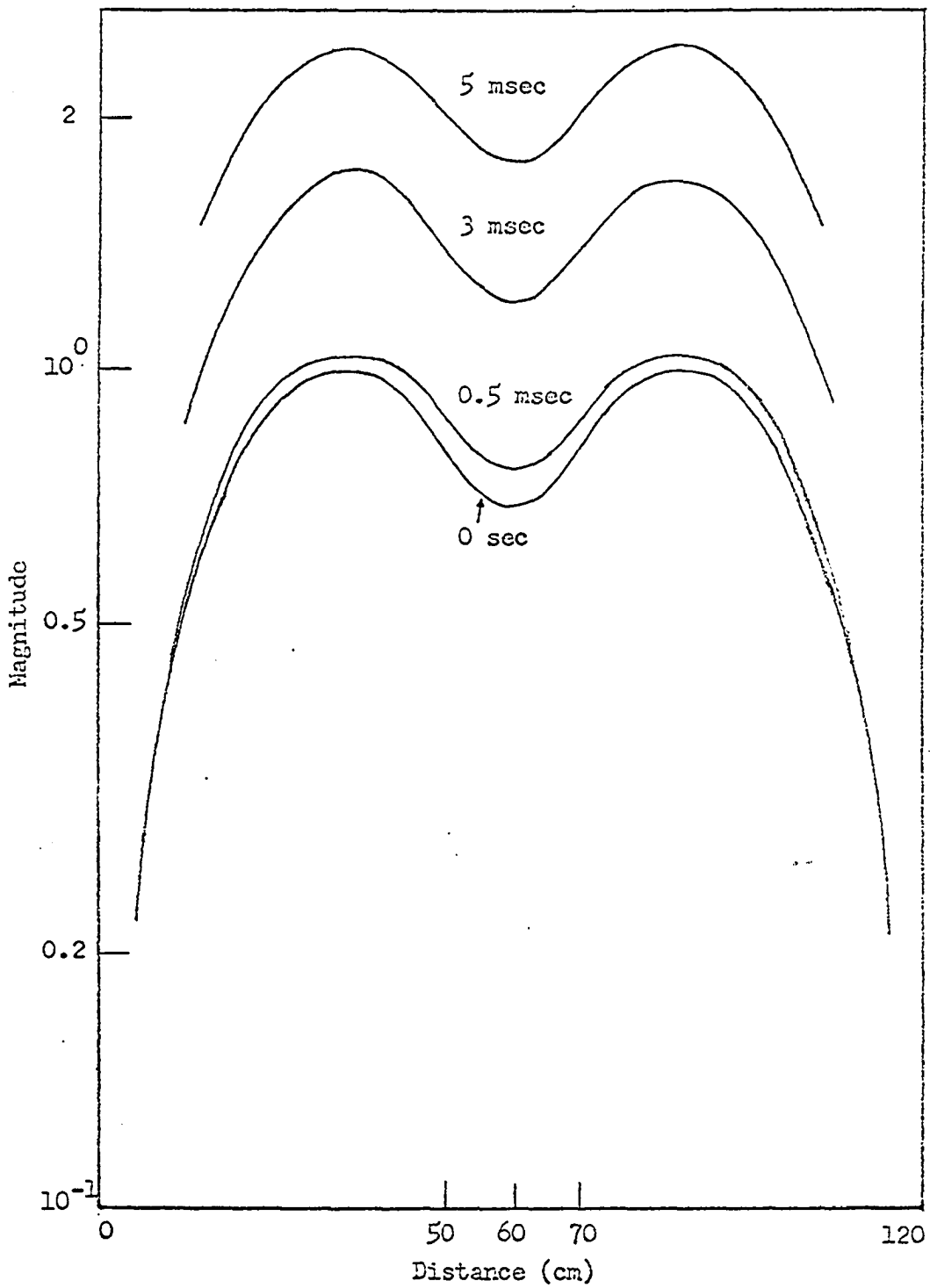

Fig. 38. Time dependent fast flux for three region two-group analysis where Σ_a=0.008 cm^{-1}

ity changes they should become important. In one case the absorption cross section in the region $50 \leq x \leq 70$ was reduced to $\Sigma_{a2}=0.015$ cm^{-1}, and the equations for the time coefficients were solved both with delayed neutrons included and with delayed neutrons removed. When the two solutions were compared, it was found that they were identical; thus the delayed neutrons had no effect in this case. In order to obtain an expression for the reactivity effect corresponding to a certain change in the absorption cross section, the following approximation is made:

$$k \text{ eff} = \frac{\nu\Sigma_f L}{\Sigma_{ao}-\delta\Sigma_a}, \text{ where L is leakage}$$

$$\delta k = \frac{\nu\Sigma_f L}{\Sigma_{ao}-\delta\Sigma_a} - 1$$

$$\frac{\delta k}{k \text{ eff}} = \frac{\nu\Sigma_f L}{\Sigma_{ao}-\delta\Sigma_a} \cdot \frac{-\Sigma_{ao}+\delta\Sigma_a}{\frac{\nu\Sigma_f L}{\Sigma_{ao}-\delta\Sigma_a}} = 1 + \frac{(\delta\Sigma_a-\Sigma_{ao})}{\nu\Sigma_f L}$$

$$= 1 + \frac{\Sigma_{ao}(-1 + \delta\Sigma_a/\Sigma_{ao})}{\nu\Sigma_f L}$$

$$= 1 + \frac{(-1 + \delta\Sigma_a/\Sigma_{ao})}{\frac{\nu\Sigma_f L}{\Sigma_{ao}}} \approx \frac{\delta\Sigma_a}{\Sigma_{ao}}$$

$$\frac{\delta k}{k} \approx \frac{\delta\Sigma_a}{\Sigma_{ao}} \qquad (44)$$

For the case of $\Sigma_{a2}=0.015$ cm^{-1}, $\frac{\delta k}{k} = 0.074$, and the reactor is prompt critical.

When the absorption cross section in the region $50 \leq x \leq 70$ was reduced to $\Sigma_a=0.01610$ cm^{-1}, it was found that $\delta k/k=0.006$, and the delayed neutrons should be important in this analysis. The time coefficients determined for this situation are shown in Figure 40, for both cases: delayed neutrons included and delayed neutrons removed. The effect of delayed neutrons is apparent.

6 mode analysis

The reactor shown in Figure 28 was also divided into six regions as shown in Figure 39. The six regions are

Region	Location
1	$0 \leq x \leq 20$
2	$20 \leq x \leq 30$
3	$30 \leq x \leq 50$
4	$50 \leq x \leq 60$
5	$60 \leq x \leq 70$
6	$70 \leq x \leq 120$

Space modes corresponding to these six regions were determined in the same manner as were the modes for the three region analysis, and the modes are displayed in Figures 41, 42, 43, and 44. Again the condition that the modes sum to the corresponding steady state fluxes is valid. Now the time dependent fluxes are expressed in the form

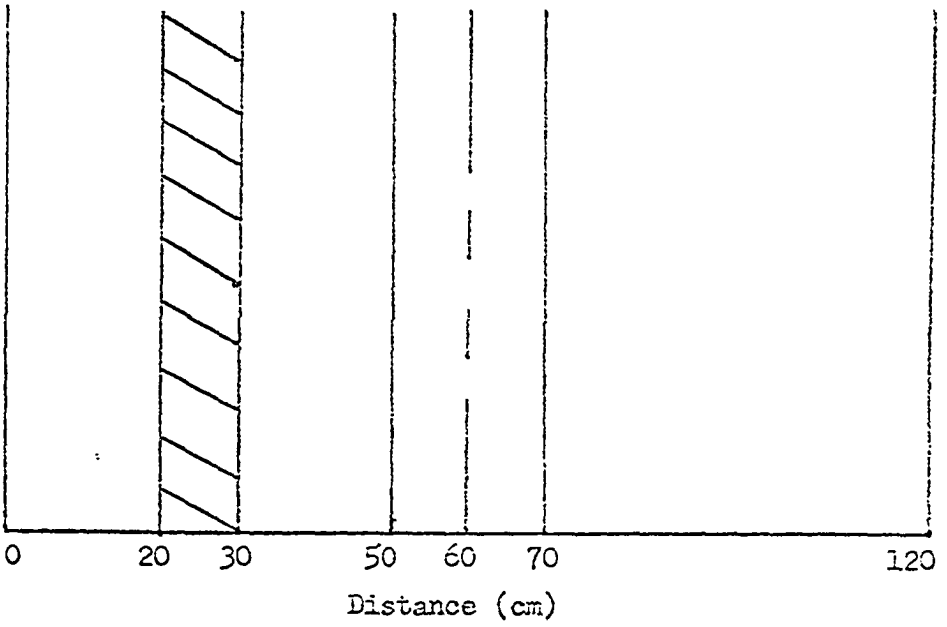

Fig. 39. Division of reference reactor for six region, two-group analysis

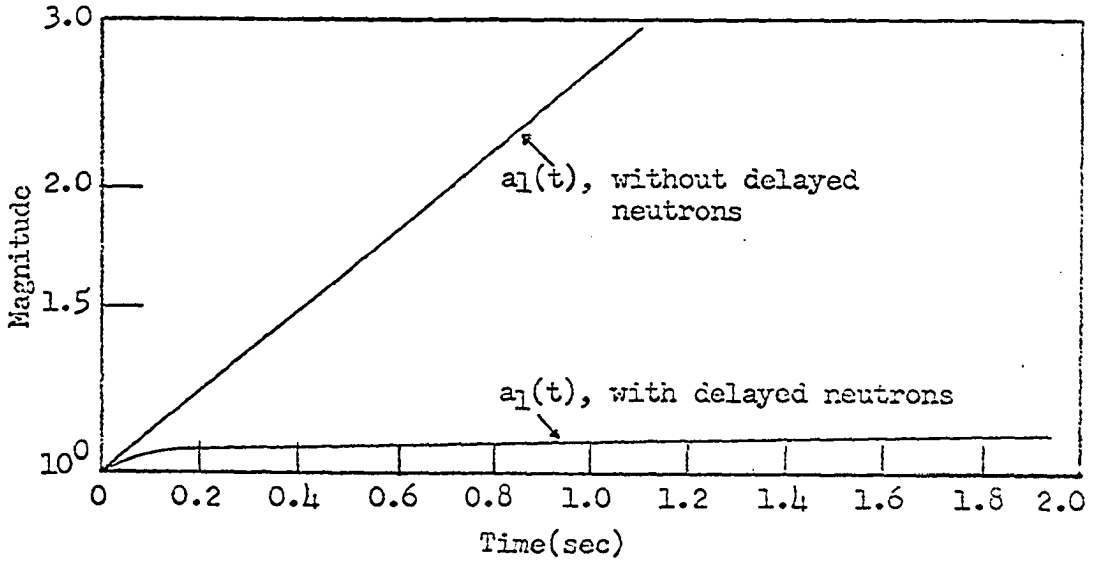

Fig. 40. Influence of delayed neutrons on time coefficient for three region, two-group analysis

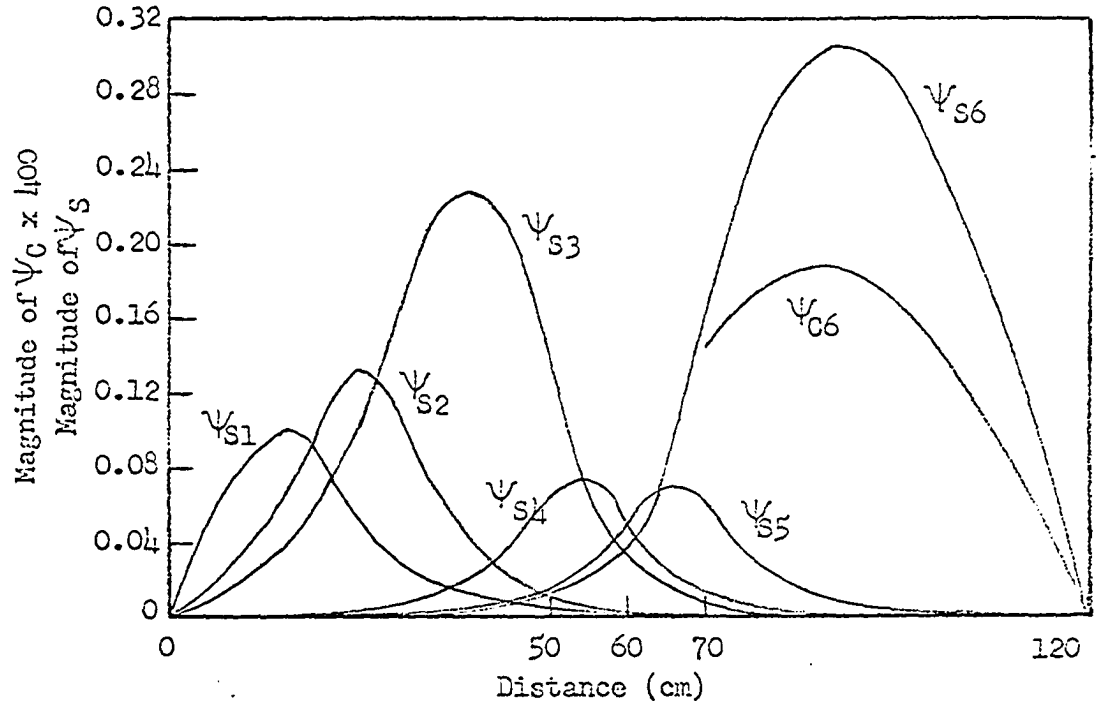

Fig. 41. Six region space modes for two-group analysis

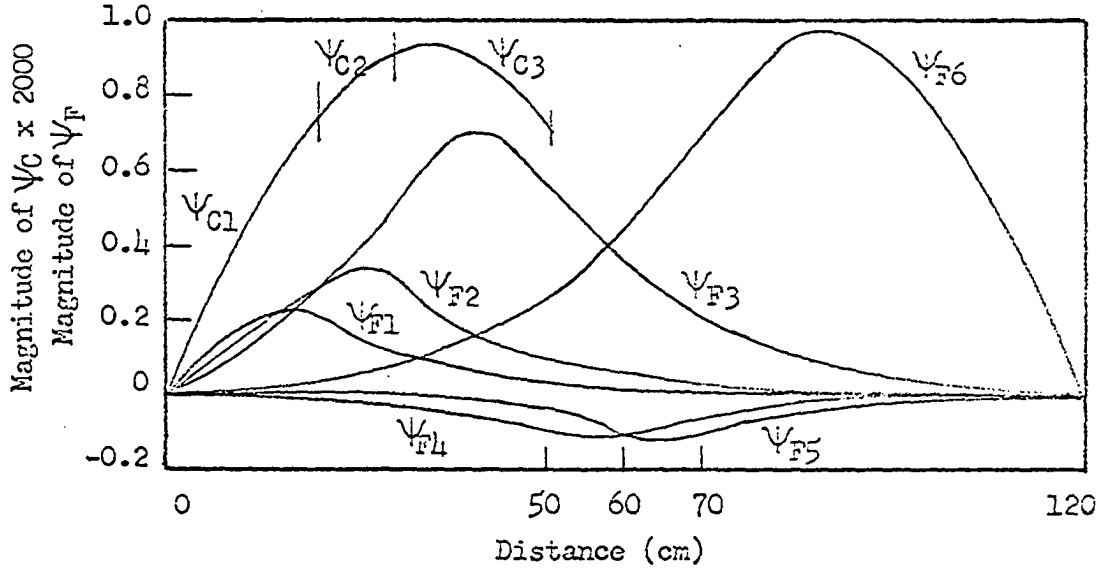

Fig. 42. Six region space modes for two-group analysis

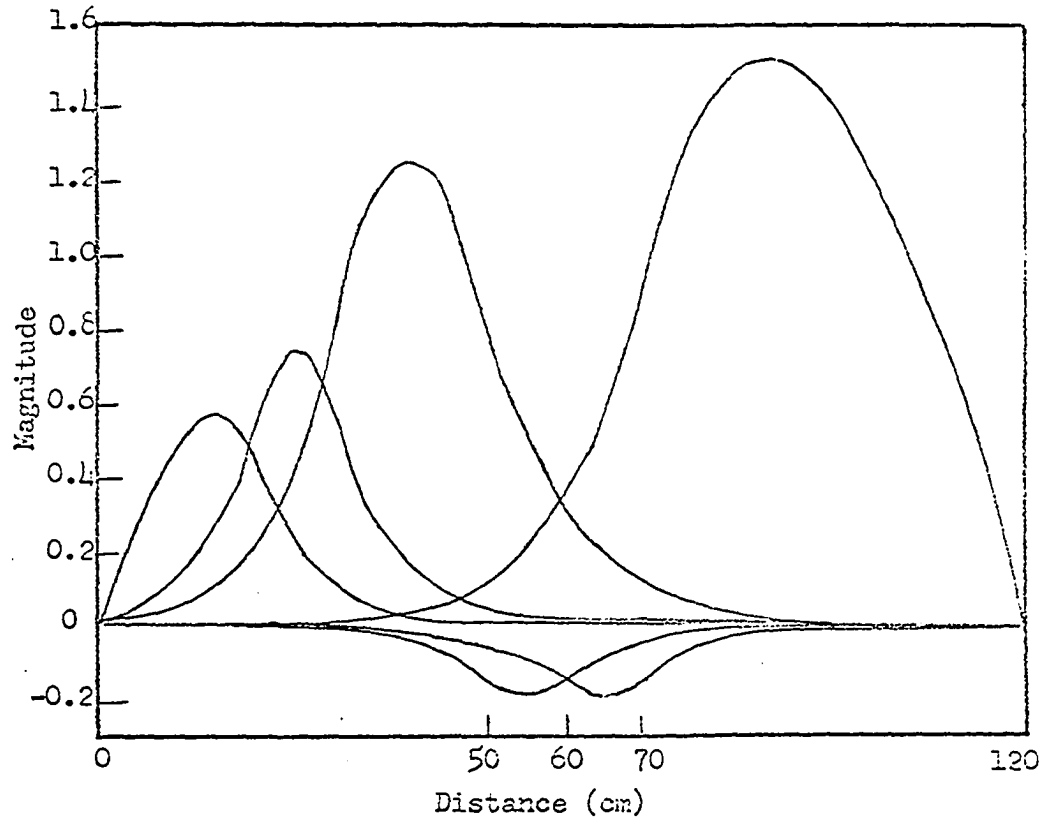

Fig. 43. Six region adjoint slow modes for two-group analysis

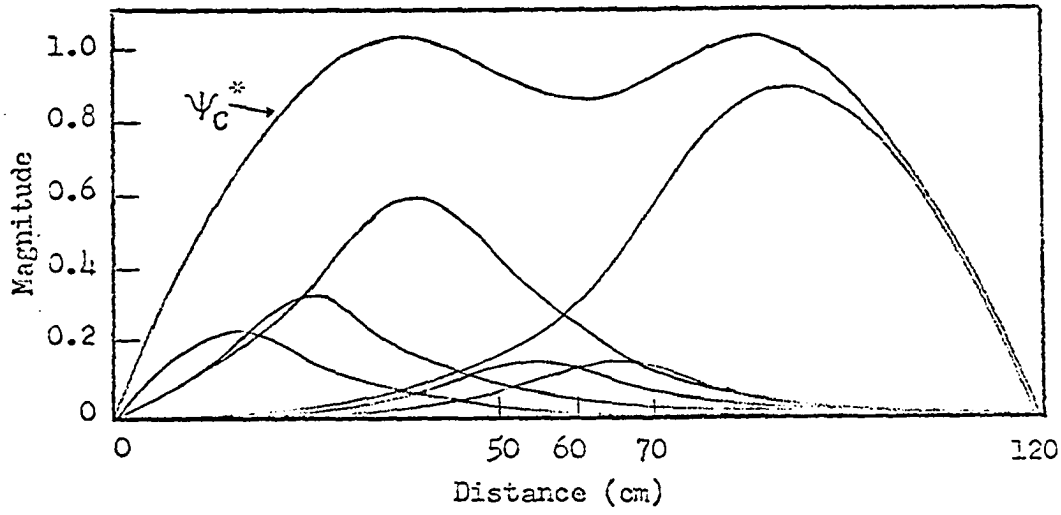

Fig. 44. Six region adjoint fast modes and adjoint precursor modes for two-group analysis

$$\phi_F(x,t) = \sum_{i=1}^{6} a_i(t)\psi_{Fi}(x);\ \phi_S(x,t) = \sum_{i=1}^{6} b_i(t)\psi_{Si}(x), \quad (45)$$

where the time coefficients are determined as solutions to a set of differential equations of the form $\Gamma\dot{\theta} = B\theta$.

The absorption cross section in the region $50 \leq x \leq 70$ was reduced stepwise to $\Sigma_a = 0.0005\ cm^{-1}$, and the matrices Γ and B were determined. The time coefficients $a_i(t)$ and $b_i(t)$ are then solutions to the differential equations $\Gamma\dot{\theta} = B\theta$. The solutions for the time coefficients were obtained by the exponential method and by the numerical method NODE, with the terms $[\psi_i * V_F^{-1}\psi_j]$ set equal to zero. The results of these two methods agreed. When the time dependent flux distributions were obtained from Equation 45, it was found that the results were not in complete agreement with those obtained from the three mode analysis, as shown in Figures 35 and 36. A comparison of the slow flux as determined by the three mode and six mode analyses is given in Figure 45. It can be seen that the six mode analysis predicts that the reactor is slightly more supercritical than the three mode analysis predicts.

Since the exponential and numerical methods converged to the same solutions for the six mode time coefficients, it is believed that the differences shown in Figure 45 should be attributed to some other problem. One possibility that exists is that three modes are not sufficient for convergence purposes. However, it is felt that a more likely explanation is

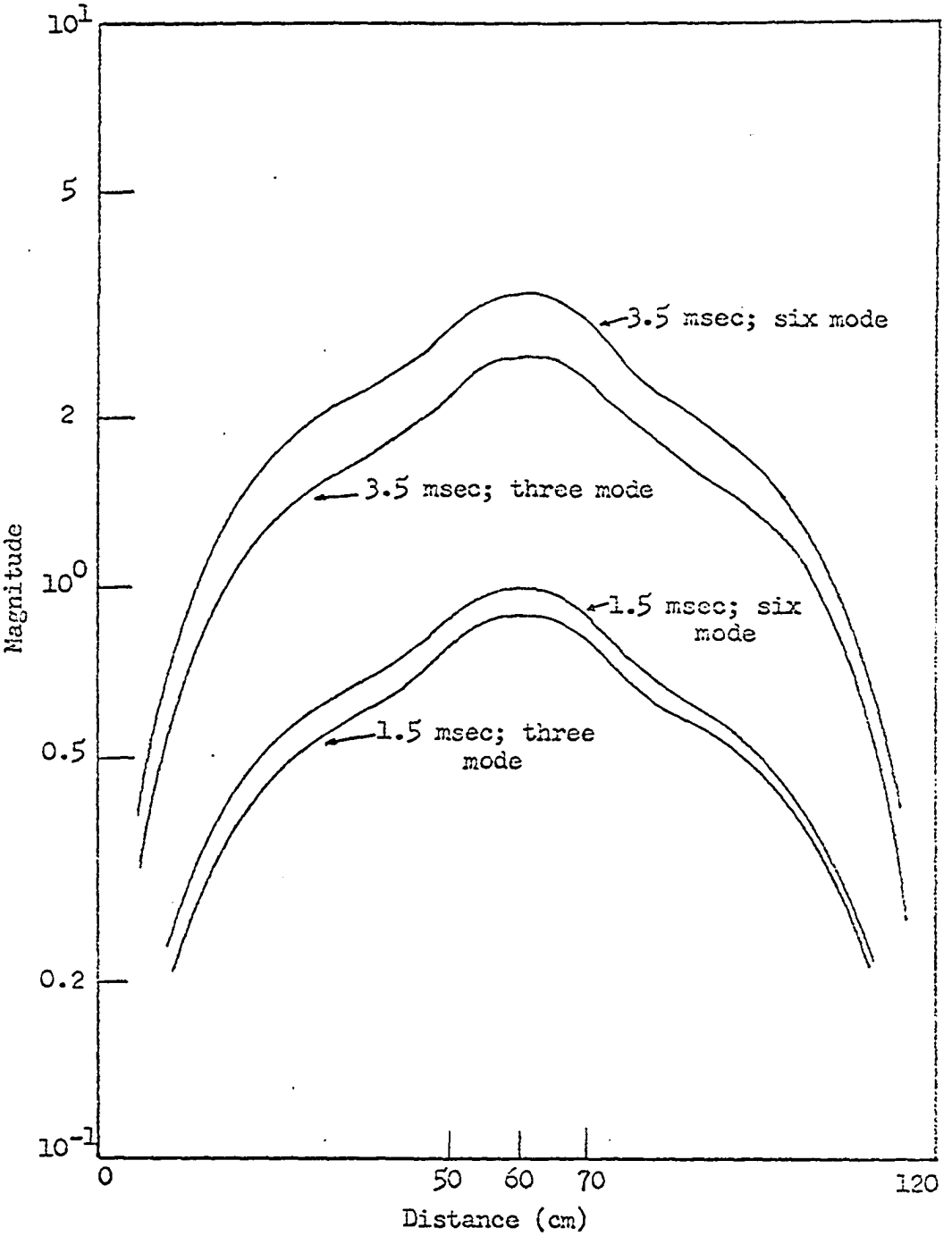

Fig. 45. Comparison of time dependent slow flux for three mode and six mode analyses

that there are numerical calculation errors involved in the generation of the elements of the matrices Γ and B. All errors involved in the numerical calculations performed in determining the critical fluxes, determining the space modes, and integrating the space modes are included in the elements of Γ and B. As indicated previously the criticality condition is that $B_o A_o = 0$, where B_o is the matrix B evaluated with all critical parameters. In the three region, two-group analysis it was found that $B_o A_o \approx [10^{-4}]$, but in the six region, two-group analysis $B_o A_o \approx [10^{-2}]$. Hence, the calculations involved in the six region analysis did involve somewhat greater inaccuracies. More support for this conclusion will be given in the next section.

The absorption cross section in the region $20 \leq x \leq 30$ was reduced stepwise to $\Sigma_a = 0.004$ cm^{-1}, and the resulting time dependent flux distributions were determined from Equation 25 and are displayed in Figures 46 and 47. The exponential method and NODE again converged to solutions for the time coefficients that agreed with each other.

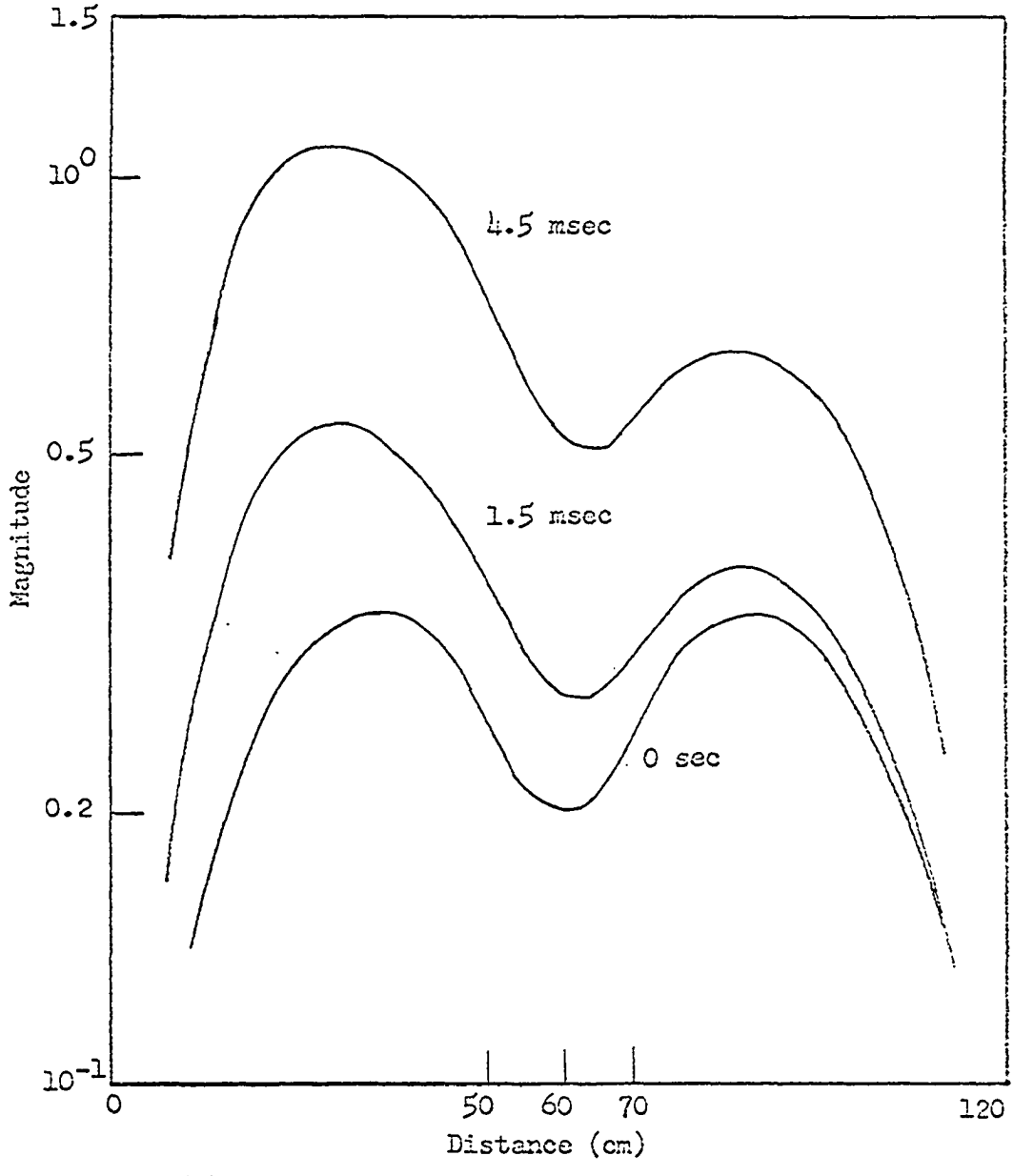

Fig. 46. Time dependent slow flux for six region, two-group analysis where $\Sigma_a = 0.004$ cm^{-1}

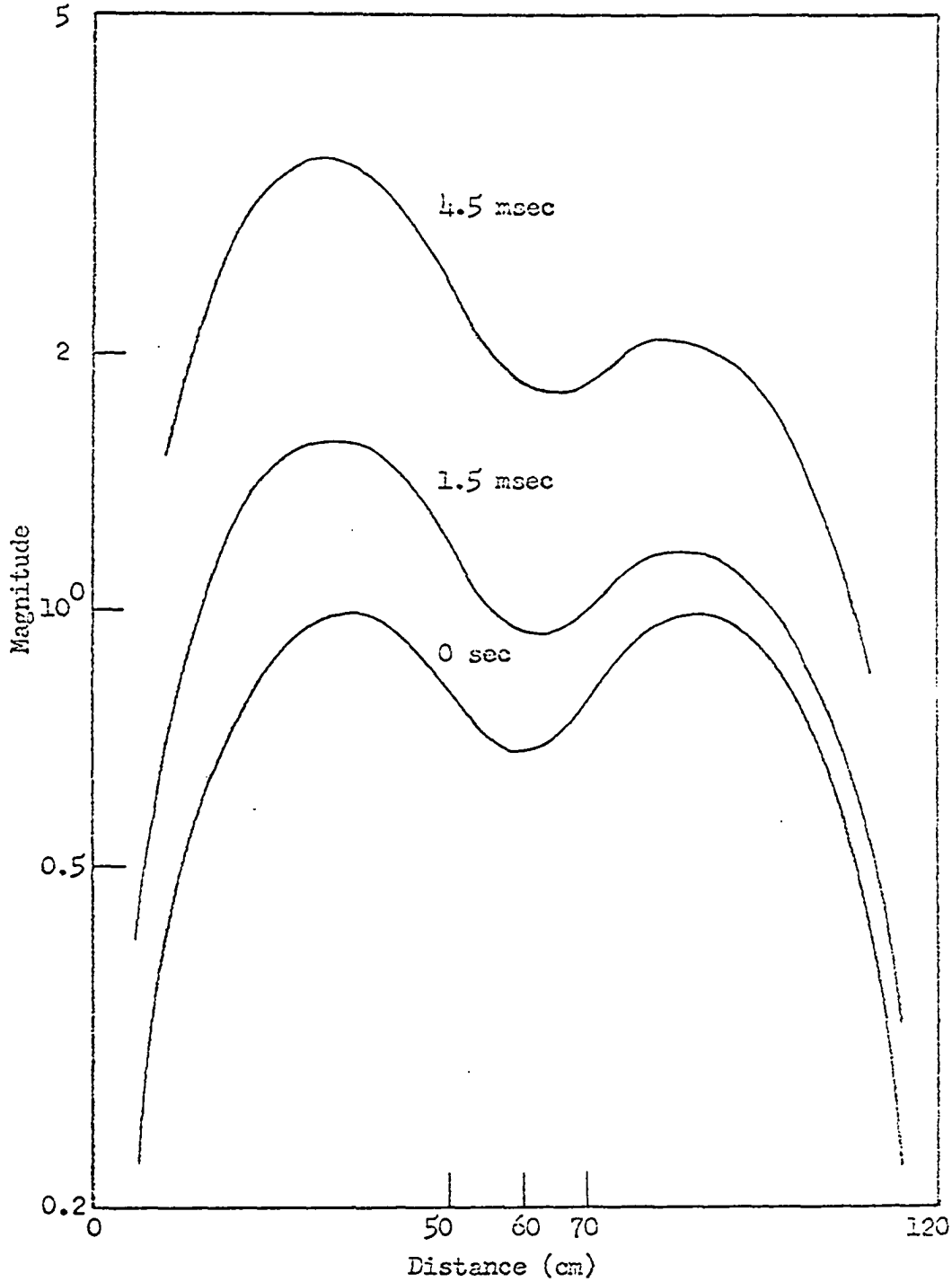

Fig. 47. Time dependent fast flux for six region, two-group analysis where $\Sigma_a = 0.004$ cm^{-1}

VIII. TWO GROUP ANALYSIS: FREQUENCY RESPONSE

The response of the reactor shown in Figure 28 to an oscillating absorber located in some region is to be determined by applying the same basic technique that was utilized in obtaining the one-group frequency response. It is assumed that the absorption cross section in some region of the reactor can be expressed in the form

$$\Sigma_a = \Sigma_{ao} + \delta\Sigma_a e^{i\omega t} .$$

Recall that the differential equations for determining the time coefficients are of the form $\Gamma\dot{\theta} = B\theta$. Also note that, as shown for the two mode case, the absorption cross section only appears in some elements of the matrix B. Hence, when the equations are written in the form

$$\Gamma\dot{\theta} = (B_o + \delta B)\theta,$$

it is found, for the two mode case, that

$$\delta B = \begin{bmatrix} 0 & 0 & 0 & 0 & 0 & 0 \\ 0 & 0 & 0 & 0 & 0 & 0 \\ 0 & 0 & \delta b_{33} & \delta b_{34} & 0 & 0 \\ 0 & 0 & \delta b_{43} & \delta b_{44} & 0 & 0 \\ 0 & 0 & 0 & 0 & 0 & 0 \\ 0 & 0 & 0 & 0 & 0 & 0 \end{bmatrix}$$

where

$$\delta b_{ij} = [\psi_{Si}^* \, \delta\Sigma_a \psi_{Sj}]'$$

Note again that the integration indicated in $[\psi_{Si}^{*}\delta\Sigma_a\psi_{Sj}]'$ is only over the region of oscillation.

Following the same procedure as in the one-group frequency analysis will lead to the set of equations

$$[i\omega\Gamma - B_o]\delta\theta = \delta B\cdot\theta_o$$

where

$$\delta\theta = \begin{bmatrix} a_1 + ib_1 \\ a_2 + ib_2 \\ c_1 + id_1 \\ c_2 + id_2 \\ e_1 + if_1 \\ e_2 + if_2 \end{bmatrix} .$$

The frequency dependent fluxes are now written, where a two mode expansion is used for illustration, as

$$\phi_F(x,\omega) = (a_1+ib_1)\psi_{F1}(x) + (a_2+ib_2)\psi_{F2}(x)$$

$$= W_F(x,\omega) + iY_F(x,\omega)$$

$$\phi_S(x,\omega) = (c_1+id_1)\psi_{S1}(x) + (c_2+id_2)\psi_{S2}(x)$$

$$= W_S(x,\omega) + iY_S(x,\omega).$$

The frequency response of the reactor shown in Figure 28 is now determined using the three expansion modes shown in

Figures 30 and 31. It is assumed that an absorber of magnitude $\delta\Sigma_a=0.002\ cm^{-1}$ is oscillated in the region $50\leq x\leq 70$. The magnitude of the frequency response for the fast and slow fluxes is shown in Figure 48 and the corresponding phase diagrams are given in Figure 49. Several features of these diagrams are worthy of note. The magnitude of the frequency response for the fast flux, evaluated at x=6 cm., has the same shape as the frequency response for the slow flux evaluated at the same point in the reactor. In fact, in all instances investigated in this three mode analysis, the magnitude diagrams for the fast flux had the same shape as the diagrams for the corresponding slow flux magnitude response. However, as seen from Figure 49, the phase response does show some differences. Also note that the effect of the delayed neutrons is apparent at low frequencies.

In Figure 50 several variations of the magnitude of the frequency response for the three mode analysis are indicated. In one instance the frequency response for the slow flux, evaluated at x=26 cm., was determined after setting the terms $[\psi_{Fi}^{*}\ V_F^{-1}\psi_{Fj}]$ equal to zero. This corresponds to setting equal to zero the time derivative of the fast flux. As can be seen from Figure 50, the frequency response was not affected by this elimination. In a second analysis the terms corresponding to $[\psi_{Si}^{*}\ V_S^{-1}\psi_{Sj}]$ were set equal to zero; that is, the time derivative of the slow flux was assumed to be

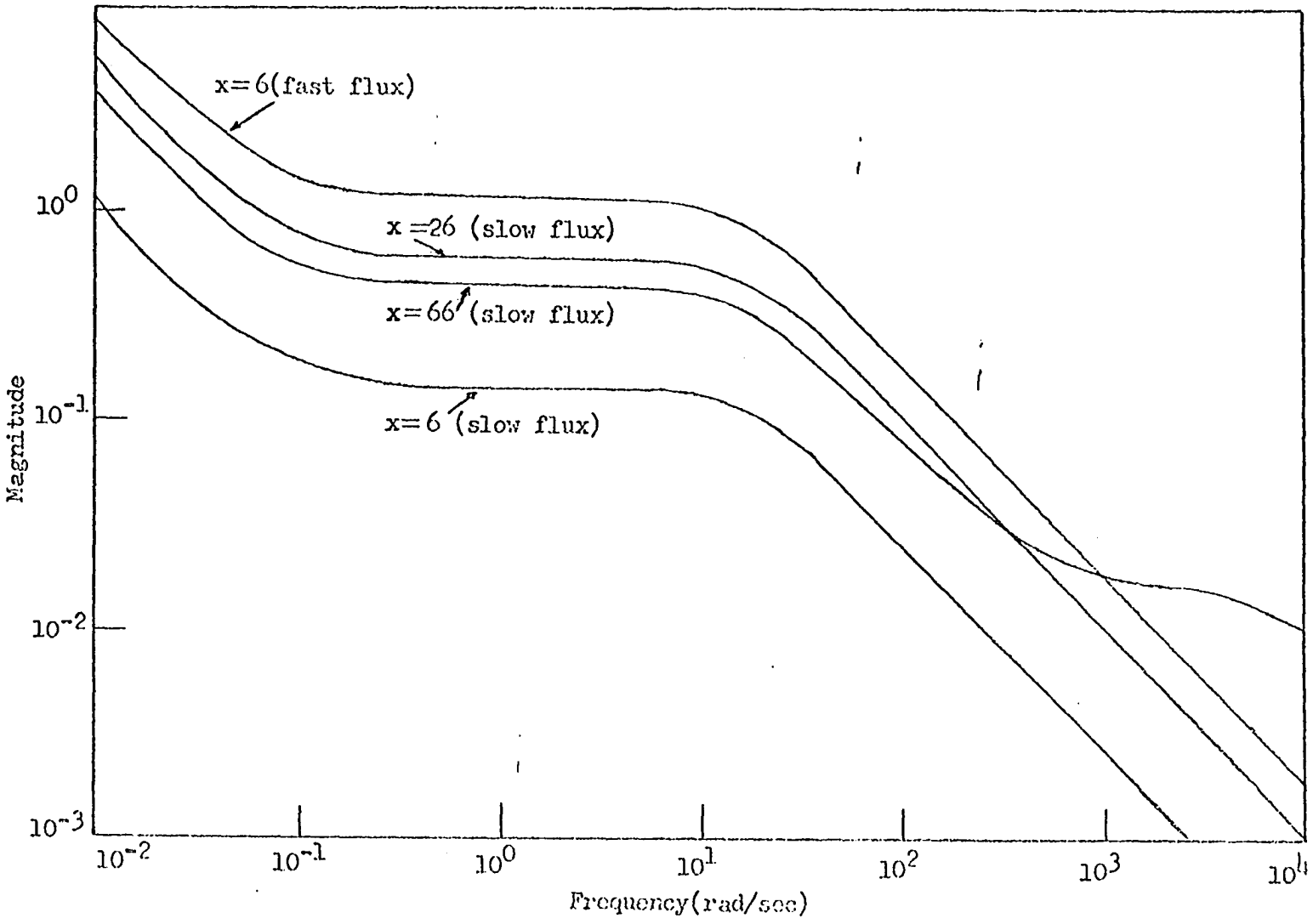

Fig. 48. Magnitude of fast and slow flux frequency response for three mode analysis

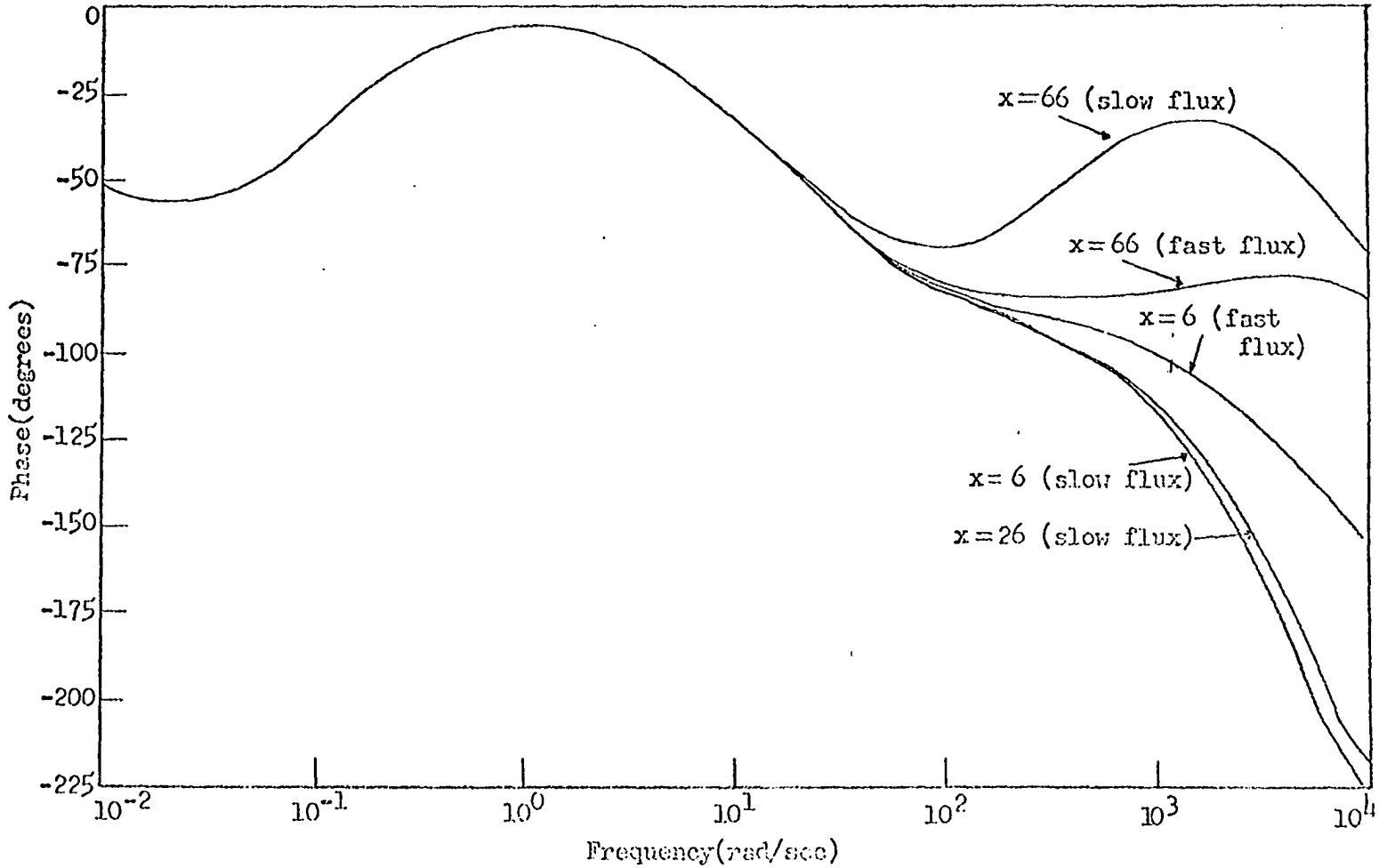

Fig. 49. Phase angle of fast and slow flux frequency response for three mode analysis

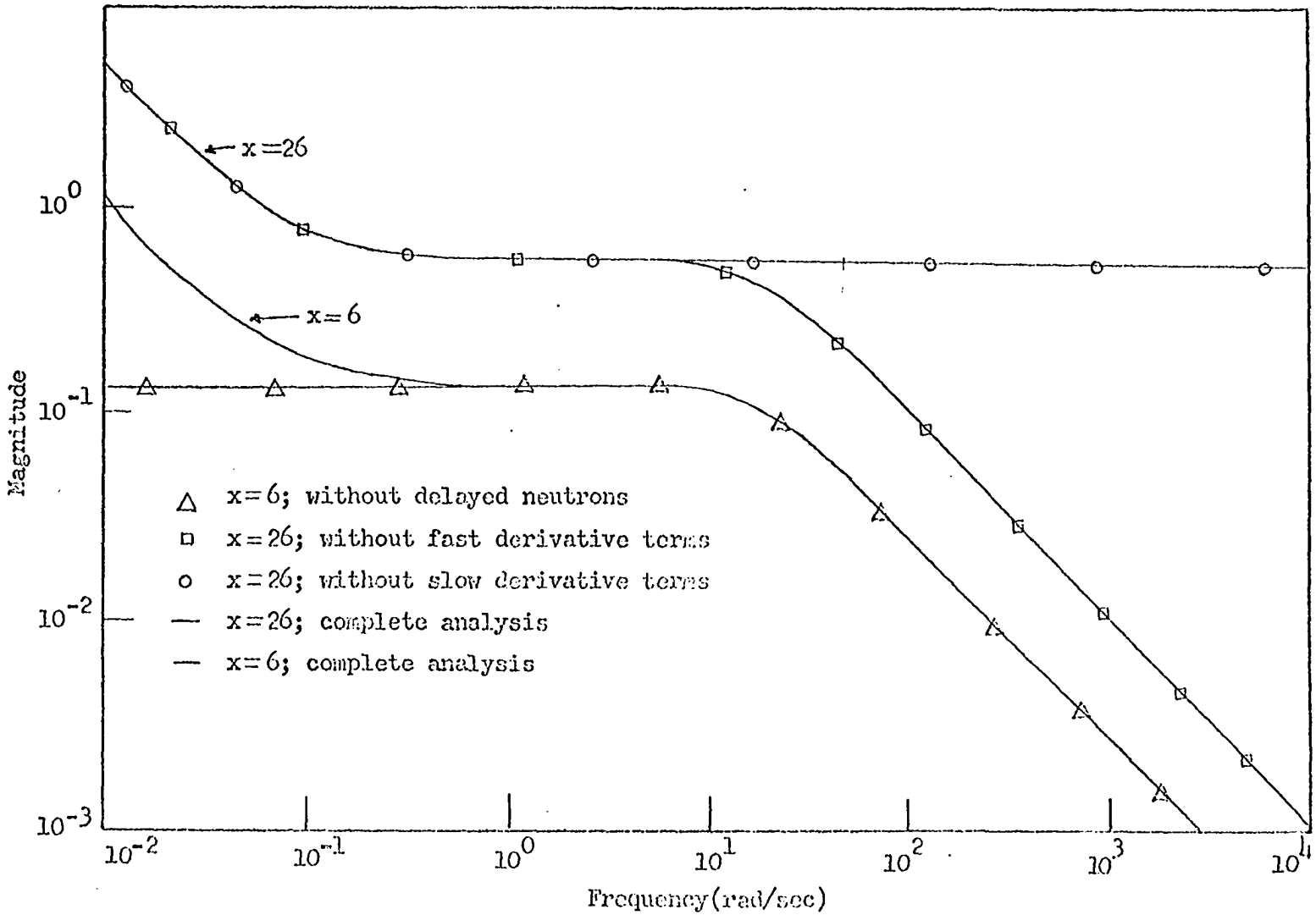

Fig. 50. Variations of frequency response for three mode analysis

zero. In this case the frequency response was affected only at frequencies greater than 10 rad/sec. It is interesting to compare the results of these analyses with the results obtained by performing an analogous analysis using the space-independent, or point, kinetic equations

$$\frac{dn}{dt} = \frac{\delta k n}{\ell} \quad \frac{-\beta n}{\ell} + \lambda c$$

$$\frac{dc}{dt} = \frac{\beta n}{\ell} \quad -\lambda c.$$

The point kinetic transfer function is given by (44)

$$G(S) \equiv \frac{\Delta N(S)}{\Delta K(S)} = \frac{n(0)\ (S+\lambda)}{\ell S(S+\beta/\ell)} = \frac{n(0)\ (j\omega+\lambda)}{\ell(j\omega)(j\omega+\beta/\ell)} \tag{46}$$

At low frequencies where $\omega << \beta/\ell$, Equation 46 reduces to

$$G(j\omega) \equiv \frac{\Delta N(j\omega)}{\Delta K(j\omega)} = \frac{n(0)(j\omega+\lambda)}{\beta(j\omega)} \tag{47}$$

Now the point transfer function is derived by first letting $\frac{dn}{dt} = 0$. The standard substitutions are made that

$$n(t) = n_o + \delta n$$

$$c(t) = c_o + \delta c$$

and initial conditions are applied. The result is

$$\frac{\delta k\ n(0)}{\ell} \quad - \frac{\beta \delta n}{\ell} + \lambda \delta c = 0$$

$$\frac{d\delta c}{dt} = \frac{\beta \delta n}{\ell} \quad -\lambda \delta c, \tag{48}$$

where the second order term $\frac{\delta k \cdot \delta n}{\ell}$ has been eliminated. Equations 48 are now Laplace transformed and solved for the

ratio $\frac{N(S)}{K(S)} = \frac{L[\delta n]}{L[\delta k]}$; the result is

$$\frac{\Delta N(S)}{\Delta K(S)} = \frac{n(0)(S+\lambda)}{\beta \cdot S} \tag{49}$$

When the substitution is made $S=j\omega$, it can be seen that Equations 49 and 47 are identical.

Also shown in Figure 50 is the result of eliminating delayed neutrons from the analysis. The frequency response for the slow flux, evaluated at x=6 cm., is shown for the situations in which delayed neutrons are included in the analysis and when they are eliminated. It is apparent that the delayed neutrons only influence the frequency response at low frequencies where $\omega \leq \lambda$.

The frequency response of the reactor shown in Figure 28 was next determined using the six region space modes displayed in Figures 41, 42, 43, and 44. When an absorber of magnitude $\delta\Sigma_a=0.002$ cm^{-1} was assumed to be oscillated in the region $50 \leq x \leq 70$, the magnitude of the frequency response for the slow flux was determined at x=6 cm. as shown in Figure 51. Also shown in Figure 51 is a comparison of this six mode analysis with the frequency response obtained by the previous three mode analysis. It can be seen that the diagrams are in agreement except at low frequencies. This difference is again thought to be due to the somewhat greater inaccuracies involved in the six mode analysis. As indicated in Figure 45 the six mode analysis tends to predict a somewhat more super-

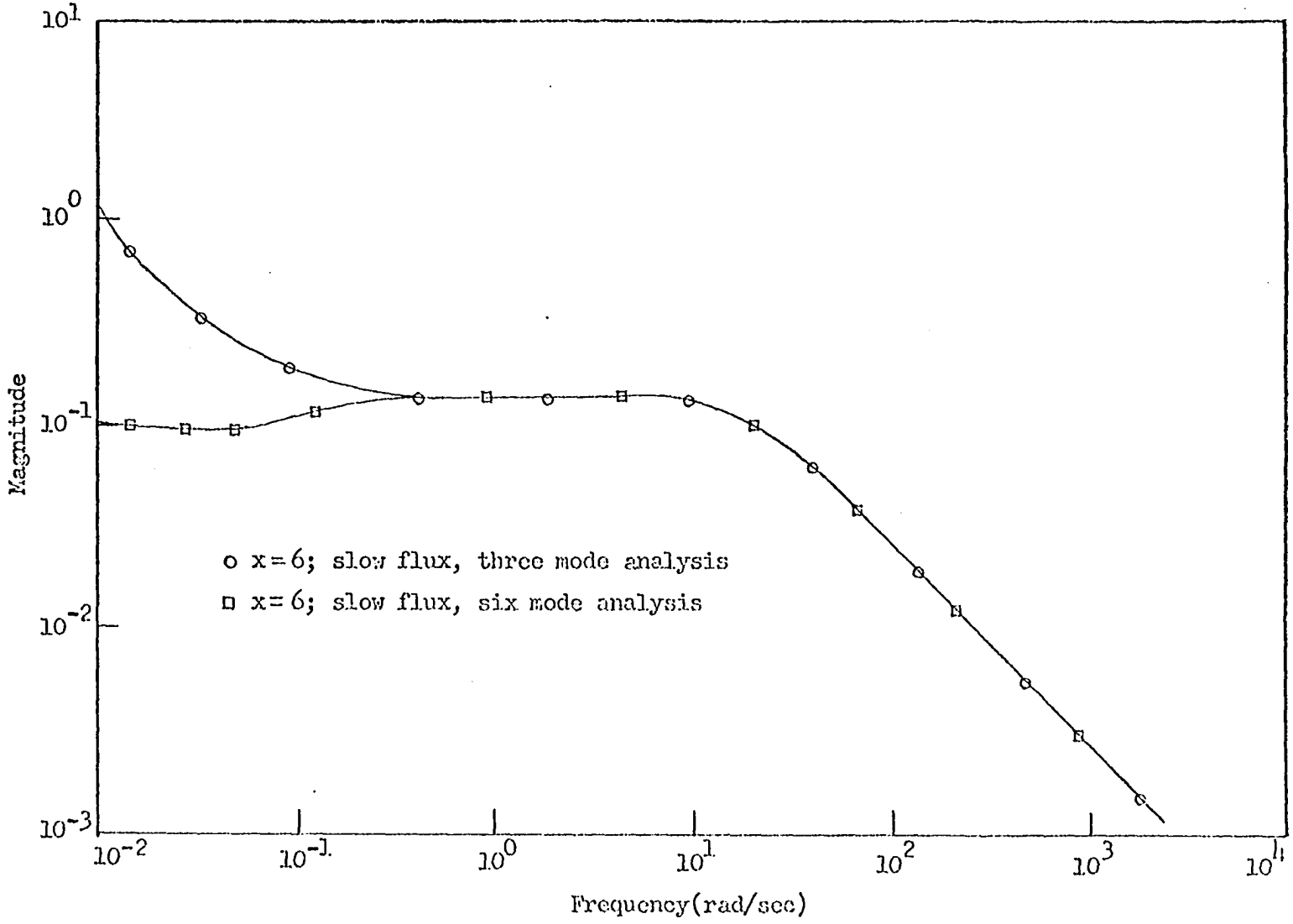

Fig. 51. Comparison of three mode and six mode frequency response for two-group analysis

critical behavior than does the three mode analysis. Reference is made to a paper by Cohn (48) in which he demonstrated, analytically, that a reactor which is very slightly super - or sub - critical will not possess a frequency response of the usual form at low frequencies.

The six mode analysis was finally used to obtain the response of the reactor in Figure 28 to an oscillating absorber of magnitude $\delta\Sigma_a = 0.0008\ cm^{-1}$ in the region $20 \leq x \leq 30$. Magnitude and phase diagrams for this analysis are shown in Figures 52, 53, and 54. Again no fast flux magnitude plots were shown because the shapes were the same as those for the corresponding slow fluxes. However, as shown in Figures 53 and 54, there was again some differences in the phase angle for corresponding fast and slow flux responses. Also note the increased roll off in magnitude for frequency responses determined at x=66 cm. and x=86 cm.

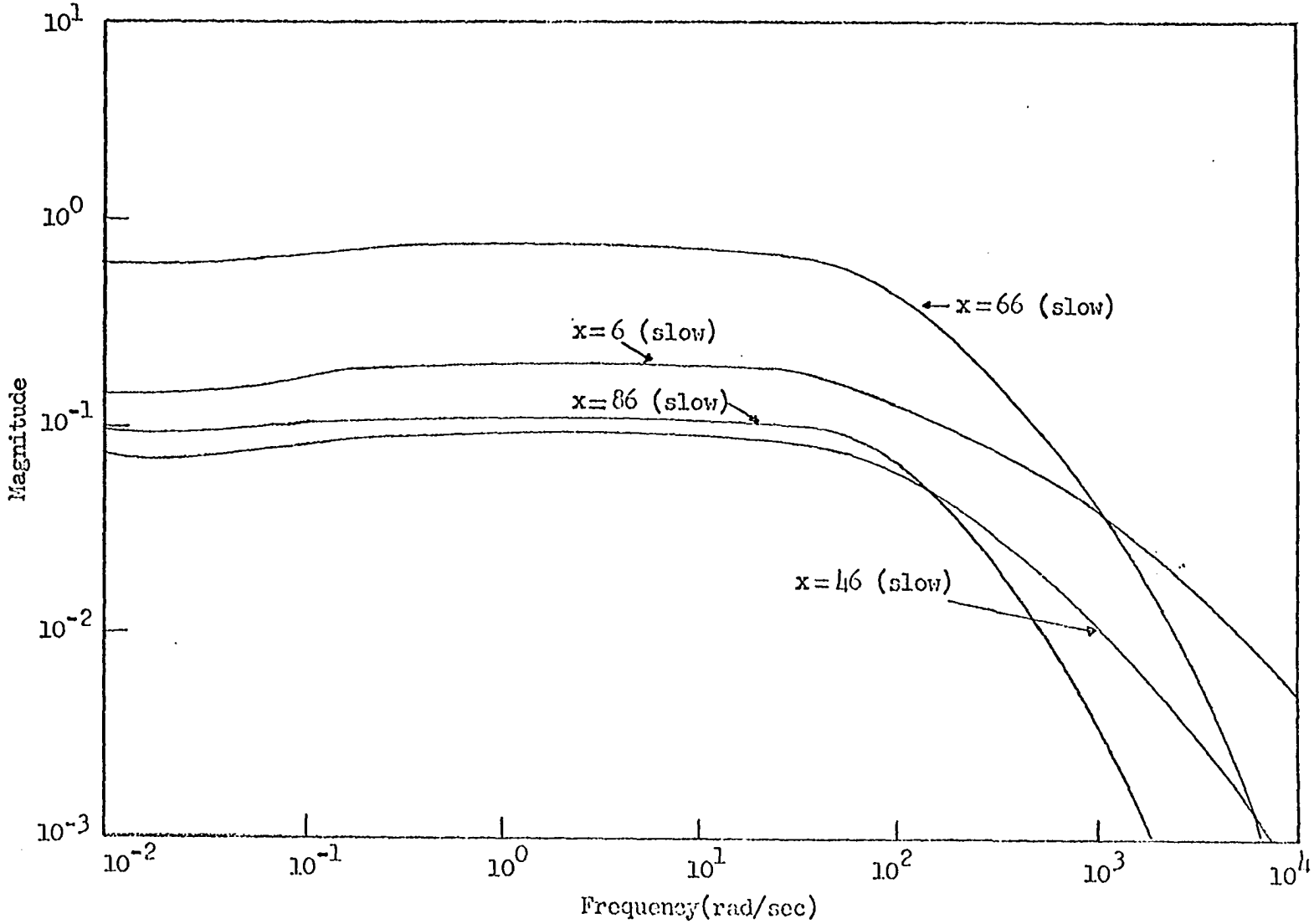

Fig. 52. Magnitude of frequency response for six node, two-group analysis

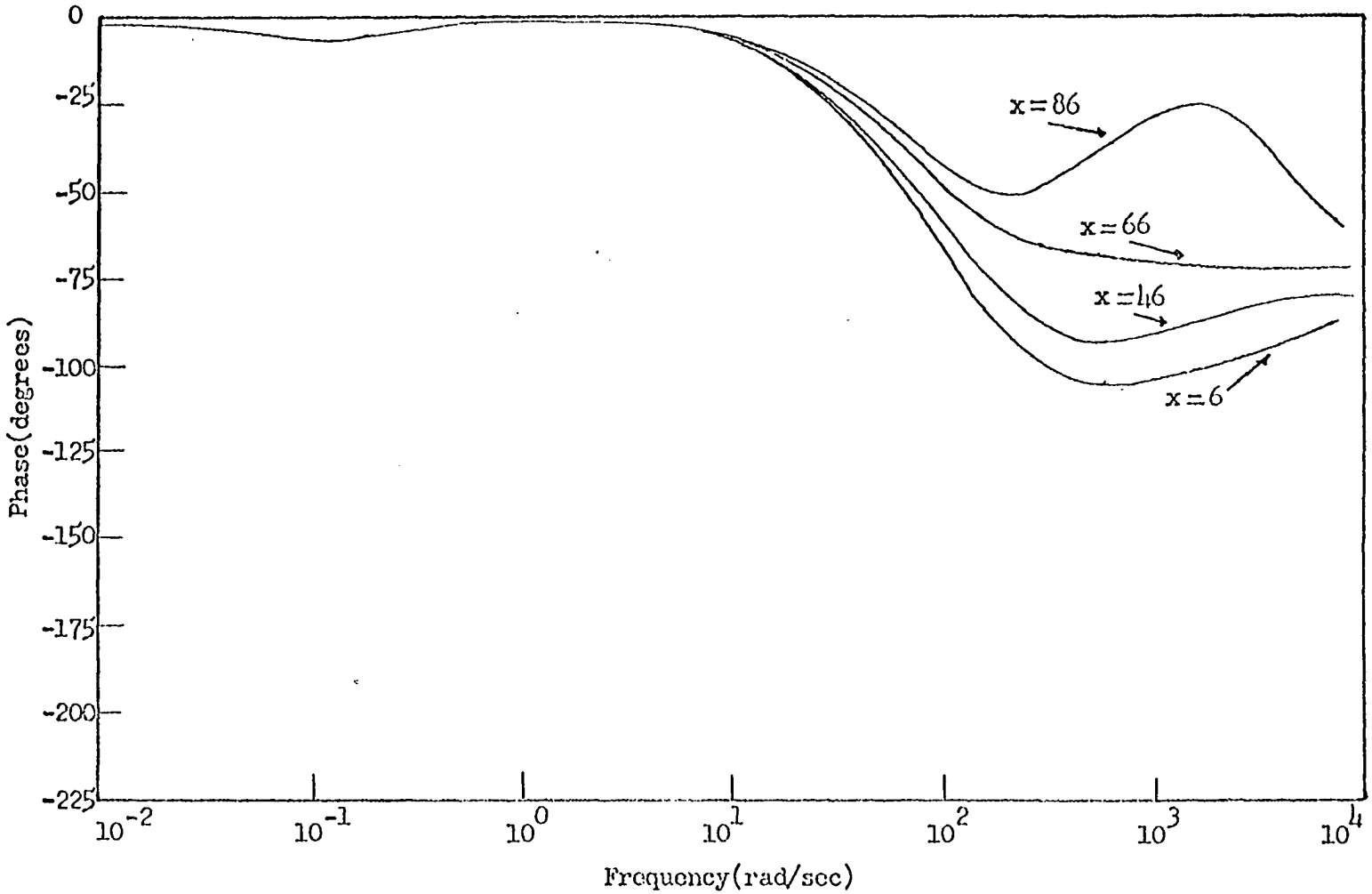

Fig. 53. Phase angle of fast flux frequency response for six mode analysis

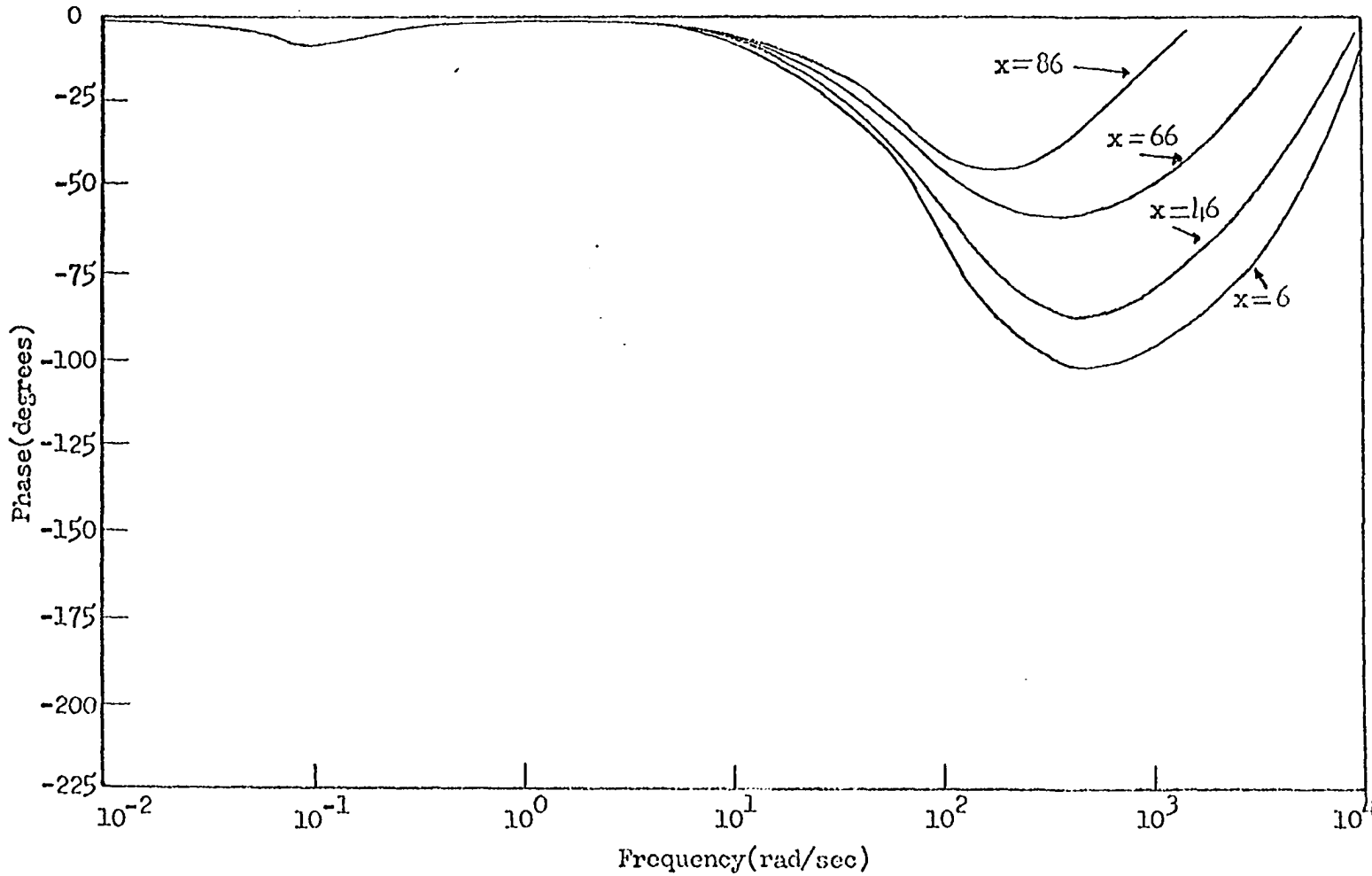

Fig. 54. Phase angle of slow flux frequency response for six mode analysis

IX. ONE GROUP ANALYSIS: RAMP RESPONSE

The purpose of this section is to illustrate that the basic technique used in this paper can be easily extended to include ramp reactivity inputs. As an example the reactor shown in Figure 1 will be analyzed using one-group diffusion theory. It is assumed that the absorption cross section in the region $10 \leq x \leq 17$ can be expressed in the form

$$\Sigma_a = (0.00818-t)\,cm^{-1}, \quad 0 \leq t \leq 0.00818 \text{ sec.}$$

The time dependent flux is written in the form

$$\phi(x,t) = \sum_{i=1}^{6} a_i(t)\psi_i(x), \tag{50}$$

where the space functions $\psi_i(x)$ are shown in Figure 14 Recall that the time coefficients $a_i(t)$ are determined as solutions to the differential equations

$$\Gamma\dot{\theta} = B\theta$$

where

$$\Gamma = [\lambda_{ij}] = [[\psi_i^* \, V^{-1}\psi_j]];$$

$$B = [b_{ij}] = [[\psi_i^*(\nu\Sigma_f - \Sigma_a)\psi_j]].$$

In this case, however, the absorption cross section in the region $10 \leq x \leq 17$ is a function of time. Hence, the matrix B is now of the form

$$B = B_o - \Sigma_{a2}(t) \cdot G,$$

where

$$B_o = [b_{oij}] = [\int_0^{10} (\nu\Sigma_f - \Sigma_a)\psi_i^*\psi_j \, dx + \int_{10}^{17} \psi_i^*(\nu\Sigma_f)\psi_j \, dx + \int_{17}^{74} \psi_i^*(\nu\Sigma_f - \Sigma_a)\psi_j \, dx]$$

$$G = [g_{ij}] = [\int_{10}^{17} \psi_i^*\psi_j \, dx]$$

$$\Sigma_{a2}(t) = (0.00818 - t) \text{ cm}^{-1}.$$

The time coefficients are thus solutions to the differential equations

$$\Gamma\dot{\theta} = B_o\theta - \Sigma_{a2}(t) \cdot G\theta \qquad (51)$$

The equations given in Equation 51 represent a set of first order differential equations with time dependent coefficients. These equations were solved by means of the numerical routine NODE with a machine running time very comparable to the step analyses. The solutions for the time coefficients a_1, a_2, and a_5 are shown in Figure 55. The time dependent flux distributions, as obtained from Equation 50, are shown in Figure 56. Note that the flux distributions shown in Figure 56 possess shapes very comparable to those for the step analysis, shown in Figure 18, but that their magnitudes are less by a factor of 10. Hence, even though a very fast ramp input was used, the difference between the ramp and step analyses was very significant.

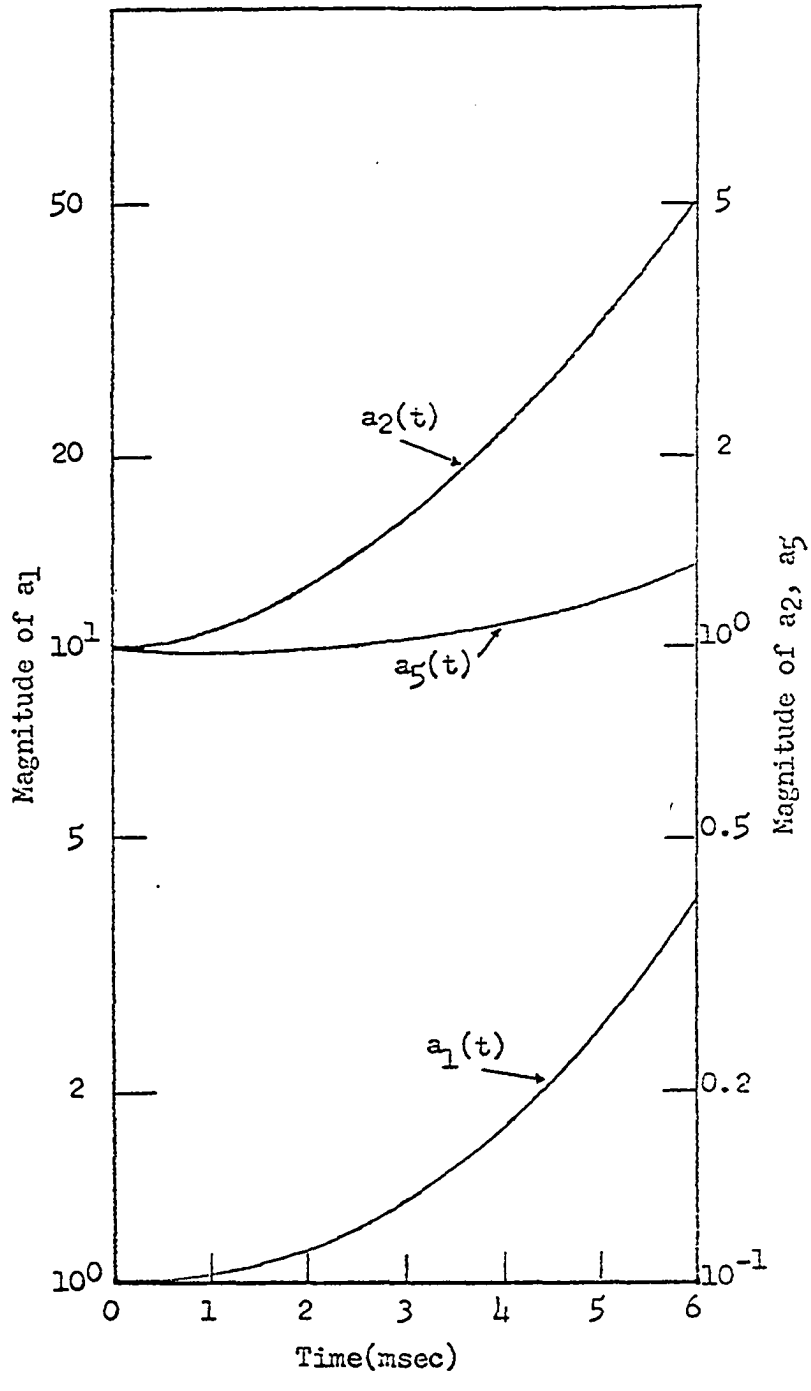

Fig. 55. Time coefficients for ramp analysis

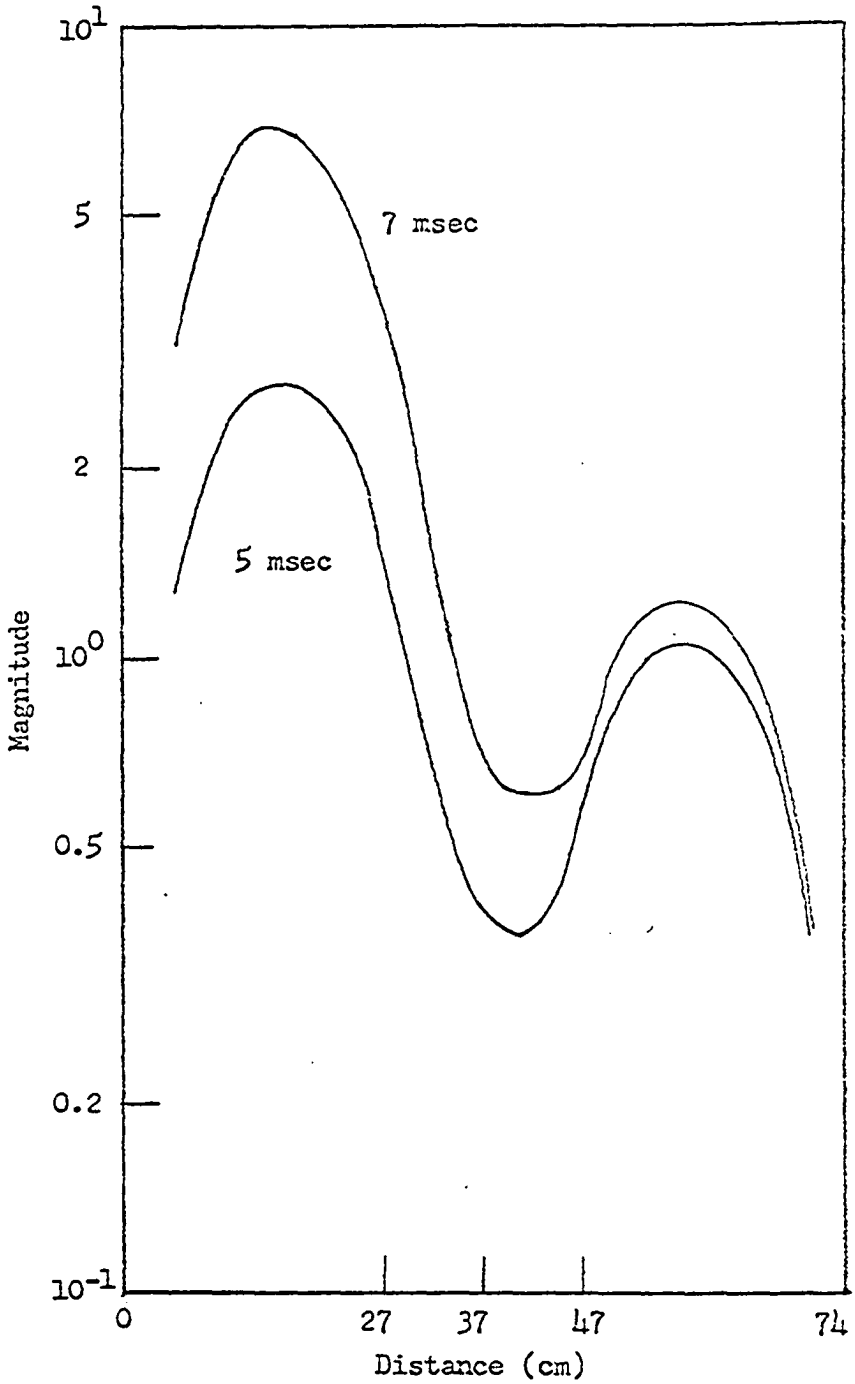

Fig. 56. Time dependent flux for ramp analysis

X. CONCLUSIONS

The modal analysis technique has been used in this paper to solve the kinetic equations for a nuclear reactor. This method involves expressing the time dependent neutron flux in the form

$$\phi(x,t) = \sum_{i=1}^{N} a_i(t)\psi_i(x)$$

where the space functions $\psi_i(x)$ and the time coefficients $a_i(t)$ need to be determined in some suitable and consistent manner. The Green's function space modes used in this paper have proven to have several desirable properties.

The Green's function space modes are relatively easy to generate. They are determined as the solution to a straightforward set of differential equations and corresponding boundary conditions, and their solution involves no source iteration. The only information needed in order to determine the modes is the solution to the steady state problem. This information may easily be obtained either by analytical means, as was done in this paper, or by the many numerical methods that are available. The problem is even simpler for a one energy group analysis since no adjoint space modes need to be determined.

It was found that an extension was required in order to generate space modes that would represent non-multiplying regions in the reactor. This problem became apparent when no

mode was determined to describe the coupling region of a coupled core reactor. Without such a mode it was not possible to correctly describe the time dependent behavior of the reactor. The same problem would arise in the case of a reflected reactor or a seed-blanket type reactor. Modes for the non-multiplying regions were determined by the relatively easy extension of creating a psuedo production operator in the non-multiplying region. This psuedo production operator was formed by a suitable division of the removal operators Σ_a or Σ_R for the coupling regions. It is quite significant that the choice of the relative division of these operators does not affect the final expression for the reactor time dependent flux.

The shape of the space modes is partially determined by the manner in which the reactor is divided into various regions. The choice as to the number of regions and their relative locations is determined by the type of perturbation that is to be made in the reactor. That is, since it is anticipated that the greatest changes in flux shape will occur in the regions nearest the region of perturbation, more regions are established in this area. Therefore, there are more space modes available to describe the time dependent flux shape in the areas where it is undergoing the greatest changes. The shape of the modes is also partially determined by the reactor critical flux distribution; in fact, the space modes

sum to this critical flux. The net result of obtaining space modes in this manner is a rapid convergence rate of the expression for the time dependent flux as compared to other modes, such as the Helmholtz modes. A rapid convergence rate is important because it results in less computer running time; in addition, fewer modes require fewer time coefficients, which simplifies the time dependent portion of the problem.

After the space modes have been established, the corresponding time coefficients are derived by means of a variational principle. Recall that the space functions do not possess orthogonality properties. In the variational technique a functional is established whose Euler equations are the neutron kinetic and adjoint kinetic equations. After a separable trial function is substituted into this functional, taking the first variation of the resulting functional leads to a set of first order, linear differential equations whose solution represents the time coefficients. These differential equations are inherently describing the dynamic behavior of a nuclear reactor, and the solution of such equations typically involves some interesting and difficult numerical problems. Four independent techniques were investigated as possibilities for solving these differential equations.

The analog computer method was mentioned only briefly. The advantage of time scaling and the disadvantage of hardware requirements were discussed. The eigenvalue method proved to

be a fast and easy method so long as the numerical method utilized was capable of obtaining the eigenvalues and eigenvectors of the problem at hand. It was noted that as the description of the reactor becomes more complex, the eigenvalue method falters due to the sizes of the matrices that result from the analysis. The numerical routine NODE was a very satisfactory technique after the fast neutron lifetime was removed from the analysis. It is not completely evident from the analyses performed in this paper whether a Runge-Kutta technique such as employed in NODE would be satisfactory for a multi-group analysis in which more than two energy groups were included. However, since the analysis in this paper was for the extreme fast and slow fluxes, it is believed that a Runge-Kutta scheme should continue to be a useful technique for more complex analyses. The exponential method gave excellent results for all investigations. The method is fast and seems to continue to be useful even for more complex analyses. That is, in the case of a more complex description of the reactor, the effect on the exponential method is only an increase in the size of the matrix U in e^{U}. This increase only results in a slightly longer convergence time on the digital computer. The larger matrices do involve some problem as far as round off error is concerned, but this does not seem to be a significant problem except for analyses involving very small perturbations to the reactor.

A very significant advantage of the overall analytical technique employed in this paper is its versatility. The technique allows one to obtain the response of a nuclear reactor to perturbations of a step, ramp, or oscillatory nature. The space modes are determined from the steady state problem and are independent of the type of perturbation that is to be made. The modes are only dependent on the region in which the perturbation is made in the manner described previously. Therefore, only the problem of determining the time coefficients is affected by the type of perturbation. A ramp perturbation is the hardest to analyze in that it requires the solution of a set of first order differential equations with non-constant coefficients. The step input problem is then somewhat easier since in this case the differential equations resulting from the variational technique are first order with constant coefficients. The response of the reactor to an oscillating absorber is the easiest problem to analyze since the differential equations for the time coefficients in this case reduce to algebraic equations. The only problem encountered in the oscillatory analysis was that of maintaining sufficient accuracy at low frequencies so that the influence of delayed neutrons is not lost. However, in all cases the overall analytical technique requires very slight adjustments in order to encompass the various types of perturbations.

The actual results obtained in this paper are displayed in various figures throughout the text. A fundamental result of the overall analysis is the demonstration that the time dependent response of a nuclear reactor is spatially dependent. Recall that the space-independent, or point, kinetic equations assume that the reactor maintains some fixed spatial distribution and that this distribution then rises exponentially. The space-time results demonstrated in this paper clearly show that the flux shape does undergo some changes in shape during a transient period, and when an asymptotic distribution is reached, it is not the same distribution as the critical. In fact, in certain cases very large flux tilting occurs. The point kinetic equations also predict that the frequency response of a reactor will be the same at any point in the reactor. The fact that the frequency response can, in fact, be very much spatially dependent is also clearly demonstrated by the frequency response diagrams displayed in this paper. It was interesting to note the comparison between the frequency responses as obtained from the point analysis and from the space-time analysis when the time derivative terms were neglected. In the space-time analysis the removal of the fast derivative terms greatly simplifies the numerical calculations, and it is significant that their removal does not affect the expression obtained for the reactor frequency response.

It was realized that it is impossible to obtain a step reactivity input in a physical sense. Thus it was interesting to note the comparison obtained for the reactor response to a step and a very rapid ramp input. The flux shapes obtained were very comparable, but the magnitude of the flux at any given time was significantly less in the case of the ramp analysis.

The extension of the basic technique employed in this paper to more neutron energy groups or more delayed neutron groups should be straightforward. The neutron kinetic equations could still be written in the matrix form

$$L\phi = V^{-1} \frac{\partial \phi}{\partial t}$$

where the matrices L, V^{-1}, and ϕ are now merely larger in size than those analyzed in this paper. However, when one tries to include feedback effects, such as xenon, in the description of the reactor, some problems develop. The kinetic equations can no longer be written in the linear form $L\phi = V^{-1} \frac{\partial \phi}{\partial t}$ since feedback effects include some non-linearities. One possible way to eliminate this difficulty is to linearize the kinetic equations by expressing all variables in terms of a steady state part and a small, time dependent part, such as

$$\phi = \phi_o + \delta\phi(t)$$

$$C = C_o + \delta C(t).$$

This linearization implies that one is limited to investigating small reactivity perturbations. The kinetic equations will now be expressible in the form

$$L\phi = V^{-1} \frac{\partial \phi}{\partial t} + R_o \ ,$$

where the matrix R_o has only steady state terms as its elements. The analysis could now be continued by dividing the operator L as before and attempting to determine space modes to describe the reactor variables. A functional would have to be derived that would include the terms R_o as part of its Euler equations. One other problem that might develop is that xenon feedback is a effect that is present at low frequencies, which is where some problems developed in this paper when considering delayed neutrons. In the case of a step reactivity input the xenon contribution to the reactor time dependent behavior would probably be described by small eigenvalues, if the eigenvalue method is used to solve the differential equations, and this also leads to problems. In any event including feedback effects into the analysis would be an interesting problem to pursue.

XI. LITERATURE CITED

1. Hurwitz, H., Jr. The derivation and integration of the pile-kinetic equations. Nucleonics 5: 61-67. 1949.

2. Glasstone, S. and Edlund, M. C. The elements of nuclear reactor theory. New York, N.Y. D. Van Nostrand Co., Inc. 1952.

3. Weinberg, A. M. and Wigner, E. P. The physical theory of neutron chain reactors. Chicago, Ill. The University of Chicago Press. 1958.

4. Ash, M. Nuclear reactor kinetics. New York, N.Y. McGraw-Hill Book Co., Inc. 1965.

5. Henry, A. F. The application of reactor kinetics to the analysis of experiments. Nuc. Sci. and Eng. 3: 52-70. 1958.

6. Lewins, J. Variational representations in reactor physics derived from a physical principle. Nuc. Sci. and Eng. 8: 95-104. 1960.

7. Gozani, T. The concept of reactivity and its application to kinetic measurements. Nukleonik 5: 55-62. 1963.

8. Hurwitz, H., Jr. Note on the theory of coefficients. U.S. Atomic Energy Commission Report KAPL-98. [Knolls Atomic Power Lab., Schenectady, N.Y.] 1948.

9. Ussachoff, L. N. Equation for the importance of neutrons, reactor kinetics and the theory of perturbation. First United Nations International Conference on the Peaceful Uses of Atomic Energy, 1st, Geneva, 1956. Paper 656. 1956.

10. Selengut, D. S. Variational analysis of multi-dimensional systems. U.S. Atomic Energy Commission Report HW-59126. [General Electric Co. Hanford Atomic Products Operation, Richland, Wash.] 1958.

11. Kadomtsev, B. B. A physical interpretation of the adjoint function (translated title). Doklady Akad. Nauk S.S.S.R. 113: 3. 1957.

12. Lewins, J. The time-dependent importance of neutrons and precursors. Nuc. Sci. and Eng. 7: 268-274. 1960.

13. Flatt, H. P. Collocation method for the numerical solution of the reactor kinetics equation. IBM Nucl. Comp. Bull. 5. 1962.

14. Kaganove, J. J. Numerical solution of the one group reactor kinetics equations. U.S. Atomic Energy Commission Report ANL-6132. [Argonne National Lab., Argonne, Ill.] 1960.

15. Hansen, K. F., Koen, B. V., and Little, W. W., Jr. Stable numerical solutions of the reactor kinetics equations. Nuc. Sci. and Eng. 22: 51-59. 1965.

16. Keepin, G. R. and Cox, C. W. General solution of the reactor kinetic equations. Nuc. Sci. and Eng. 8: 670-690. 1960.

17. Kaplan, S., Henry, A. F., Marglois, S. G., and Taylor, J. J. Space-time reactor dynamics. Third International Conference on the Peaceful Uses of Atomic Energy 3: 41. New York, N.Y., United Nations. 1964.

18. Henry, A. F. and Curlee, N. J. Verification of a method for treating neutron space-time problems. Nuc. Sci. and Eng. 4: 727-744. 1958.

19. Lewins, J. The approximate separation of kinetics problems into time and space functions by a variational principle. J. Nuc. Energy 12, Part A: 108-112. 1960.

20. Lewins, J. The reduction of the time-dependent equations for nuclear reactors to a set of ordinary differential equations. Nuc. Sci. and Eng. 9: 399-407. 1961.

21. Kaplan, S. and Margolis, S. G. Delayed neutron effects during flux tilt transients. Nuc. Sci. and Eng. 7: 276-277. 1960.

22. Varga, R. S. Numerical solution of the two-group diffusion equation in x-y geometry. U.S. Atomic Energy Commission Report WAPD-159. [Westinghouse Electric Corp. Atomic Power Division, Pittsburgh, Pa.] 1956.

23. Cadwell, W. R., Henry, A. F., and Vigilotti, A. J. WIGLE- A program for the solution of the two-group space-time diffusion equations in slab geometry. U.S. Atomic Energy Commission Report WAPD-TM-416. [Westinghouse Electric Corp. Atomic Power Division, Pittsburgh, Pa.] 1964.

24. Avery, R. Theory of coupled reactors. Second International Conference on the Peaceful Uses of Atomic Energy 12: 182. New York, N.Y., United Nations. 1958.

25. Kaplan, S. and Bewick, J. A. Space and time synthesis by the variational method. U.S. Atomic Energy Commission Report WAPD-BT-28. [Westinghouse Electric Corp. Atomic Power Division, Pittsburgh, Pa.] 1963.

26. Crandall, S. H. Engineering Analysis. New York, N.Y. McGraw-Hill Book Co., Inc. 1956.

27. Foderaro, A. and Garabedian, H. L. Two group reactor kinetics. Nuc. Sci. and Eng. 14: 22-29. 1962.

28. Loewe, W. E. Space-dependent effects in the response of a nuclear reactor to forced oscillations. Nuc. Sci. and Eng. 21: 536-549. 1965.

29. Kaplan, S. The property of finality and the analysis of problems in reactor space-time kinetics by modal expansions. Nuc. Sci. and Eng. 9: 357-361. 1961.

30. Cohn, R. Some topics in reactor kinetics. Second International Conference on the Peaceful Uses of Atomic Energy 11: 302. United Nations. 1958.

31. Henry, A. F. The application of inhour modes to the description of nonseparable reactor transients. Nuc. Sci. and Eng. 20: 338-351. 1964.

32. Habetler, G. J. and Martino, M. A. Existence theorems and spectral theory for the multigroup diffusion model. American Mathematical Society Symposia in Applied Mathematics-Nuclear Reactor Theory, Proceedings. 1961.

33. Dougherty, D. E. and Shen, C. N. The space-time neutron kinetic equations obtained by the semidirect variational method. Nuc. Sci. and Eng. 13: 141-148. 1962.

34. Calame, G. P. and Federighi, F. D. A variational procedure for determining spatially dependent thermal spectra. Nuc. Sci. and Eng. 10: 190-201. 1961.

35. Wylie, C. R., Jr. Advanced engineering mathematics. New York, N.Y. McGraw-Hill Book Co., Inc. 1960.

36. Pennington, R. H. Introductory computer methods and numerical analysis. New York, N.Y. The Macmillan Co. 1965.

37. Kuo, Shan S. Numerical methods and computers. Reading, Mass. Addison-Wesley Publishing Co., Inc. 1965.

38. Hildebrand, F. B. Introduction to numerical analysis. New York, N.Y. McGraw-Hill Book Co., Inc. 1956.

39. Clark, M., Jr. Numerical methods of reactor analysis. New York, N.Y. Academic Press, Inc. 1964.

40. Pluta, P. R. Coupled core kinetic behavior. AEC Symposium Series #7, Neutron Dynamics and Control, CONF-650413. [U.S. Atomic Energy Commission Div. Tech. Information, Springfield, Virginia.] 1966.

41. Gill, S. A process for the step-by-step integration of differential equations in an automatic digital computing machine. Camb. Phil. Soc. Proc. 47: 96. 1951.

42. Pipes, L. A. Matrix methods for engineering. Englewood Cliffs, N.J. Prentice-Hall, Inc. 1963.

43. Frazer, R. A., Duncan, W. J., and Collar, A. R. Elementary matrices. New York, N.Y. Cambridge University Press. 1938.

44. Pipes, L. A. Applied mathematics for engineers and physicists. New York, N.Y. McGraw-Hill Book Co., Inc. 1958.

45. Hildebrand, F. B. Methods of applied mathematics. Englewood Cliffs, N.J. Prentice-Hall, Inc. 1952.

46. Friedman, B. Principles and techniques of applied mathematics. New York, N.Y. John Wiley and Sons, Inc. 1956.

47. Glasstone, S. and Edlund, M. C. The elements of nuclear reactor theory. Princeton, N.J. D. Van Nostrand Co., Inc. 1952.

48. Cohn, C., Johnson, R. J., and Macdonald, R. N. Calculating space-dependent reactor transfer functions using static techniques. Nuc. Sci. and Eng. 26: 198-206. 1966.

XII. ACKNOWLEDGMENTS

I wish to thank Dr. Richard Danofsky for his assistance and interest during the initiation and completion of this project. I also gratefully acknowledge support by the Atomic Energy Commission by the award of a special fellowship in nuclear engineering, administered by Oak Ridge Associated Universities.